

**Analytical
and Numerical
Solutions of the
Transport
Equation
for an Exchangeable
Solute in a
Layered Soil**



November 1989
Agronomy and Soils Departmental Series No. 139
Alabama Agricultural Experiment Station
Auburn University
Lowell T. Frobish, Director
Auburn University, Alabama



ANALYTICAL AND NUMERICAL SOLUTIONS OF THE TRANSPORT EQUATION
FOR AN EXCHANGEABLE SOLUTE IN A LAYERED SOIL

Feike J. Leij and J.H. Dane

Graduate Student and Professor
of Agronomy and Soils

Alabama Agricultural Experiment Station
Auburn University
Auburn University, Alabama
Lowell T. Frobish, Director

CONTENTS

	<i>page</i>
LIST OF FIGURES	v
ABSTRACT	ix
INTRODUCTION	1
THEORY	3
Analytical Solution of the ADE for a Nonreactive Solute in a Homogeneous Medium	3
Analytical Solution of the ADE for a Nonreactive Solute in a Two-layer Medium	8
Numerical Solution of the ADE for an Exchangeable Solute in a Homogeneous Medium	11
Numerical Solution of the ADE for an Exchangeable Solute in a Layered Medium	15
Additional Remarks about the Numerical Solution of the ADE .	20
RESULTS AND DISCUSSION	27
Numerical and Analytical Results for Transport of a Non-reactive Solute	28
The Effect of Nonlinear Exchange on Solute Transport . . .	43
The Influence of Soil Layers with Different Transport Properties on Solute Transport	52
SUMMARY AND CONCLUSIONS	63
LITERATURE CITED	65
APPENDIX A. Analytical Solution of the ADE for the Second Layer of a Porous Medium Using a First-type Condition	68
APPENDIX B. Analytical Solution of the ADE for the Second Layer of a Porous Medium Using a Third-type Condition	73
APPENDIX C. Analytical Solution of the ADE for a Two-layer Medium Using a Third-type Condition at the Inlet and a Combined First- and Third-type Condition at the Interface .	77
APPENDIX D. Numerical Integration with the Gauss Chebyshev formula	80

APPENDIX E. Expressions for a_i , b_i , c_i , and f_i to Solve the ADE for a Non-layered Soil and a Layered Soil	81
APPENDIX F. List of Parameter Values for Simulations	83
APPENDIX G. Listing of Computer Programs	86

FIRST PRINTING, NOVEMBER 1989

*Information contained herein is available
to all without regard to race, color, sex,
or national origin*

LIST OF FIGURES

FIG.1. Schematic of the problem and grid system for the numerical solution of transport in a homogeneous soil. The solid circles refer to grid points with known values and the open circles refer to grid points with unknown values 13

FIG.2. Schematic of the problem and grid system at the interface for the numerical solution of transport in a layered soil. The solid circles and triangles refer to grid points with known values and the open circles and triangles refer to grid points with unknown values 16

FIG.3A. The influence of the space step, Δx , on the numerical solution of the ADE. The solid lines are based on the analytical solution 22

FIG.3B. The influence of the time step, Δt , on the numerical solution of the ADE. The solid lines are based on the analytical solution 22

FIG.4. Numerical solution of the ADE with zero dispersion using two different approximations for $\partial X/\partial t$ as presented in Eq.(22) and (32). The solid line represents the theoretical step front 24

FIG.5A. Numerical solution of the ADE for a homogeneous soil using a first-type condition 29

FIG.5B. Numerical solution of the ADE for a homogeneous soil using a third-type condition 29

FIG.6A. Validation of the analytical solution of the ADE for a two-layer medium using a first-type condition 31

FIG.6B. Validation of the analytical solution of the ADE for a two-layer medium using a third-type condition 31

FIG.7A. Validation of the numerical solution of the ADE for a two-layer medium using a first-type condition 32

FIG.7B. Validation of the numerical solution of the ADE for a two-layer medium using a third-type condition 32

FIG.7C. Validation of the numerical solution of the ADE for a two-layer medium using a third-type condition at the inlet and a second-type condition at the interface 33

FIG. 8A. Numerical solution of the ADE for a two-layer medium ($D_1 < D_2, v_1 < v_2$) using a first-type condition	34
FIG. 8B. Numerical solution of the ADE for a two-layer medium ($D_1 < D_2, v_1 < v_2$) using a third-type condition	34
FIG. 8C. Numerical solution of the ADE for a two-layer medium ($D_1 < D_2, v_1 < v_2$) using a third-type condition at the inlet ² and ¹ a second-type condition at the interface	35
FIG. 9A. Numerical solution of the ADE for a two-layer medium ($D_1 > D_2, v_1 > v_2$) using a first-type condition	36
FIG. 9B. Numerical solution of the ADE for a two-layer medium ($D_1 > D_2, v_1 > v_2$) using a third-type condition	36
FIG. 9C. Numerical solution of the ADE for a two-layer medium ($D_1 > D_2, v_1 > v_2$) using a first-type condition at the inlet ² and ¹ a second-type condition at the interface	37
FIG. 10A. Analytical solution of the ADE for a two-layer medium ($D_1 < D_2, v_1 = v_2$) using a first-type condition	38
FIG. 10B. Analytical solution of the ADE for a two-layer medium ($D_1 < D_2, v_1 = v_2$) using a third-type condition	38
FIG. 11A. Analytical solution of the ADE for a two-layer medium ($D_1 > D_2, v_1 = v_2$) using a first-type condition	39
FIG. 11B. Analytical solution of the ADE for a two-layer medium ($D_1 > D_2, v_1 = v_2$) using a third-type condition	39
FIG. 12A. Analytical solution of the ADE for a two-layer medium ($D_1 = D_2, v_1 < v_2$) using a first-type condition	41
FIG. 12B. Analytical solution of the ADE for a two-layer medium ($D_1 = D_2, v_1 < v_2$) using a third-type condition	41
FIG. 13A. Analytical solution of the ADE for a two-layer medium ($D_1 = D_2, v_1 > v_2$) using a first-type condition	42
FIG. 13B. Analytical solution of the ADE for a two-layer medium ($D_1 = D_2, v_1 > v_2$) using a third-type condition	42
FIG. 14A. The effect of front retardation on transport. Analytical solution of the ADE using $R = 1$	44
FIG. 14B. The effect of front retardation on transport. Analytical solution of the ADE using $R = 38.5$	44

FIG. 15A.	The effect of nonlinear exchange on transport. Numerical solution of the ADE for unfavorable exchange	46
FIG. 15B.	The effect of nonlinear exchange on transport. Numerical solution of the ADE for linear exchange	46
FIG. 15C.	The effect of nonlinear exchange on transport. Numerical solution of the ADE for favorable exchange	47
FIG. 16.	The effect of front sharpening on transport. Numerical solution of the ADE for favorable exchange	47
FIG. 17A.	The effect of nonlinear exchange on dispersion: concentration profiles for various exchange isotherms using a moving coordinate system after 1 d	49
FIG. 17B.	The effect of nonlinear exchange on dispersion: concentration profiles for various exchange isotherms using a moving coordinate system after 2 d	49
FIG. 17C.	The effect of nonlinear exchange on dispersion: concentration profiles for various exchange isotherms using a moving coordinate system after 3 d	50
FIG. 17D.	The effect of nonlinear exchange on dispersion: concentration profiles for various exchange isotherms using a moving coordinate system after 4 d	50
FIG. 18A.	Numerical solution of the ADE for a pulse input during unfavorable exchange	51
FIG. 18B.	Numerical solution of the ADE for a pulse input during linear exchange	51
FIG. 18C.	Numerical solution of the ADE for a pulse input during favorable exchange	52
FIG. 19.	The effect of layers with different dispersion coefficients on solute transport. Numerical solution of the ADE for a two-layer medium ₂ using a third-type condition with: (a) $D_1 = D_2 = 10 \text{ cm}^2/\text{d}$, and (b) $D_1 = 10 \text{ cm}^2/\text{d}$ and $D_2 = 100 \text{ cm}^2/\text{d}$	54

FIG. 20A.	The effect of layers with different exchange capacities on solute transport. Numerical solution of the ADE for a two-layer medium using a third-type condition with $(S_T)_1 = (S_T)_2 = 0$ cmol/kg	56
FIG. 20B.	The effect of layers with different exchange capacities on solute transport. Numerical solution of the ADE for a two-layer medium using a third-type condition with $(S_T)_1 = 0$ and $(S_T)_2 = 2$ cmol/kg	56
FIG. 20C.	The effect of layers with different exchange capacities on solute transport. Numerical solution of the ADE for a two-layer medium using a third-type condition at the inlet and a second-type condition at the interface with $(S_T)_1 = 0$ and $(S_T)_2 = 2$ cmol/kg	57
FIG. 21.	The effect of layers with different exchange isotherms on solute transport. Numerical solution of the ADE for a two-layer medium with: (a) $(dY/dX)_1 = 1$ and $(dY/dX)_2 = 3X^2$ and (b) $(dY/dX)_1 = 1$ and $(dY/dX)_2 = \frac{1}{3}X^{-2/3}$	58
FIG. 22.	Concentration profiles in a hypothetical sand with a third-type inlet condition: nonlayered profile (a), and profile with a hypothetical clay layer using a third-type interface condition (b), and second-type interface condition (c)	60
FIG. 23.	Concentration profiles in a hypothetical clay with a third-type inlet condition: nonlayered profile (a), and profile with a hypothetical sand layer using a third-type interface condition (b), and second-type interface condition (c)	62

ABSTRACT

The study of solute transport in layered media is important to investigate how solute movement can be slowed by incorporating a retarding layer in the soil profile and to examine the influence of soil heterogeneity on solute transport. This is conveniently done by comparing transport through layered media with transport through homogeneous media.

A relatively straightforward implicit finite difference method was used to simulate reactive solute transport in layered and homogeneous soil profiles. The effects of numerical dispersion and the differences between the use of a concentration and a flux boundary condition at the inlet were demonstrated for a homogeneous soil. Analytical solutions were obtained for a medium consisting of two layers. Using a flux-type condition at the inlet boundary and interface resulted in discontinuities in solute concentrations at these positions.

The importance of the exchange capacity and the exchange isotherm for the simulation of solute transport was investigated for some hypothetical cases. Both of these phenomena have a strong impact on solute transport. Several examples of a solute pulse traveling through a two-layer medium were presented. Simulation of solute transport through a soil profile, in which a soil layer with low permeability characteristics (soil barrier) was embedded, showed that the adsorption capacity of the barrier was not fully utilized to retard the solute because of dispersive transport.

INTRODUCTION

Transport of chemicals in soils is of great interest in a number of areas in agriculture and engineering. This interest is aroused by the potential of chemicals (fertilizers, pesticides, wastes etc.) to move from the soil surface through the unsaturated zone of the soil towards the groundwater. This process generally results in a deterioration of the quality of soil and water resources. Once a chemical or solute reaches the groundwater, spread of the chemical is greatly facilitated by streamflow within the aquifer system. Therefore, the description of solute movement through the unsaturated zone is an important research topic.

The two objectives of this study were to (1) simulate 1-D transport of inorganic salts through homogeneous and layered soils and (2) investigate the effects of linear versus nonlinear exchange. Layering of soil, with layers of different physical and chemical properties, is of interest due to the influence artificial or natural barriers might have in slowing or preventing the movement of certain chemicals. The effects of layering are also important to the study of transport in heterogeneous media. A layered medium, consisting of a series of homogeneous soil layers, is conceptually equal to a heterogeneous soil. The second objective is important to determine how much effort should be made to determine exchange properties. The influence of the cation exchange capacity and the exchange isotherms are investigated for some hypothetical cases with conditions similar to our later experimental work (19).

Although solute transport in porous media is most often described with the advection dispersion equation (ADE) a number of different approaches have been proposed to model transport because the application of the ADE might not be justified for many instances in the field (15). However, the use of the ADE offers distinct advantages because of its deterministic nature. For a limited number of situations, analytical solutions are available. In most cases, however, numerical methods need to be employed, because the specific conditions for which analytical solutions exist are not encountered in the field. Unfortunately, these methods do not permit as much insight into the effects of physical and chemical processes on solute transport as analytical solutions do, and they are susceptible to computational errors. When long-term predictions of the behavior of chemicals in the soil need to be made, careful consideration should be given to the choice of the numerical model and the processes to be modeled.

A vast amount of work has been published on the numerical solution of the ADE simulating chemical transport in soils. Finite difference methods are quite popular for this purpose, because of their relatively straightforward formulation of the problem (27). However, the somewhat more complicated finite element method has been used as well (*e.g.*, 26). The latter method has distinct advantages when systems with irregular boundaries are considered. Another method is that of characteristics, which is less vulnerable to the numerical problems which plague finite difference solutions.

Because of the simple geometry of the media and the nature of this study, viz. the examination of the importance of various physical and chemical properties on solute transport, the numerical solution of the ADE was carried out with a finite difference method. Verification of the solution was accomplished with comparison to analytical solutions and mass balance calculations.

THEORY

The problem of transport of a nonlinearly exchanging solute is formulated for a homogeneous porous medium and for a porous medium consisting of distinct layers. Analytical solutions are given for transport in a (homogeneous) one-layer and a two-layer medium subject to a flux- and a concentration-type boundary condition at the inlet and the interface. Numerical solutions of the ADE are also given for these cases, but in addition solutions are presented for a flux-type condition at the inlet of the soil and a combined flux- and concentration-type at the interface of soil layers.

Analytical Solution of the ADE for a Nonreactive

Solute in a Homogeneous Medium

For a number of cases, involving simple boundary and initial conditions and linearly exchanging solutes, analytical solutions of the ADE are available. These solutions can be utilized to predict transport, to determine transport parameters, or to validate numerical solutions obtained for the same conditions. For 1-D steady-state flow, transport of a nonreactive solute in a homogeneous soil column with

length L can be described as follows:

$$\frac{\partial C}{\partial t} = D \frac{\partial^2 C}{\partial x^2} - v \frac{\partial C}{\partial x} \quad 0 < x < L \quad t > 0 \quad (1)$$

where C is the solute concentration expressed in mass per volume of solution [ML^{-3}], t is time [T], D is the dispersion coefficient [L^2T^{-1}], v is the mean pore water velocity [LT^{-1}], and x is the coordinate in the direction of flow [L]. The dispersion coefficient quantifies two mechanisms which contribute to solute spreading, viz., molecular diffusion and mechanical dispersion. A common expression for the dispersion coefficient is:

$$D = D_0/\lambda + \alpha|v| \quad (2)$$

where D_0 is the coefficient of molecular diffusion in a free solution [L^2T^{-1}], λ is the tortuosity factor, α is the dispersivity [L], and $|v|$ is the absolute value of v .

Although we assumed nonreactive solute transport, i.e., $R=1$, it should be noted that transport of a linearly exchanging solute can be described by making the substitutions $v=v^*$ and $D=D^*$, where $v^*=v/R$ and $D^*=D/R$.

The choice of the initial and boundary conditions deserves careful attention. If they do not represent the physical system, the mathematical solution based on these conditions is of little practical use. It is assumed that the initial concentration in the column is constant:

$$C(x,0) = C_1 \quad 0 < x < L \quad (3)$$

A great deal of attention has been paid to the proper formulation of the boundary conditions for the ADE (11, 16, 34). We considered the following boundary conditions at the inlet:

$$C|_{x_{\downarrow}0} = C_0 \quad (\text{first-type}) \quad t > 0 \quad (4-a)$$

$$\left(-D \frac{\partial C}{\partial x} + vC\right)|_{x_{\downarrow}0} = vC_0 \quad (\text{third-type}) \quad t > 0 \quad (4-b)$$

where $x_{\downarrow}0$, sometimes denoted as $x \rightarrow 0^+$, implies that $x=0$ is approached from inside the column. The first-type condition (Eq.(4-a)) suggests that the concentration at the interface of influent solution (eluent) is continuous, whereas the third-type condition (Eq.(4-b)) implies that the flux is continuous at the interface. For solute displacement experiments, the latter condition is the more realistic one.

In contrast with the first- or concentration-type condition, the third- or flux-type condition leads to conservation of mass. However, this condition has a few drawbacks. First, one might question the use of a dispersion coefficient close to the interface (11). For practical reasons we will accept its validity. Second, the third-type condition leads to a discontinuity in solute concentration at the inlet. Physically, this will not occur at the microscopic level because of molecular diffusion.

To put these conditions in perspective, it is helpful to formulate the theoretical boundary condition at the inlet as:

$$C|_{x \uparrow 0} = C|_{x_{\downarrow}0} \quad t > 0 \quad (5-a)$$

$$\left(-\theta_0 D_0 \frac{\partial C}{\partial x} + \theta_0 v_0 C\right)|_{x \uparrow 0} = \left(-\theta_1 D_1 \frac{\partial C}{\partial x} + \theta_1 v_1 C\right)|_{x_{\downarrow}0} \quad t > 0 \quad (5-b)$$

$$C(x, t) = C_0 \quad x \leq -L_0 \quad t > 0 \quad (5-c)$$

where θ is the volumetric water content [$L^3 L^{-3}$], L_0 is the arbitrary length of a boundary layer outside the soil column [L], and the subscripts 0 and 1 refer to the eluent and the soil column, respectively. All concentrations are resident concentrations (21). The conditions expressed in Eq.(5) are of little practical use because the location of L_0 is generally not known. Therefore, Eq.(5-c) is omitted and it is assumed that the applied solution is well mixed with eluent concentration C_0 . Note that the concentration of the eluent is now a flux-averaged concentration. Eq.(4-a) and (4-b) then follow from Eq.(5-a) and (5-b). We prefer the use of Eq.(4-b) because of mass preservation, accepting the discontinuity in concentration due to the use of two different types of concentration, i.e., a flux-type for the eluent and a resident-type for the soil. Solutions of the ADE subject to Eq.(4-a) can also be useful (34). Therefore both Eq.(4-a) and (4-b) will be used.

For the outlet, the boundary condition can be formulated as:

$$\left. \frac{\partial C}{\partial x} \right|_{x=L} = 0 \quad t > 0 \quad (6-a)$$

where it is assumed that the concentration is macroscopically continuous over the outlet boundary. This condition is invoked for diffusive transport in finite media, e.g., mass transport by molecular diffusion or heat transport with thermal insulation at $x=L$. In these cases, no transport will occur across the surface at $x=L$. Physically, it is difficult to imagine how dispersive transport will vanish during transient advective transport across the outlet boundary. Furthermore, van Genuchten and Parker (34) argue that in analogy to the macroscopic

discontinuity at the inlet, using Eq.(4-b), a similar discontinuity might occur at the outlet. This invalidates Eq.(6-a). The problem of formulating a boundary condition at $x=L$ can be avoided by assuming that the medium is in effect semi-infinite, i.e.:

$$\left. \frac{\partial C}{\partial x} \right|_{x \rightarrow \infty} = 0 \quad t > 0 \quad (6-b)$$

Based on the considerations outlined by van Genuchten and Parker (34), we decided to use this outlet condition for our analytical solutions. It should be noted that the differences between solutions for finite and semi-infinite media are usually rather small (33).

The analytical solution of Eq.(1) subject to Eq.(3), (4-a) and (6-b), i.e., for a semi-infinite medium with a first-type condition at the inlet, is given by (18):

$$C(x,t) = C_1 + \frac{1}{2}(C_0 - C_1) \left\{ \operatorname{erfc} \left[\frac{x-vt}{2\sqrt{Dt}} \right] + \operatorname{erfc} \left[\frac{x+vt}{2\sqrt{Dt}} \right] \exp\left(\frac{vx}{D}\right) \right\} \quad (7)$$

whereas for the third-type condition at the inlet (i.e., Eq.(1) subject to Eq.(3), (4-b) and (6-b)), the solution is given by:

$$C(x,t) = C_1 + \frac{1}{2}(C_0 - C_1) \left\{ \operatorname{erfc} \left[\frac{x-vt}{2\sqrt{Dt}} \right] + \sqrt{\frac{4v^2 t}{\pi D}} \exp\left[-\frac{(x-vt)^2}{4Dt}\right] - \left(1 + \frac{vx}{D} + \frac{v^2 t}{D}\right) \exp\left(\frac{vx}{D}\right) \operatorname{erfc} \left[\frac{x+vt}{2\sqrt{Dt}} \right] \right\} \quad (8)$$

The evaluation of erfc with standard tables is rather tedious. The function is available as a library function for a number of computer languages. However, it can also be approximated with a series expansion (1). Van Genuchten and Alves (33) provided approximations for the function $\exp(A)\operatorname{erfc}(B)$ which can be programmed easily.

Analytical Solution of the ADE for a Nonreactive
Solute in a Two-layer Medium

Analytical solutions can also be developed for transport in media consisting of homogeneous layers. A variety of solutions does already exist for heat conduction in composite media (21). Solutions for transport have been reported by Shamir and Harleman (28), and Al-Niami and Rushton (3). Shamir and Harleman (28) used a first-type inlet condition and an outlet condition at infinity for each layer, whereas Al-Niami and Rushton (3) used a first-type inlet condition and a finite outlet condition for each layer. Neither solution leads to conservation of mass. We solved this problem assuming that each layer is in effect semi-infinite, using a first or a third-type condition at the inlet of each layer. The solution procedure becomes more tedious with the increase of the number of layers. Therefore, we only considered a medium consisting of two homogeneous layers, with an interface located at $x=L_1$. The flow is perpendicular to the interface.

The solution of the ADE for the first layer was already discussed in the section on analytical solutions for a homogeneous medium. Mathematically, the presence of a second layer does not influence the solution for the first layer because the outlet condition of the first layer was chosen at infinity. Physically, this seems a reasonable assumption for steady flow if no extreme differences in dispersion coefficients between the layers exist, i.e., upstream dispersion is negligible.

The ADE for the second layer is given by:

$$\frac{\partial C}{\partial t} = D_2 \frac{\partial^2 C}{\partial x^2} - v_2 \frac{\partial C}{\partial x} \quad L_1 < x < L_2 \quad t > 0 \quad (9)$$

subject to:

$$C(x, 0) = C_1 \quad L_1 < x < L_2 \quad (10-a)$$

$$C \Big|_{x \uparrow L_1} = C \Big|_{x \downarrow L_1} \quad t > 0 \text{ (first-type)} \quad (10-b)$$

$$(-\theta_1 D_1 \frac{\partial C}{\partial x} + \theta_1 v_1 C) \Big|_{x \uparrow L_1} = (-\theta_2 D_2 \frac{\partial C}{\partial x} + \theta_2 v_2 C) \Big|_{x \downarrow L_1} \quad t > 0 \text{ (third-type)} \quad (10-c)$$

$$\frac{\partial C}{\partial x} \Big|_{x \rightarrow \infty} = 0 \quad t > 0 \quad (10-d)$$

where the subscripts 1 and 2 refer to the first and second layer. We assumed that the initial concentration, C_1 , is equal for both layers. For a first-type condition, the problem is solved in conjunction with Eq.(7), whereas Eq.(8) was used to solve the problem for a third-type condition. From now on it is understood that the term condition refers to the boundary condition at the inlet of a homogeneous layer or a nonlayered soil. Using Eq.(11) from Parker and van Genuchten (22), it can be shown that Eq.(10-b) implies that the volume averaged or resident concentration is continuous at the interface, while Eq.(10-c) implies that the flux-averaged concentration is continuous.

The analytical solution of Eq.(9), subject to (10-a), (10-d), and (10-b) or (10-c), was obtained with Laplace transforms. Appendices A and B contain the details of the respective solution procedures. For a first- and third-type condition, the results are, respectively:

$$C(x,t) = \frac{(C_o - C_1)(x-L_1)}{\sqrt{16\pi D_2}} \int_0^t \left\{ \operatorname{erfc} \left[\frac{L_1 - v_1 \tau}{\sqrt{4D_1 \tau}} \right] + \exp \left(\frac{v_1 L_1}{D_1} \right) \operatorname{erfc} \left[\frac{L_1 + v_1 \tau}{\sqrt{4D_1 \tau}} \right] \right\} \times$$

$$\times \left\{ \frac{1}{(t-\tau)^{3/2}} \exp \left[- \frac{(x-L_1 - v_2(t-\tau))^2}{4D_2(t-\tau)} \right] \right\} d\tau + C_1 \quad (11)$$

$$C(x,t) = \frac{v_2(C_o - C_1)}{\sqrt{4D_2}} \int_0^t \left\{ \operatorname{erfc} \left[\frac{L_1 - v_1 \tau}{\sqrt{4D_1 \tau}} \right] + \exp \left(\frac{v_1 L_1}{D_1} \right) \operatorname{erfc} \left[\frac{L_1 + v_1 \tau}{\sqrt{4D_1 \tau}} \right] \right\} \times$$

$$\times \left\{ \frac{1}{\sqrt{\pi(t-\tau)}} \exp \left[- \frac{(x-L_1 - v_2(t-\tau))^2}{4D_2(t-\tau)} \right] + \right.$$

$$\left. - \frac{v_2}{\sqrt{4D_2}} \exp \left(\frac{v_2(x-L)}{D_2} \right) \operatorname{erfc} \left[\frac{x-L+v_2(t-\tau)}{\sqrt{4D_2(t-\tau)}} \right] \right\} d\tau + C_1 \quad (12)$$

The integrals appearing in these solutions were evaluated with help of the Gauss-Chebyshev formula, discussed in Appendix D.

If we deal with resident-type concentrations, both concentration and flux are continuous across the interface and the solutions given by Eq.(11) and (12) will not yield the exact concentration profile. The transport problem where both the flux and concentration are continuous resembles the one of heat flow in composite media with no contact resistance at the interface (8). To solve this problem analytically, the (simplifying) assumption that the first layer is, in effect, semi-infinite cannot be used. The exit and inlet condition of respectively the first and second layer consist of the two interface conditions (Eq.(10-b) and (10-c)). Appendix C contains the mathematical statement of the problem as well as the solution for the concentration of both layers in the Laplace domain.

Numerical Solution of the ADE for an Exchangeable

Solute in a Homogeneous Medium

To describe transport of a reactive solute we rewrite Eq.(1) as follows:

$$\theta \frac{\partial C}{\partial t} + \rho \frac{\partial S}{\partial t} = \theta D \frac{\partial^2 C}{\partial x^2} - \theta v \frac{\partial C}{\partial x} \quad (13)$$

where ρ is the dry bulk density of the soil [ML^{-3}] and S is the adsorbed concentration of the solute expressed as mass of solute per mass of dry soil [MM^{-1}].

Equation (13) needs to be rewritten to solve for the dependent variable, C . We assumed that a unique relationship, the exchange isotherm, exists between the adsorbed ions and those present in the liquid phase. It should be noted that the relationship between S and C generally also depends on the total ionic strength and other chemical species present (23). Such dependency can be included implicitly by experimentally determining the exchange isotherm under conditions similar to those for which the ADE needs to be solved. The adsorbed concentration can be expressed in terms of the liquid concentration, C , using the chainrule:

$$\frac{\partial S}{\partial t} = \frac{dS}{dC} \frac{\partial C}{\partial t} \quad (14)$$

It is convenient to introduce the following dimensionless concentrations to describe transport of nonlinearly exchanging solutes (17):

$$X=C/C_T \quad (15-a)$$

$$Y=S/S_T \quad (15-b)$$

where X is the dimensionless concentration of the solute in the liquid phase, C_T is the total amount of solute in the liquid phase per volume of solution [ML^{-3}], Y is the dimensionless concentration of the solute in the adsorbed phase, and S_T is the total amount of solute in the adsorbed phase per mass of soil [MM^{-1}]. Substitution of these dimensionless quantities in Eq.(13) and the use of Eq.(14) yields:

$$R \frac{\partial X}{\partial t} = D \frac{\partial^2 X}{\partial x^2} - v \frac{\partial X}{\partial x} \quad (16)$$

where the dimensionless retardation factor, R , is defined as follows:

$$R = 1 + \frac{\rho S_T}{\theta C_T} \frac{dY}{dX} \quad (17)$$

The familiar form of the ADE is obtained by dividing Eq.(16) by R :

$$\frac{\partial X}{\partial t} = D^* \frac{\partial^2 X}{\partial x^2} - v^* \frac{\partial X}{\partial x} \quad (18)$$

where $v^* = v/R$ and $D^* = D/R$.

Eq.(16) will be solved for the following initial and boundary conditions:

$$X(x,0) = X_i(x) \quad 0 < x < L \quad (19-a)$$

$$X|_{x \downarrow 0} = X_0 \quad (\text{first-type}) \quad t > 0 \quad (19-b)$$

$$\left(-D \frac{\partial X}{\partial x} + vX\right)|_{x \downarrow 0} = vX_0 \quad (\text{third-type}) \quad t > 0 \quad (19-c)$$

$$\frac{\partial X}{\partial x}|_{x \uparrow L} = 0 \quad t > 0 \quad (19-d)$$

The numerical solution is achieved with the implicit Crank-Nicolson method. Using a grid system with spatial spacing Δx and temporal spacing Δt , where $x_i = (i-1)\Delta x$ and $t_j = j\Delta t$ ($i=1,2,\dots,n$ and $j=0,1,\dots$), the central difference approximation of Eq.(16) is:

$$\begin{aligned} \frac{R_i^j}{\Delta t} (X_i^{j+1} - X_i^j) = & \frac{D}{2\Delta x^2} (X_{i+1}^{j+1} - 2X_i^{j+1} + X_{i-1}^{j+1} + X_{i+1}^j - 2X_i^j + X_{i-1}^j) + \\ & - \frac{v}{4\Delta x} (X_{i+1}^{j+1} - X_{i-1}^{j+1} + X_{i+1}^j - X_{i-1}^j) \quad i=2,3,4,\dots,n-1 \end{aligned} \quad (20)$$

A schematic of the problem, along with the grid system used for the numerical approximation, is shown in figure 1.

The approximation of the initial condition is:

$$X_i^0 = X_i \quad 2 \leq i \leq n \quad (21-a)$$

The inlet condition ($x=0$) was approximated by:

$$X_1^j = X_0 \quad (\text{first-type}) \quad j \geq 0 \quad (21-b)$$

$$- \frac{D}{4\Delta x} (X_2^{j+1} - X_0^{j+1} + X_2^j - X_0^j) + \frac{v}{2} (X_1^{j+1} + X_1^j) = vX_0 \quad (\text{third-type}) \quad j \geq 0 \quad (21-c)$$

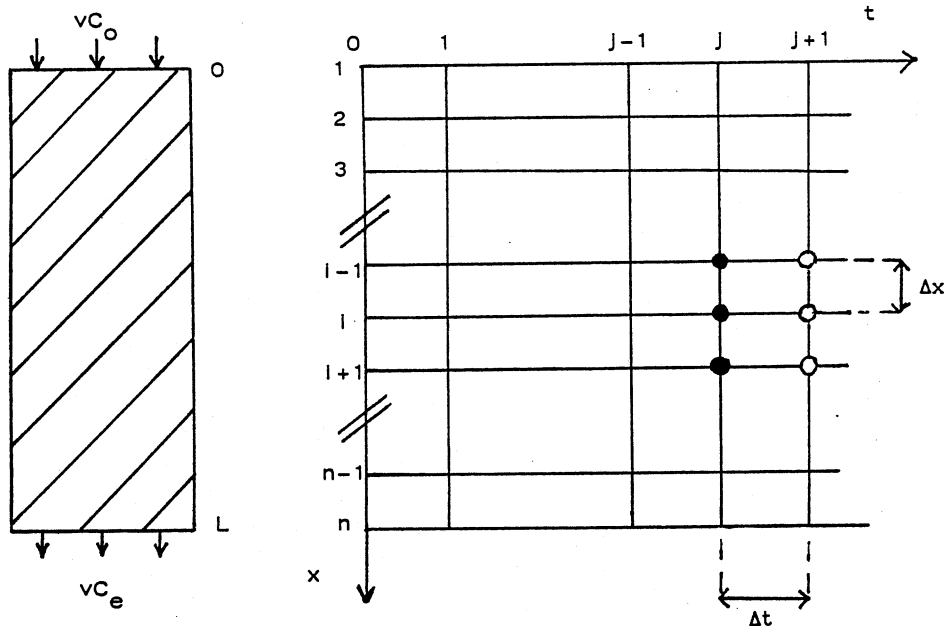


FIG. 1. Schematic of the problem and grid system for the numerical solution of transport in a homogeneous soil. The solid circles refer to grid points with known values and the open circles refer to grid points with unknown values.

where $i=0$ is a fictitious node located at $x=-\Delta x$. The central difference approximation for the outlet condition was written as:

$$X_{n+1}^{j+1} - X_{n-1}^{j+1} + X_{n+1}^j - X_{n-1}^j = 0 \quad j \geq 0 \quad (21-d)$$

where the column exit is located at $(n-1)\Delta x=L$ and $i=n+1$ represents a fictitious node located at $L+\Delta x$. The value of X_1^0 depends on the condition at the inlet of the soil. For the first-type the value is given by (21-a), whereas for the third-type condition X_1^0 was approximated according to Barry et al. (4).

To solve the above set of equations, all unknown variables at time t^{j+1} need to be expressed in terms of known variables at the previous time t^j . The variables at the fictitious nodes $i=0$ and $n+1$ were expressed in variables at column nodes using the central difference approximation of the ADE at $x=0$ and $x=L$. It is convenient to define $G=D/(2\Delta x^2)$ and $H=v/(4\Delta x)$ to rewrite Eq.(20) as:

$$\begin{aligned} (-G-H) X_{i-1}^{j+1} + \left[\frac{R_i^j}{\Delta t} + 2G \right] X_i^{j+1} + (-G+H) X_{i+1}^{j+1} = \\ (G+H) X_{i-1}^j + \left[\frac{R_i^j}{\Delta t} - 2G \right] X_i^j + (G-H) X_{i+1}^j \end{aligned} \quad (22)$$

This equation needs to be solved for $i=2, \dots, n-1$ along with the two equations for the inlet and outlet condition. The resulting system of equations can be written in matrix form:

$$\begin{bmatrix}
 b_1 & c_1 & \dots & \dots & \dots & 0 \\
 a_2 & b_2 & c_2 & & & \vdots \\
 \vdots & a_3 & b_3 & c_3 & & \vdots \\
 \vdots & & & & & \vdots \\
 \vdots & & & & & \vdots \\
 \vdots & & & & & \vdots \\
 0 & \dots & \dots & a_{n-1} & b_{n-1} & c_{n-1} \\
 & & & a_n & b_n &
 \end{bmatrix}
 \begin{bmatrix}
 X_1 \\
 X_2 \\
 X_3 \\
 \vdots \\
 X_{n-1} \\
 X_n
 \end{bmatrix}
 =
 \begin{bmatrix}
 f_1 \\
 f_2 \\
 f_3 \\
 \vdots \\
 f_{n-1} \\
 f_n
 \end{bmatrix}
 \quad (23)$$

The n by n matrix is a tridiagonal band matrix for which the unknowns X^{j+1} are conveniently solved with the Thomas algorithm (25). Expressions for the coefficients a_i , b_i , c_i and f_i are provided in Appendix E.

Numerical Solution of the ADE for an Exchangeable Solute in a Layered Medium

In most soils, the physical and chemical properties will not be constant with depth, e.g., S_T might decrease with depth whereas ρ generally increases with depth. This section is concerned with abrupt changes in properties as they occur in naturally layered soils or artificially constructed media. Each layer is assumed to be homogeneous, with constant parameter values, and the layers are separated by a sharp interface. A schematic of the problem is provided in figure 2A.

The ADE for transport within the k -th layer is written as:

$$R_k \frac{\partial X}{\partial t} = D_k \frac{\partial^2 X}{\partial x^2} - v_k \frac{\partial X}{\partial x} \quad (24)$$

The same initial, inlet, and outlet conditions are used as for the homogeneous medium in the previous section.

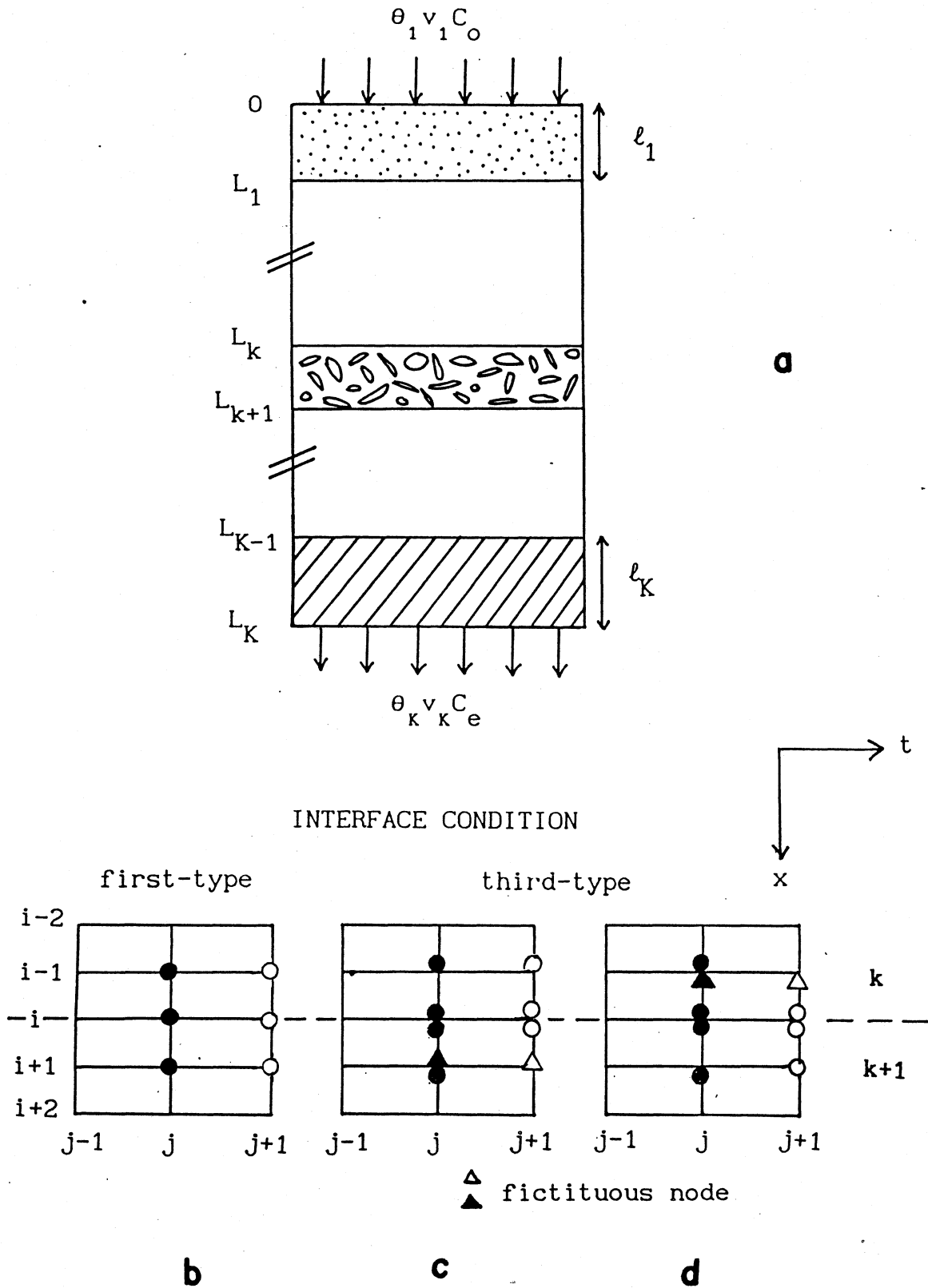


FIG. 2. Schematic of the problem and grid system at the interface for the numerical solution of transport in a layered soil. The solid circles and triangles refer to grid points with known values and the open circles and triangles refer to grid points with unknown values.

The interface condition can be expressed in a similar way as in the section on the analytical solution of solute transport in a two-layer medium. For the interface between layer k and $k+1$, where spatial node i is located at $x=L_k$, these conditions are, respectively:

$$X|_{x \uparrow L_k} = X|_{x \downarrow L_k} \quad (\text{first-type}) \quad (25-a)$$

$$(-(\theta D)_k \frac{\partial X}{\partial x} + (\theta v)_k X)|_{x \uparrow L_k} = (-(\theta D)_{k+1} \frac{\partial X}{\partial x} + (\theta v)_{k+1} X)|_{x \downarrow L_k} \quad (\text{third-type}) \quad (25-b)$$

In addition to a first- and third-type condition, a second-type condition was introduced by combining Eq.(25-a) and (25-b):

$$(\theta D)_k \frac{\partial X}{\partial x}|_{x \uparrow L_k} = (\theta D)_{k+1} \frac{\partial X}{\partial x}|_{x \downarrow L_k} \quad (\text{second-type}) \quad (25-c)$$

The second-type condition, in conjunction with the ADE on both sides of the interface, stipulates that both concentration and flux are continuous at the interface.

The solution of Eq.(24) subject to Eq.(19-a), (19-d), and (1) Eq.(19-b) and (25-a), (2) Eq.(19-c) and (25-b), or (3) Eq.(19-c) and (25-c) was accomplished with the Crank-Nicolson method. The space-time grid system is set up in such a way that a node is located at each interface. The numerical approximation of the ADE for the nodes inside each (homogeneous) layer is analogous to that discussed in the previous section.

For a first-type (interface) condition, Eq.(24) was solved with a central difference scheme where the concentration at the interface of layers k and $k+1$ was solved by using weighted coefficients. The grid system is shown in figure 2B. For example, for the coefficient a_1

(Eq.(23)) we get $a_i = w_k a_{i-1} + w_{k+1} a_{i+1}$ where the weights w_k and w_{k+1} depend on the solute residence time in the space increments on either side of the interface. The solute flux at the interface in layers k , J_k , and $k+1$, J_{k+1} , at spatial node i and temporal node j , can be approximated with the following simple explicit expressions:

$$J_k = (\theta v)_k X_i^j - \frac{(\theta D)_k}{\Delta x} (X_i^j - X_{i-1}^j) \quad (26-a)$$

$$J_{k+1} = (\theta v)_{k+1} X_i^j - \frac{(\theta D)_{k+1}}{\Delta x} (X_{i+1}^j - X_i^j) \quad (26-b)$$

The weight factors for layers k and $k+1$ (w_k and w_{k+1}), were then obtained from the solute fluxes at the interface ($x=L_k$), where the concentration at the previous time equals X_i^j :

$$w_k = \frac{1}{1 + (J_k/J_{k+1})} \quad (27-a)$$

$$w_{k+1} = 1 - w_k \quad (27-b)$$

The solution procedure is similar as outlined for the numerical solution of solute transport in a homogeneous medium. Regular and weighted coefficients a , b , c , and f are listed in Appendix E.

For the third-type (interface) condition, two different approximations for Eq.(25-b) were used to obtain the concentration at the interface of layers k and $k+1$, viz. $\lim_{x \uparrow L_k} X_i^{j+1} = X_{i \uparrow}^{j+1}$ (figure 2C) and

$\lim_{x \downarrow L_k} X_i^{j+1} = X_{i \downarrow}^{j+1}$ (figure 2D). A notation similar to that for $X_{i \uparrow}^{j+1}$ and $X_{i \downarrow}^{j+1}$

was used for the coefficients and concentrations involved in obtaining these variables. The two approximations of Eq.(25-b) are formulated in such a way that Eq.(23) could be used to formulate all equations:

$$\begin{aligned}
& - \frac{1}{\Delta x} \left(\frac{D}{v} \right)_k \left[X_{i+1\uparrow}^{j+1} - X_{i-1\uparrow}^{j+1} + X_{i+1\uparrow}^j - X_{i-1\uparrow}^j \right] + X_{i\uparrow}^{j+1} + X_{i\uparrow}^j \cong \\
& - \frac{2}{\Delta x} \left(\frac{D}{v} \right)_{k+1} \left[X_{i+1\downarrow}^j - X_{i\downarrow}^j \right] + X_{i\downarrow}^{j+1} + X_{i\downarrow}^j \quad (28-a)
\end{aligned}$$

$$\begin{aligned}
& - \frac{2}{\Delta x} \left(\frac{D}{v} \right)_k \left[X_{i\uparrow}^j - X_{i-1\uparrow}^j \right] + X_{i\uparrow}^{j+1} + X_{i\uparrow}^j \cong \quad (28-b) \\
& - \frac{1}{\Delta x} \left(\frac{D}{v} \right)_{k+1} \left[X_{i+1\downarrow}^{j+1} - X_{i-1\downarrow}^{j+1} + X_{i+1\downarrow}^j - X_{i-1\downarrow}^j \right] + X_{i\downarrow}^{j+1} + X_{i\downarrow}^j
\end{aligned}$$

It should be noted that $X_{i+1\uparrow}$ and $X_{i-1\downarrow}$ are concentrations at fictitious nodes located at $L_k + \Delta x$ and $L_k - \Delta x$, respectively. They are obtained by using the central difference approximation of Eq.(24) for layers k and $k+1$. A system of equations as given by Eq.(23) can be obtained, except that $n+k-1$ equations need to be solved, where k is the total number of layers.

Finally, the second-type interface condition was approximated by:

$$(\theta D)_k \left[X_{i\uparrow}^{j+1} - X_{i-1\uparrow}^{j+1} + X_{i\uparrow}^j - X_{i-1\uparrow}^j \right] = (\theta D)_{k+1} \left[X_{i+1\downarrow}^{j+1} - X_{i\downarrow}^{j+1} + X_{i+1\downarrow}^j - X_{i\downarrow}^j \right] \quad (29)$$

where the same grid system was used as for the first-type condition (figure 2B).

The coefficients of the matrix system are listed in Appendix E. The subscript i denotes the row number of the matrix. The coefficients a , b , c , and f depend on location and time, because D , v , θ , ρ , S_T , and dY/dX vary with each layer and dY/dX varies with time.

Additional Remarks about the Numerical Solution of the ADE

It is well known that the numerical solution of the ADE is considerably more difficult than the solution of the heat equation (14). In fact, the numerical solution of the ADE might not be accurate due to numerical dispersion or because of numerical oscillations. These numerical oscillations occur especially around the solute front, whereas numerical dispersion occurs at low values of D when the advection term is dominant. By adjusting the increments of the grid system, some improvement can be achieved. Unfortunately, efforts to reduce numerical dispersion might increase numerical oscillations and vice versa. Huyakorn and Pinder (14) suggested keeping the Peclet number ($Pe=v\Delta x/D$) less than 2 and the Courant number ($Cr=v\Delta t/\Delta x$) less than 1. The latter condition is also referred to as the Courant-Friedrichs-Lewy stability criterion (24).

Excessive rounding errors, which lead to unstable numerical solutions, are avoided if the tridiagonal matrix, given by Eq.(23), is diagonally dominant (7), i.e., if for elements on the diagonal of the matrix the following holds:

$$|p_{ii}| \geq \sum_{\substack{j=1 \\ j \neq i}}^n |p_{ij}| \quad i=1,2,\dots,n \quad (30)$$

where p_{ij} is an element at row i and column j of the matrix. In our case, using a Crank-Nicolson scheme, this leads to the requirement that $|b_i| \geq |a_i| + |c_i|$. From the expressions provided in Appendix E, it is obvious that no excessive rounding error will occur in a homogeneous soil, regardless of the size of Δx and Δt . However, the values of Δx

and Δt are important to obtain an accurate numerical approximation of the differential equation.

As an illustration, we consider 1-D transport of a nonreactive solute in a homogeneous soil with a dimensionless initial concentration $X_i=0.05$. The ADE is solved numerically for a first-type or Dirichlet boundary condition at the inlet for different values of Δx and Δt . The soil properties, relevant for solute transport, used in this example and for all later examples, are listed in Appendix F. These properties were chosen somewhat arbitrarily. Although the units of the parameters are listed, any consistent set of units would do. In fact, one might prefer to state and solve the problem in dimensionless form.

Some results are presented in figure 3A, which shows numerical solutions employing three different space increments (0.05, 0.5, and 2.5 cm) and a constant time step (0.005 d), as well as the analytical solution (solid line). The three solutions are very similar for the selected values of D and v . As expected, some deviations from the analytical solution began to occur for $\Delta x=2.5$ when $Pe=2.5$ exceeded the recommended maximum of 2. Figure 3B contains results for various values of Δt and a constant Δx of 0.5 cm. The Courant condition is satisfied if $\Delta t < 0.01$ d. However, the results indicate that a smaller Δt is desirable; the numerical and the analytical solutions are almost identical when $\Delta t \leq 0.001$. Some deviations between analytical and numerical solutions occur at the outlet ($x=12$ cm), because of the use of a semi-infinite versus a finite length (Eq.(6-b) and Eq.(19-d), respectively). It should be noted that the Crank-Nicolson method is a

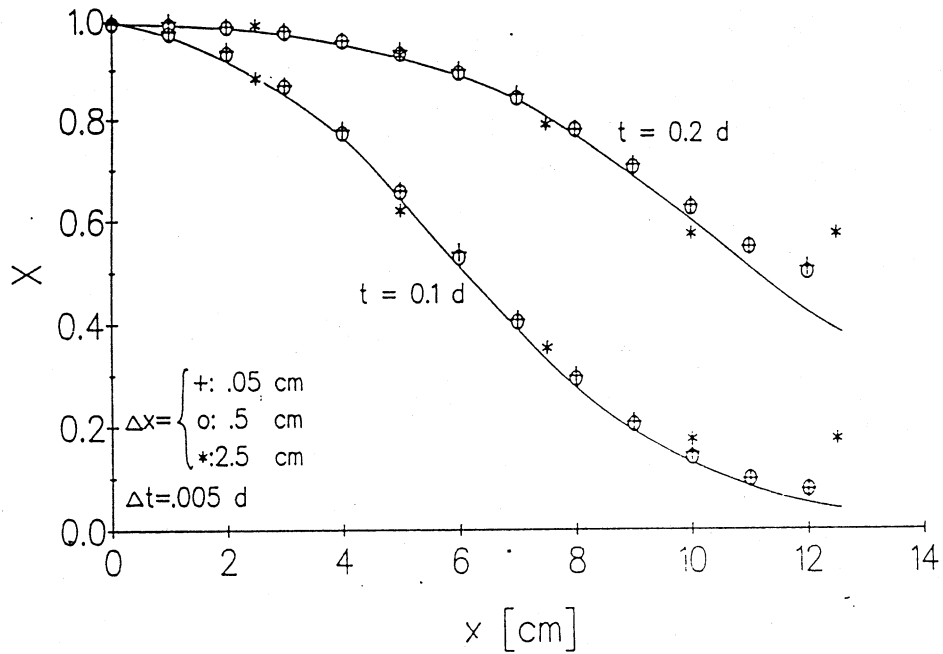


FIG.3A. The influence of the space step, Δx , on the numerical solution of the ADE. The solid lines are based on the analytical solution.

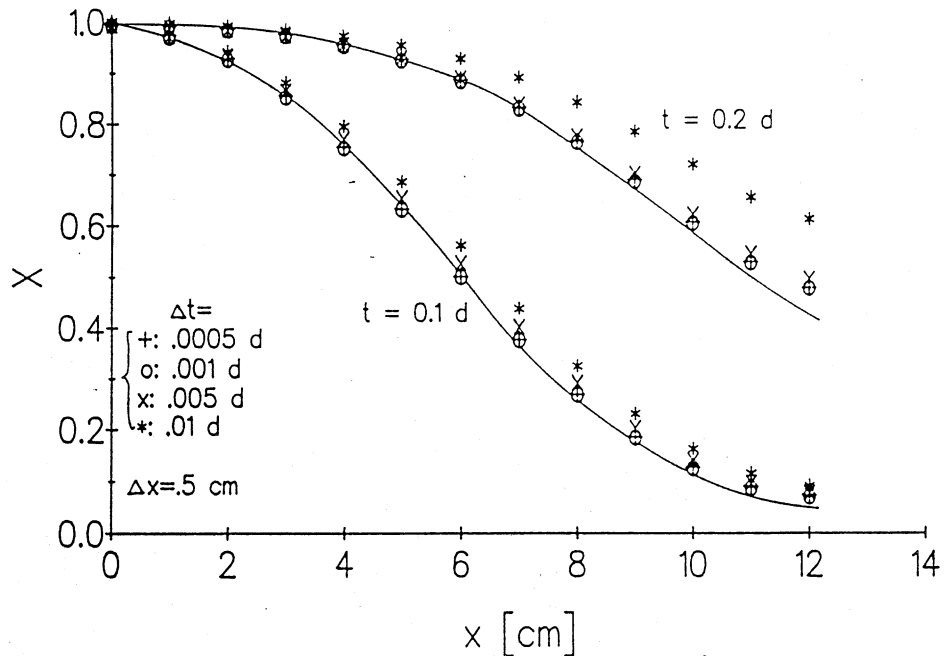


FIG.3B. The influence of the time step, Δt , on the numerical solution of the ADE. The solid lines are based on the analytical solution.

second-order method, which approximates the derivative of a function f according to:

$$f(x_0) = \frac{f(x_0+h)-f(x_0-h)}{2h} - \frac{h^2}{6} f^{(3)}(\xi) \quad \xi \in [x_0-h, x_0+h] \quad (31)$$

where $f^{(3)}$ is the third derivative of f . The last term of Eq.(31) represents the error term associated with this approximation. A higher order expansion leads to a reduction of the error.

Application of a higher order expansion for the time derivative might partly correct the problem of numerical dispersion (32). A simple example of reducing numerical dispersion by using a weighted expression for the time derivative was provided by Stone and Brian (29):

$$\frac{\partial X}{\partial t} = \frac{1}{6} \frac{X_{i+1}^{j+1} - X_{i+1}^j}{\Delta t} + \frac{2}{3} \frac{X_i^{j+1} - X_i^j}{\Delta t} + \frac{1}{6} \frac{X_{i-1}^{j+1} - X_{i-1}^j}{\Delta t} \quad (32)$$

The effect of numerical dispersion is demonstrated by assuming zero dispersion (figure 4). The results were obtained by using either Eq.(22) or a variation of Eq.(22) by substituting Eq.(32) for the $\frac{\partial X}{\partial t}$ term. The exact solution of the ADE resembles a step front ($D=0$ and $R=1$). Both numerical solutions compare poorly with the actual solute front, although the use of Eq.(32) leads to a somewhat steeper front. Numerous other techniques have been used to deal with this phenomenon (cf. 2).

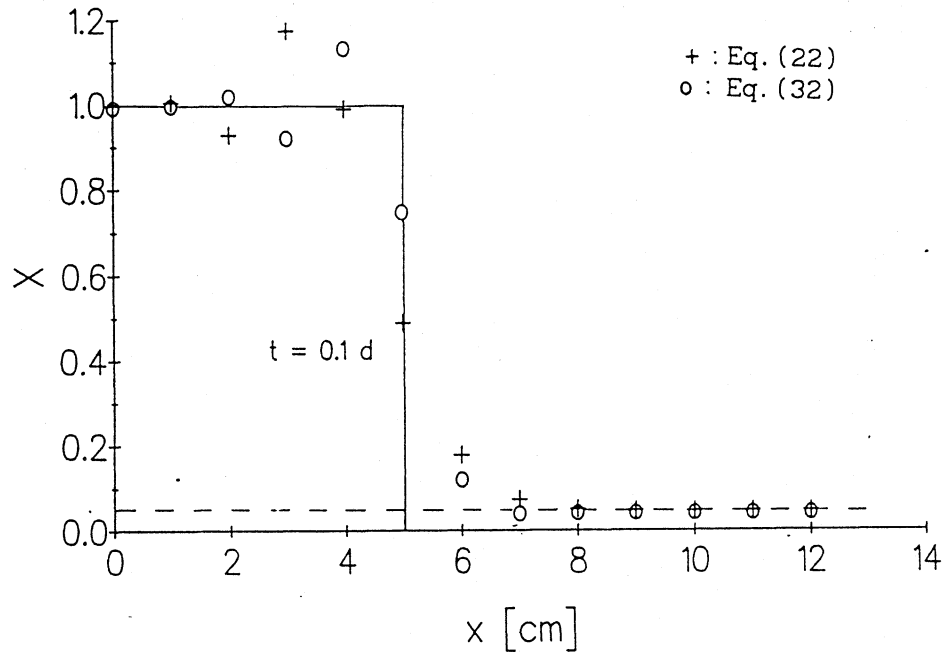


FIG. 4. Numerical solution of the ADE with zero dispersion using two different approximations for $\partial X/\partial t$ as presented in Eq.(22) and (32). The solid line represents the theoretical step front.

Besides comparison with analytical solutions, the accuracy of the numerical solution can also be evaluated with the help of a mass balance. We will do this by comparing the net influx of solute, denoted as FLUX [M], with the amount of solute which has accumulated in the column according to the numerical solution, denoted as ACC [M].

The net amount of solute which enters a hypothetical soil column during steady flow in a time interval $\Delta t = t_{j+1} - t_j$, is given by the following flux term:

$$\text{FLUX}_{j+1} = v\theta AC_T \int_{t_j}^{t_{j+1}} \left\{ X(x,t) \Big|_{x \uparrow 0} - X(x,t) \Big|_{x \downarrow L} \right\} dt \quad (33)$$

where A is the area of the column perpendicular to the direction of flow [L²]. The net amount of solute which has accumulated in the column during this period of time is given by:

$$\text{ACC}_{j+1} = A \int_0^L \left\{ \theta C_T [X(x, t_{j+1}) - X(x, t_j)] + \rho S_T [Y(x, t_{j+1}) - Y(x, t_j)] \right\} dx \quad (34)$$

where L is the length of the column in the direction of flow [L], and $X(x, t_j)$ and $Y(x, t_j)$ denote the dimensionless solute concentrations in liquid and adsorbed phase, respectively. $X(x, t_j)$ can be determined mathematically or experimentally. Because of the continuity principle, the net accumulation should be equal to the net influx. This provided a useful tool to check the accuracy of the numerically determined $X(x_i, t_{j+1})$.

Denoting the solute concentration of the eluent solution as X_{in} , Eq. (33) was approximated as:

$$\text{FLUX}_{j+1} \cong Av\theta C_T \left[(X_{in} - \frac{1}{2}(X_n^j + X_n^{j+1})) \right] \Delta t \quad (35-a)$$

$$X_{in} = \begin{cases} X_o & 0 < t < t_o \\ 0 & \text{elsewhere} \end{cases} \quad (35-b)$$

where t_o is finite for pulse displacement and infinite for step displacement. The integration to obtain the accumulation term is performed by using the trapezoidal rule, which is convenient to use for transport in layered media.

Two mass balance equations were used, viz. a relative mass balance (RMB) over the time interval $[t_j, t_{j+1}]$ and an overall relative mass balance (ORMB) over the interval $[0, t_{j+1}]$. The error criterion based on the first balance is defined as:

$$\text{RMB}_{j+1} = \left\{ \left| \text{FLUX}_{j+1} - \text{ACC}_{j+1} \right| / \text{ACC}_{j+1} \right\} * 100\% \quad (36)$$

To determine the mass balance over the whole time period, t_{j+1} , the amount of solute present at $t=0$ is subtracted from the amount present at t_{j+1} to yield the overall term SUMACC_{j+1} . The total net supply of solute to the column, SUMFLU_{j+1} , and the overall mass balance are respectively defined as:

$$\text{SUMFLU}_{j+1} = \sum_{j=1}^{j+1} \text{FLUX}_j \quad (37-a)$$

and:

$$\text{ORMB}_{j+1} = \left\{ \left| \text{SUMFLU}_{j+1} - \text{SUMACC}_{j+1} \right| / \text{SUMACC}_{j+1} \right\} * 100\% \quad (37-b)$$

As stated before, the accuracy of the numerical solution depends on the size of the space and time increments, but also on the number of calculations (rounding error). The question then arises, concerning what the appropriate sizes of Δx and Δt should be to obtain an accurate solution using a minimum number of calculations.

The value for Δt during the calculations was optimized with the help of the overall relative mass balance criterion. Two bounds on ORMB were used, namely a lower bound of 0.5% and an upper bound of 3%. The value of Δt for the next time t_{j+1} was increased in case $\text{ORMB} < 0.5\%$ and

decreased when $ORMB > 3\%$. A numerical scheme which adjusts both Δx and Δt to solve the 1-D flow problem was reported by Dane and Mathis (12).

At this point we refer to Appendix G, which contains listings of various WATFIV programs of numerical solutions used in this study. The programs HOMSOIL and VARTIM calculate solute concentrations in homogeneous media with a fixed and a variable time step, respectively. Transport in layered media was solved with the programs LAY1 and LAY3 for a first- and third-type condition, respectively, with a fixed time step. The program LAY1 was modified to solve the ADE for a second-type interface condition (i.e., LAY2). The various parameters for each problem are specified in the declaration section of the program. The value of the retardation coefficient was determined with the subroutine EXCHAN and the amount of adsorbed solute with the routine ADSORB. Subroutine TRIDIA contains the Thomas algorithm to solve the dimensionless liquid concentrations. For most problems, a fixed time step was used, and values for ORMB were generally less than 1%, depending on the type of problem.

RESULTS AND DISCUSSION

The first section of this chapter compares some of the analytical and numerical solutions for layered with solutions for nonlayered media. Furthermore, concentration profiles for layered media were investigated with analytical solutions using a first- or a third-type condition at the inlet of each layer. In the remaining sections we will use only a third-type condition at the inlet of the soil and a second- or third-type condition at the interface of soil layers (Appendix E).

Some basic effects of nonlinear exchange on solute transport will be demonstrated for pulse and step input in the second section. The third section discusses the effect of layers, with different values for their transport parameters, on the transport of a solute pulse, along with two different scenarios of reducing contaminant movement in a soil profile for a step input. Most numerical values of the parameters were chosen for illustrative purposes. All relevant values are listed in Appendix F.

Numerical and Analytical Results for Transport
of a Nonreactive Solute

We start by examining the influence of the inlet boundary condition on the mass balance. Numerical solutions of the ADE for a first- and a third-type condition, obtained with the program HOMSOIL, are presented in figure 5A and 5B, respectively. The values for Δt and Δx were 0.005 d and 0.5 cm, respectively. These values were also used for all later calculations, unless specified otherwise. Included in figure 5A and 5B are values of RMB and ORMB. For a third-type condition, $X(0,t)$ gradually approaches X_0 (figure 5B), whereas for the first-type condition, $X(0,t)$ is instantly equal to X_0 (figure 5A). In the latter case, too much solute is forced into the column, resulting in a significant overall mass balance error, particularly at the early stage. In contrast, the third-type condition preserved mass. The mass balance criterion to determine the value of a variable Δt can therefore not be used for a first-type condition. Using a variable time step for a third-type condition resulted in a CPU time which was one fifth of

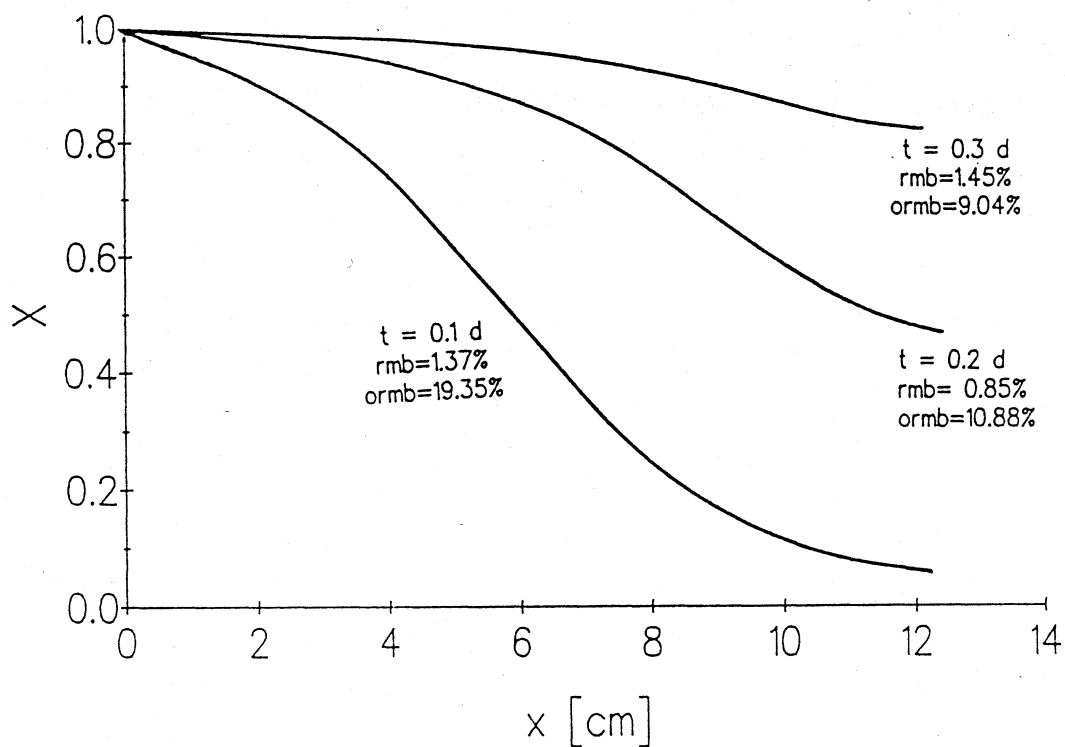


FIG.5A. Numerical solution of the ADE for a homogeneous soil using a first-type condition.

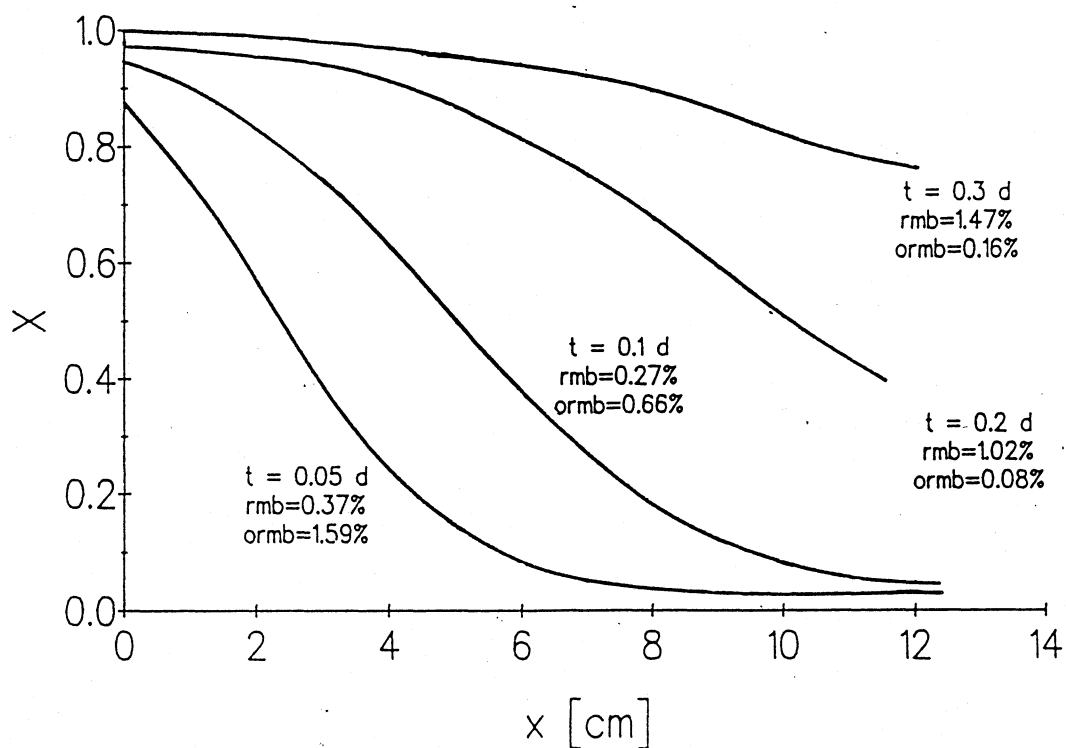


FIG.5B. Numerical solution of the ADE for a homogeneous soil using a third-type condition.

the CPU time for a fixed time step (0.005 d). The value for ORMB varied during the calculations, but was well below 1% for both schemes (HOMSOIL and VARTIM), except during the very early stages of simulation.

Next, we considered transport in a two-layer medium, with the interface at $x=6$ cm. One way of validating the analytical and numerical solutions for this problem is to use the same parameter values for both layers and compare the solution to the one for a homogeneous medium. The analytical solutions according to Eq.(11) and (12) are shown in figure 6A (first-type condition) and 6B (third-type condition), respectively, along with the solutions for a homogeneous medium (Eq.(7) and (8), respectively). Figure 7A, 7B, and 7C show the results obtained with LAY1, LAY3, and LAY2, respectively, as well as the results obtained with HOMSOIL (solid lines). The results indicate close agreement between the solutions for the "homogeneous" and the "two-layer" media.

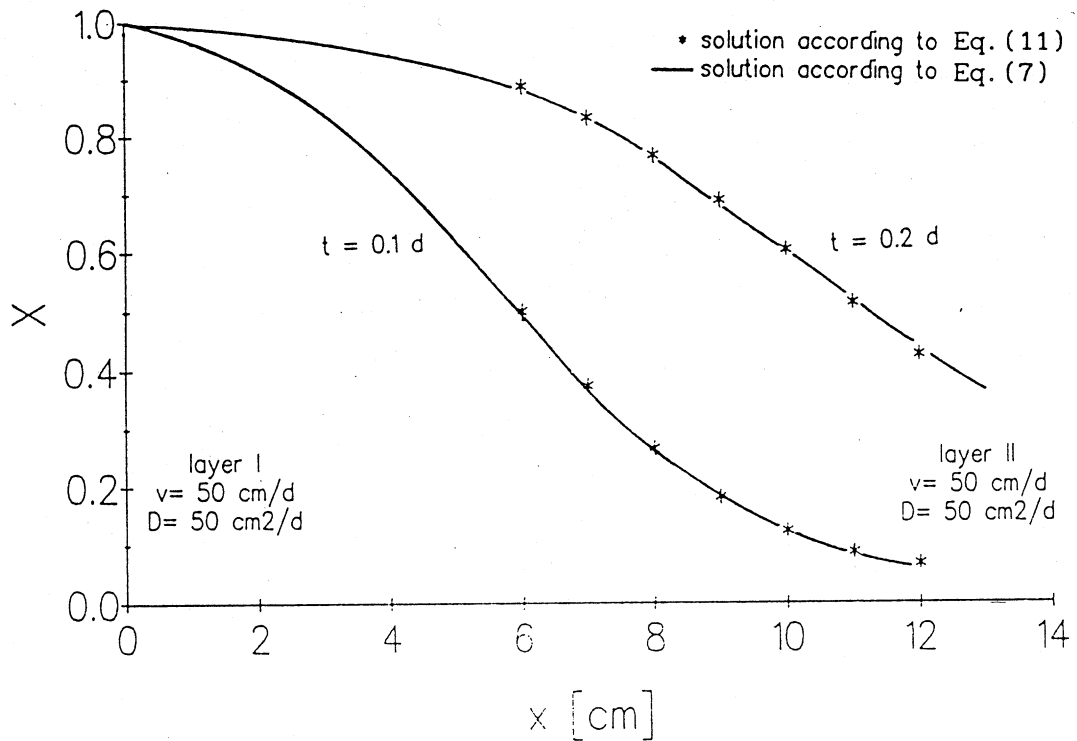


FIG.6A. Validation of the analytical solution of the ADE for a two-layer medium using a first-type condition.

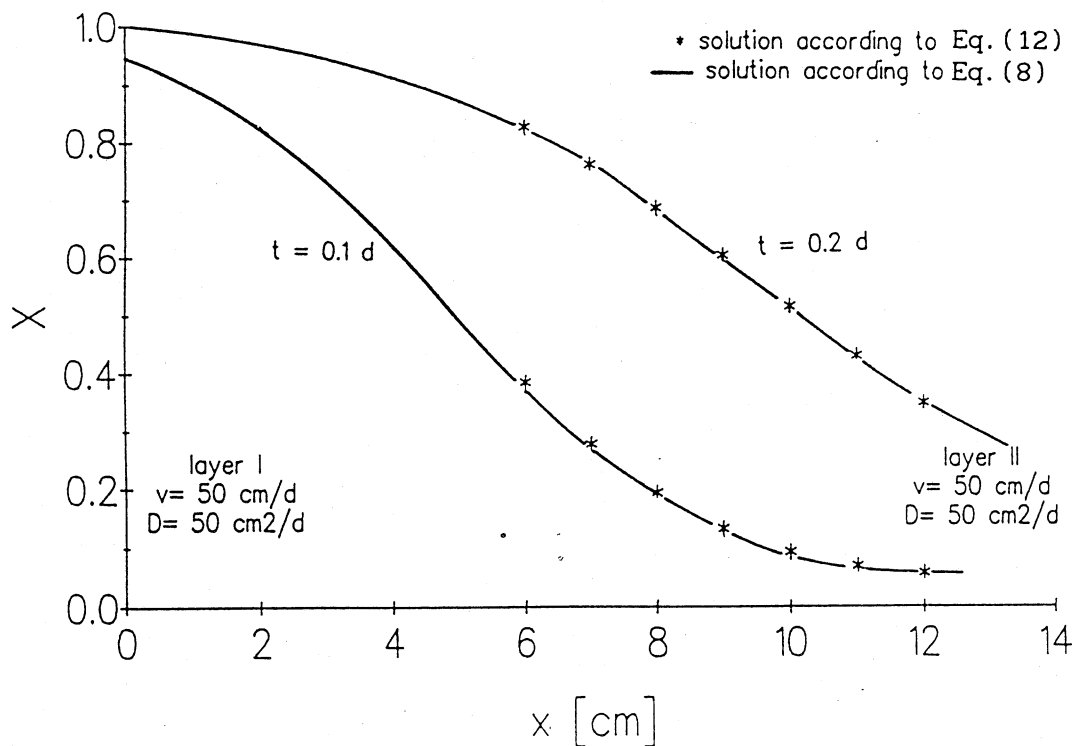


FIG.6B. Validation of the analytical solution of the ADE for a two-layer medium using a third-type condition.

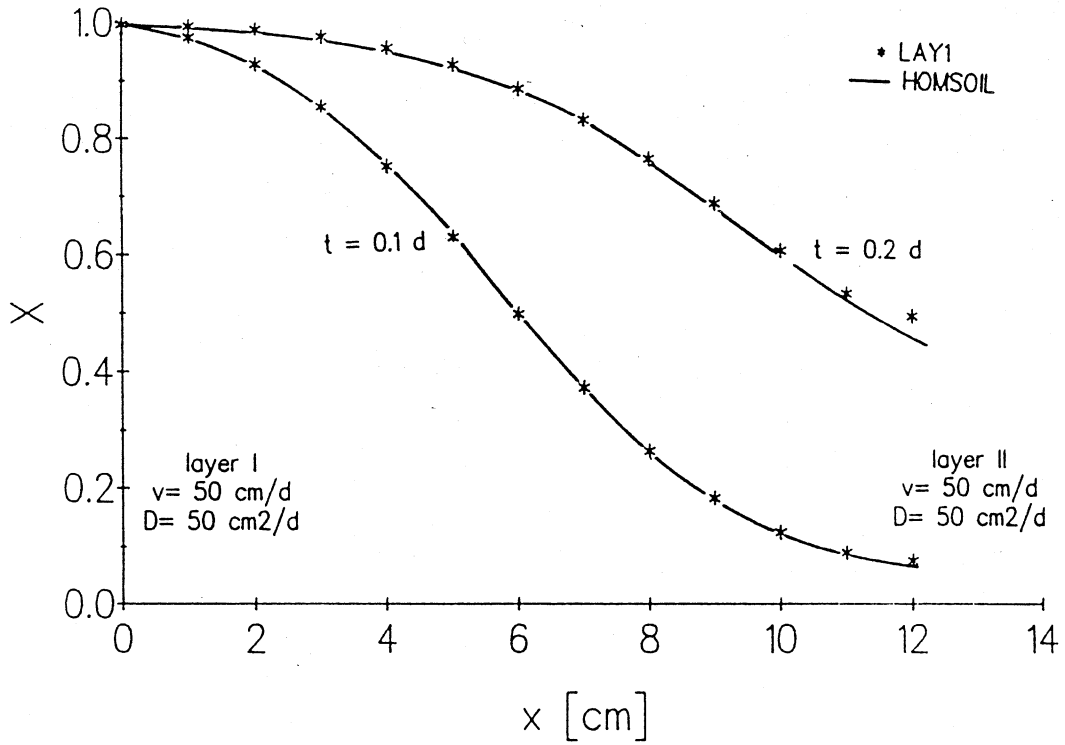


FIG. 7A. Validation of the numerical solution of the ADE for a two-layer medium using a first-type condition.

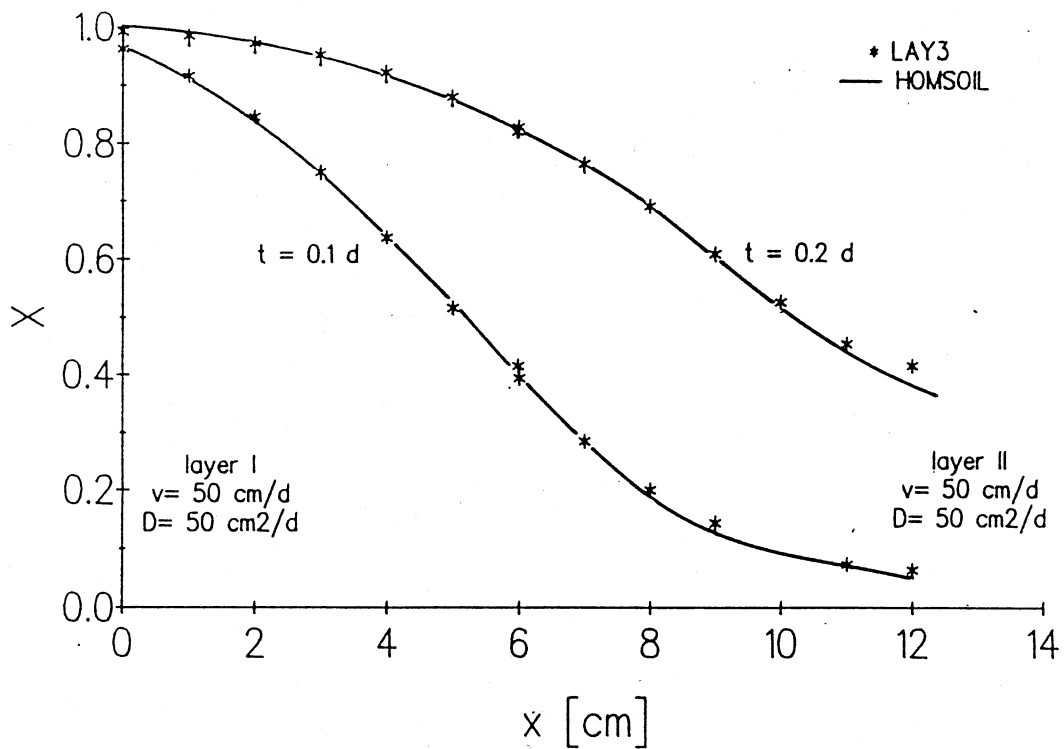


FIG. 7B. Validation of the numerical solution of the ADE for a two-layer medium using a third-type condition.

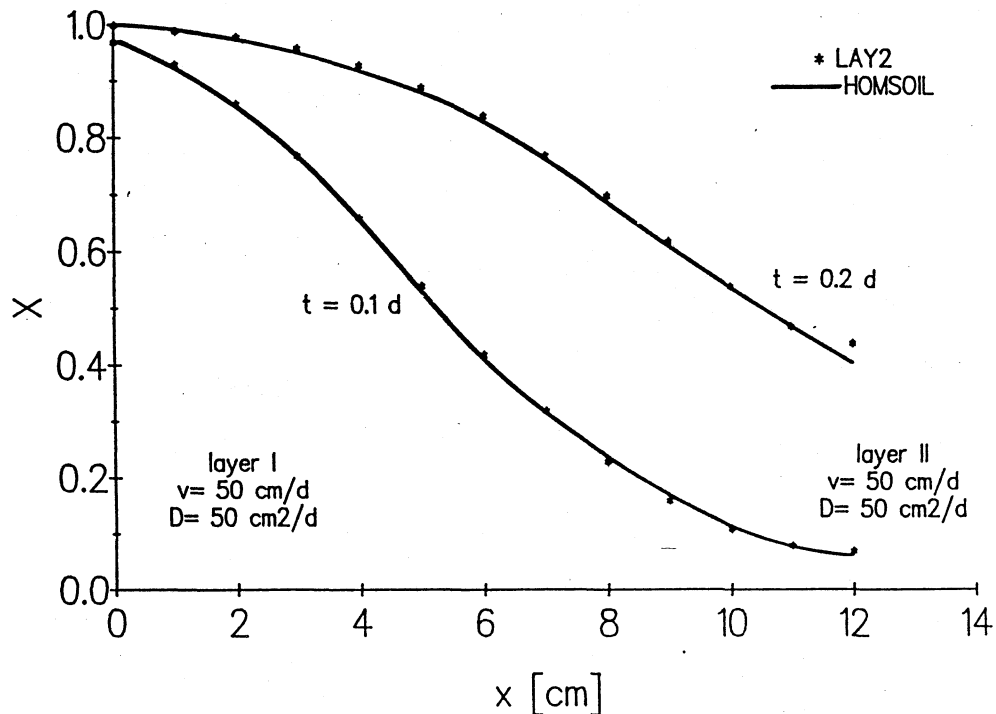


FIG.7C. Validation of the numerical solution of the ADE for a two-layer medium using a third-type condition at the inlet and a second-type condition at the interface.

Transport during steady flow in a two-layer medium was investigated for a medium with $v_1 = 25$ cm/d, $D_1 = 12.5$ cm²/d, and $\theta_1 = 0.4$ (i.e., the first layer parameter values), and $v_2 = 100$ cm/d, $D_2 = 100$ cm²/d, and $\theta_2 = 0.1$. Figure 8 shows the numerically calculated concentration profiles for a first-, third-, and second-type condition at the interface (VWC denotes θ). Because the D value is smaller in the first layer, the solute front in the first layer is steeper than in the second layer. The concentration profiles obtained with a second- and a third-type condition are very similar except at the interface. The use of a third-type condition results in a discontinuity of the (resident) concentration, whereas the profile is continuous for a second-type

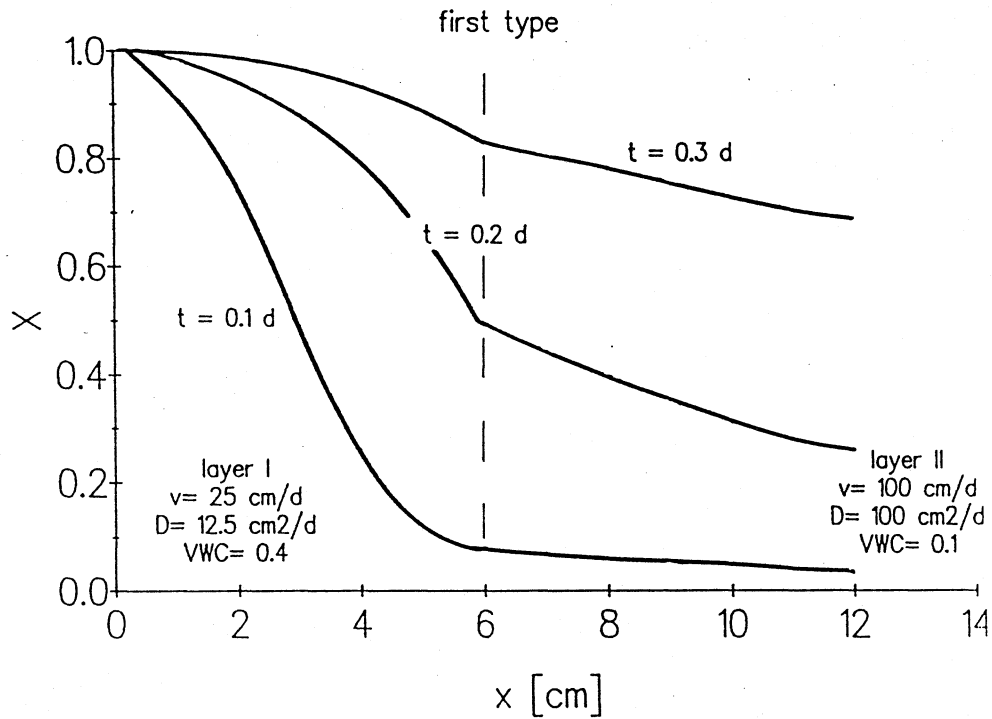


FIG.8A. Numerical solution of the ADE for a two-layer medium ($D_1 < D_2$, $v_1 < v_2$) using a first-type condition.

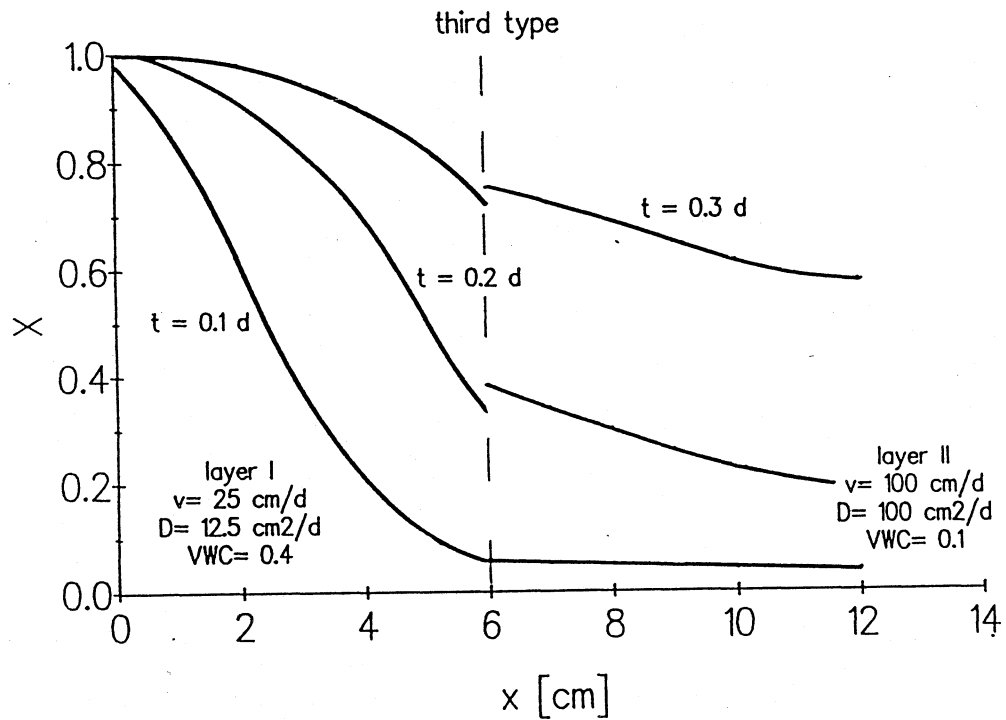


FIG.8B. Numerical solution of the ADE for a two-layer medium ($D_1 < D_2$, $v_1 < v_2$) using a third-type condition.

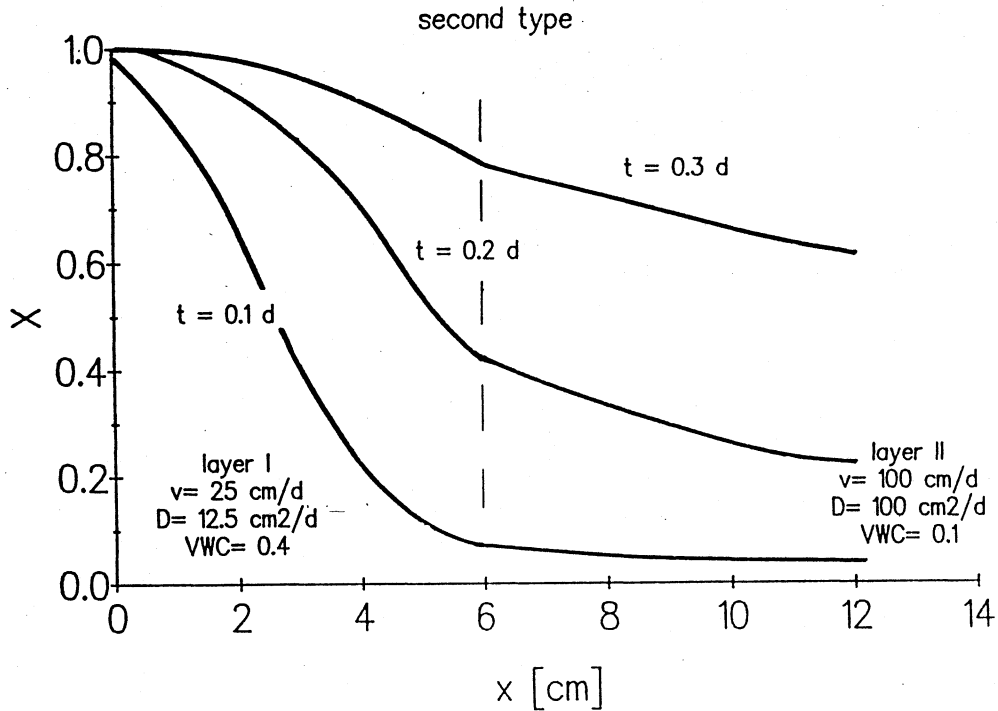


FIG. 8C. Numerical solution of the ADE for a two-layer medium ($D_1 < D_2$, $v_1 < v_2$) using a third-type condition at the inlet and a second¹-type condition at the interface.

condition. For a third-type condition, the concentration increased with position across the interface. Note that in both cases the flux and the flux-averaged concentration are continuous at the interface. Figure 9 contains the results if the layers are interchanged. The concentration profiles are now steeper in the second layer, because of the small D -value compared to the first layer. For a third-type condition, the (resident) concentration decreased across the interface.

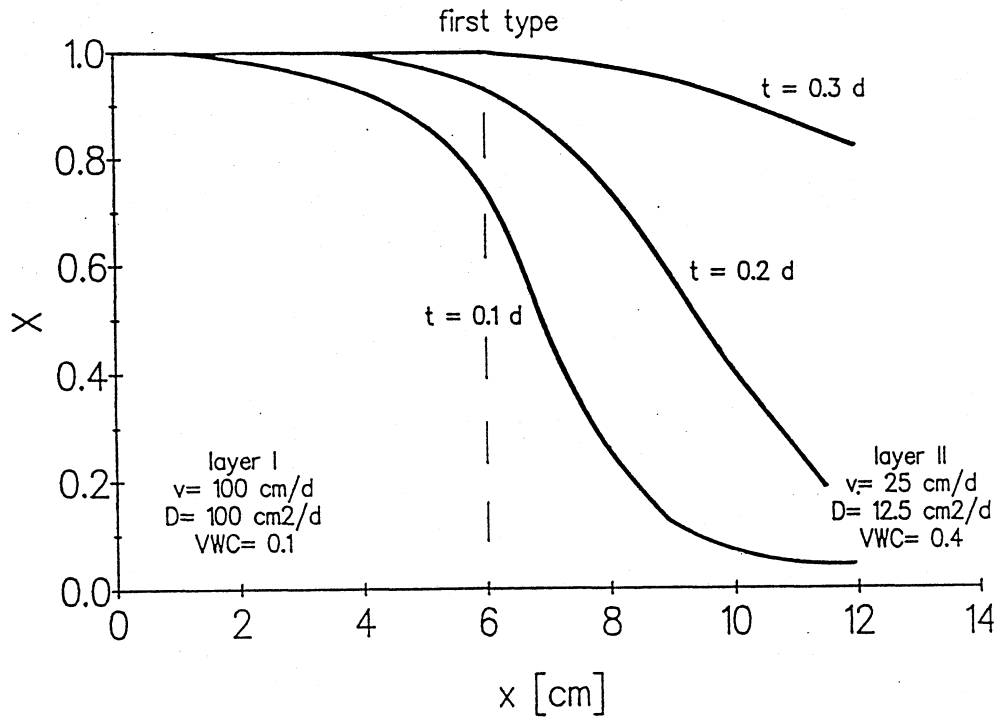


FIG.9A. Numerical solution of the ADE for a two-layer medium ($D_1 > D_2$, $v_1 > v_2$) using a first-type condition.

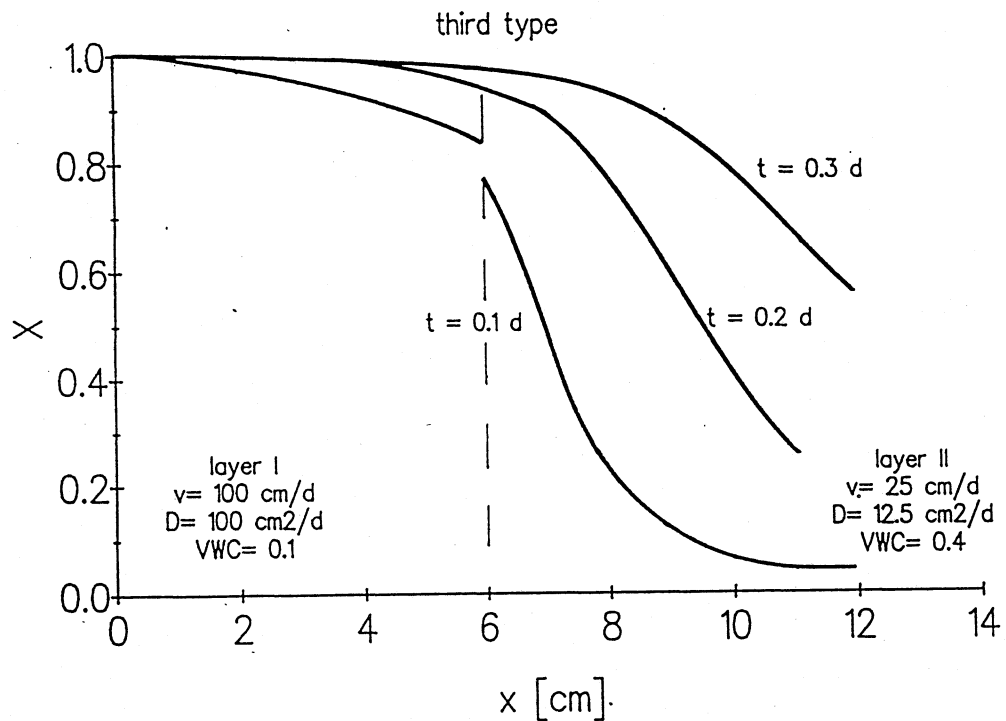


FIG.9B. Numerical solution of the ADE for a two-layer medium ($D_1 > D_2$, $v_1 > v_2$) using a third-type condition.

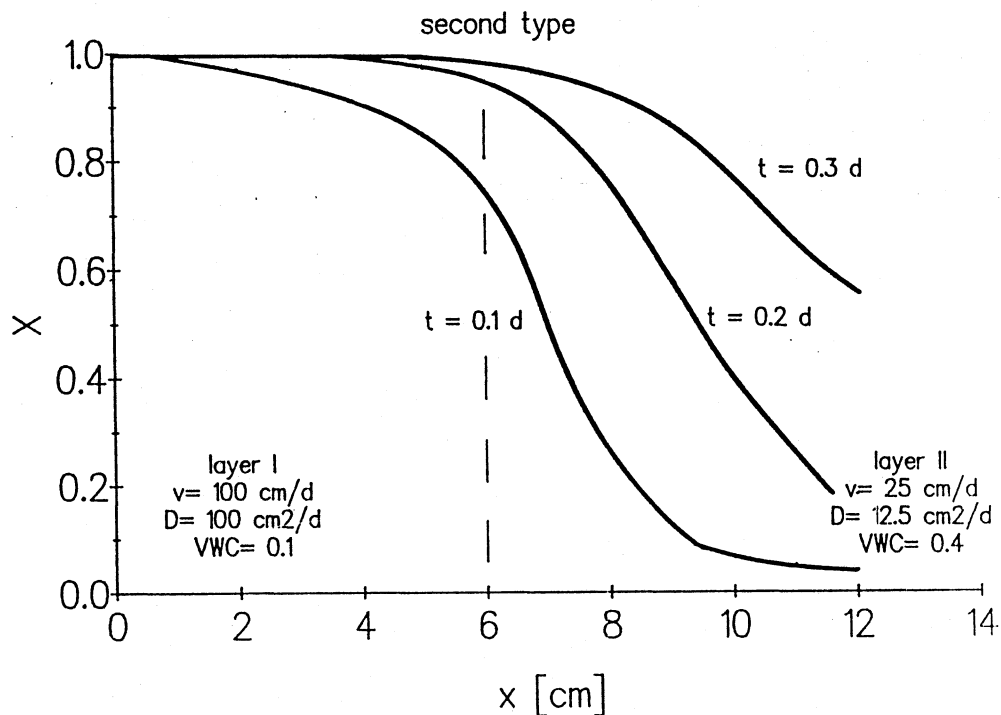


FIG.9C. Numerical solution of the ADE for a two-layer medium ($D_1 > D_2$, $v_1 > v_2$) using a first-type condition at the inlet and a second-type at the interface.

We investigated the influence of different parameter values further by using analytical solutions. First we examined the influence of dispersion, using somewhat artificially large differences in D -values. In figure 10, the D -value in the first layer is smaller than in the second layer, whereas in figure 11 the D -values are interchanged. The error in the mass balance can be evaluated by comparing the first-type solution (figure 10A and 11A) with the third-type solution (figure 10B and 11B). For a layered medium, the repeated application of the first-type condition leads to an increase in the mass balance error of the solution compared to a homogeneous medium (cf. figure 5). For a third-type condition, a discontinuity in

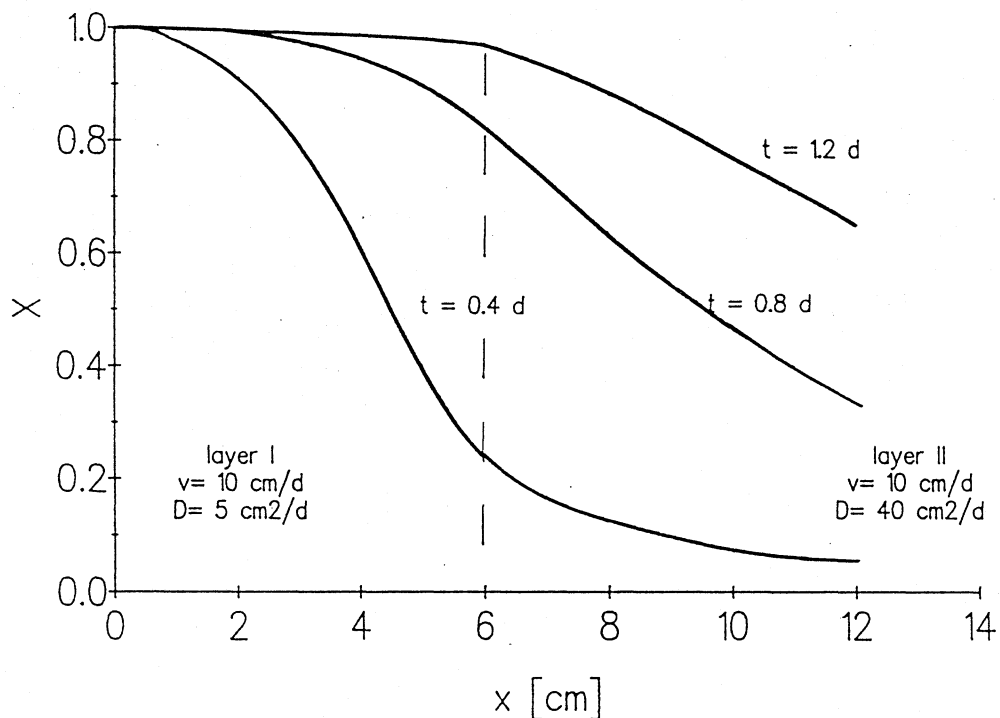


FIG.10A. Analytical solution of the ADE for a two-layer medium ($D_1 < D_2$, $v_1 = v_2$) using a first-type condition.

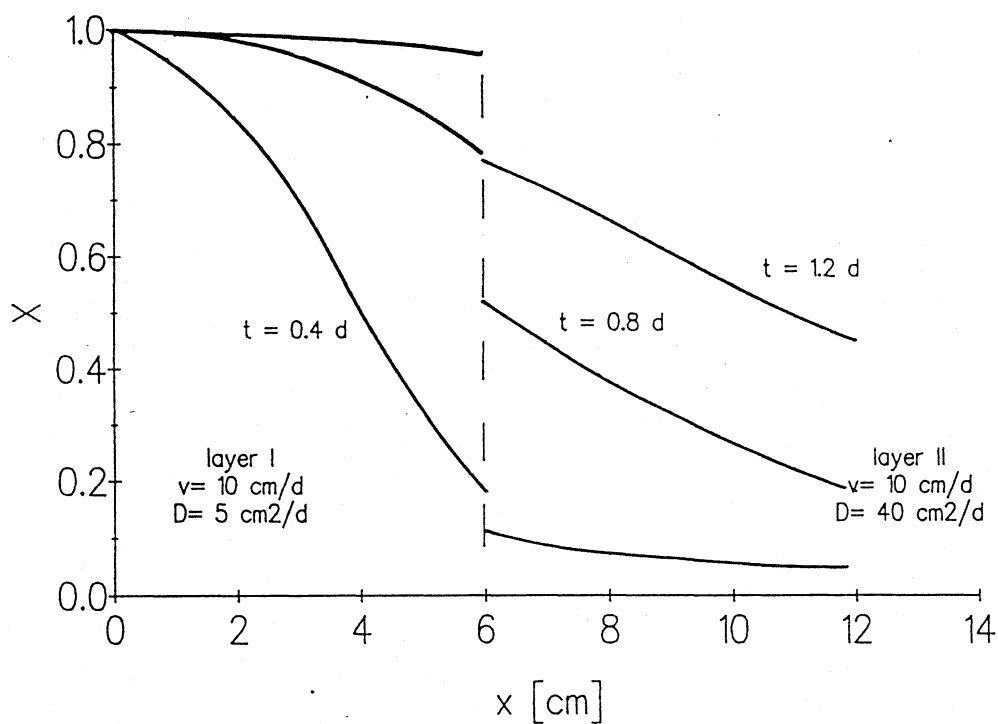


FIG.10B. Analytical solution of the ADE for a two-layer medium ($D_1 < D_2$, $v_1 = v_2$) using a third-type condition.

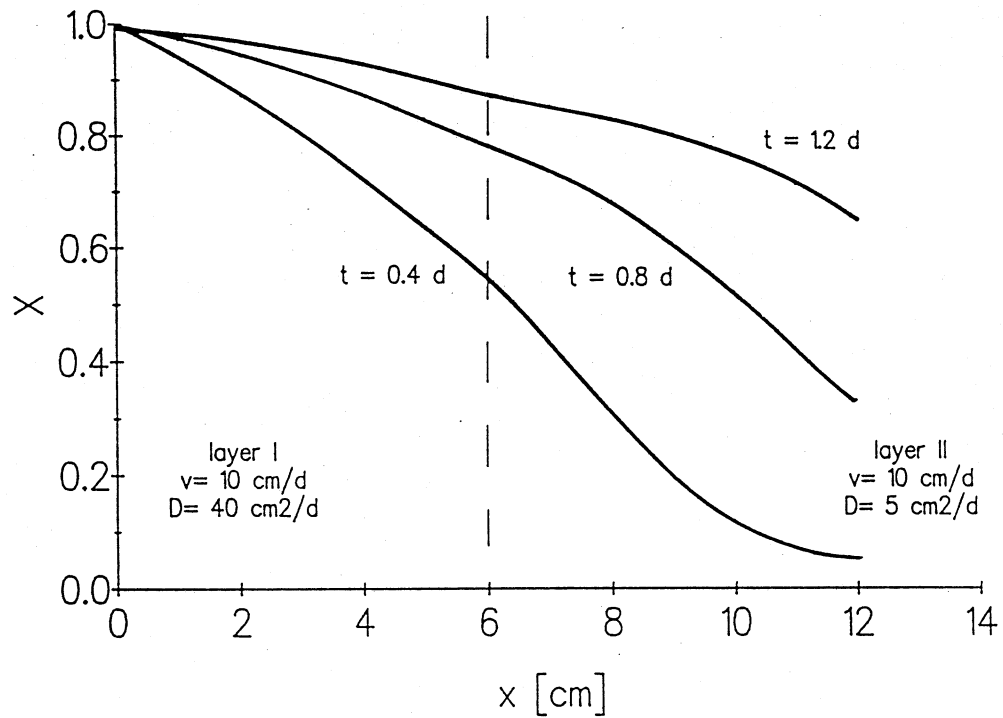


FIG. 11A. Analytical solution of the ADE for a two-layer medium ($D_1 > D_2$, $v_1 = v_2$) using a first-type condition.

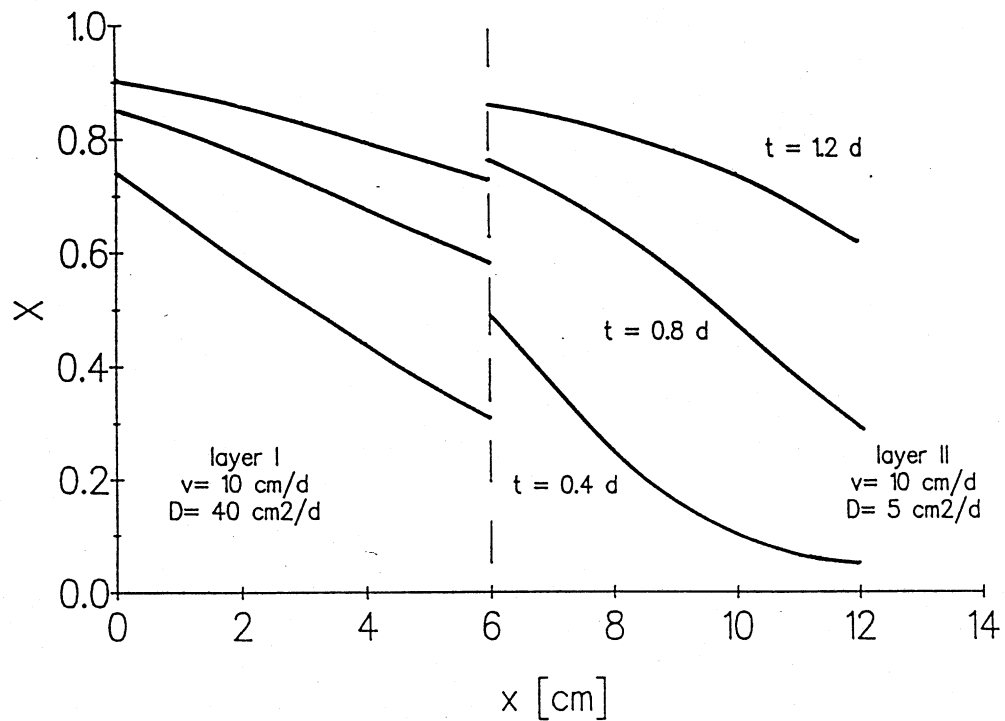


FIG. 11B. Analytical solution of the ADE for a two-layer medium ($D_1 > D_2$, $v_1 = v_2$) using a third-type condition.

concentration can be observed at the interface. This discontinuity is similar to the one at the inlet where flux-averaged concentrations, rather than resident concentrations, are continuous. During heat transport in composite media, a similar discontinuity arises if there is a contact resistance. Heat flow across the interface is then described with a 'radiation' boundary condition using a heat transfer coefficient.

Next, we investigated the influence of differences in v -values on the concentration profile for steady-state flow. In figure 12, the pore-water velocity is smaller in the first than in the second layer. Figure 13 shows the concentration profiles if the layers are interchanged. The solute front is steeper in the low velocity layer. For a third-type condition, the concentration is lower in the low velocity layer than in the high velocity layer at the interface. The values of the advective and dispersive fluxes are, respectively, lower and higher in the low velocity layer than in the high velocity layer because of the differences in θ . We note again that the flux-averaged concentration is continuous at the interface.

From these examples it can be concluded that the use of a first-type condition leads to large mass balance errors in layered media. For a third-type condition, the discontinuity of the resident concentration at the interface depends both on the differences in v and D . If these differences are not too large, the analytical solution using a third-type condition gives a good approximation of the actual concentration profile. The latter can be obtained by assuming that both concentration and flux are continuous at the interface (cf. figures 8B and 8C and figures 9B and 9C).

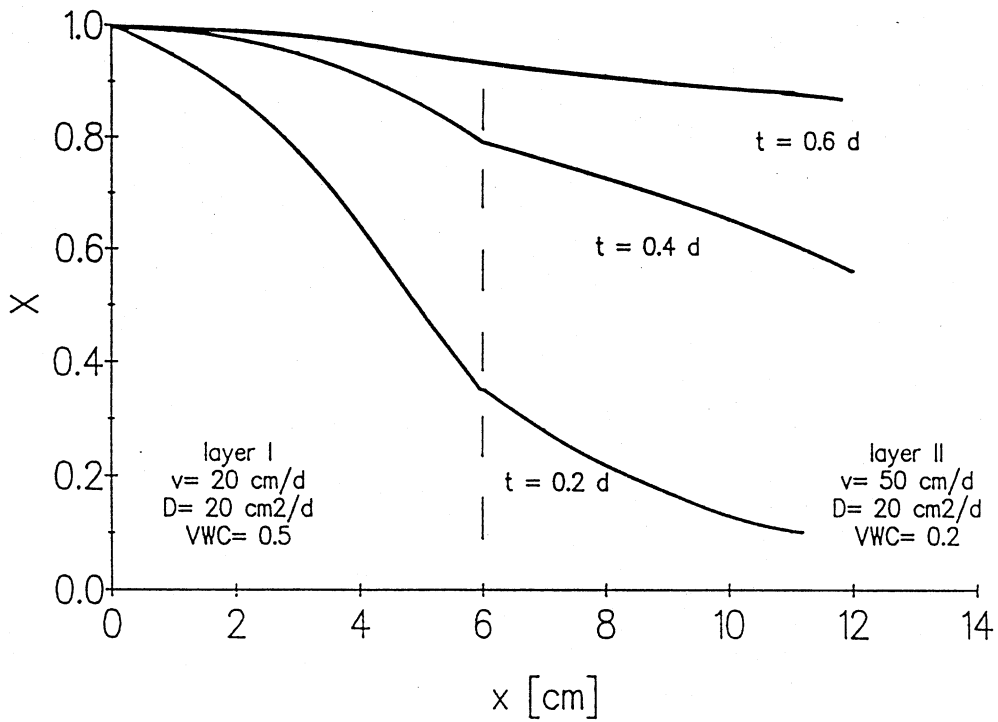


FIG.12A. Analytical solution of the ADE for a two-layer medium ($D_1 = D_2$, $v_1 < v_2$) using a first-type condition.

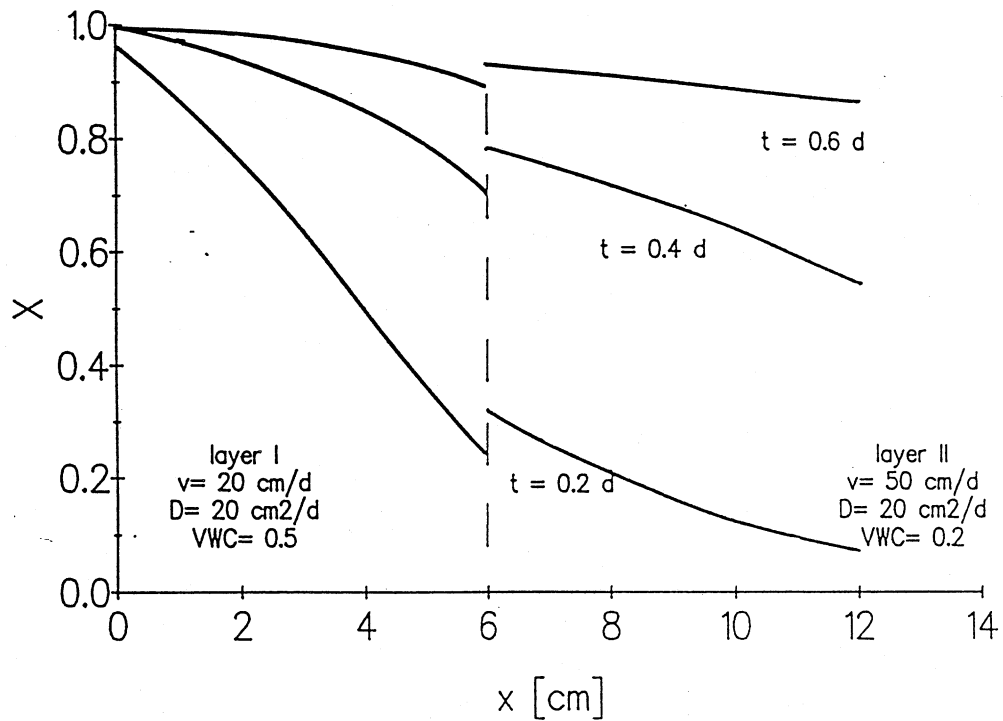


FIG.12B. Analytical solution of the ADE for a two-layer medium ($D_1 = D_2$, $v_1 < v_2$) using a third-type condition.

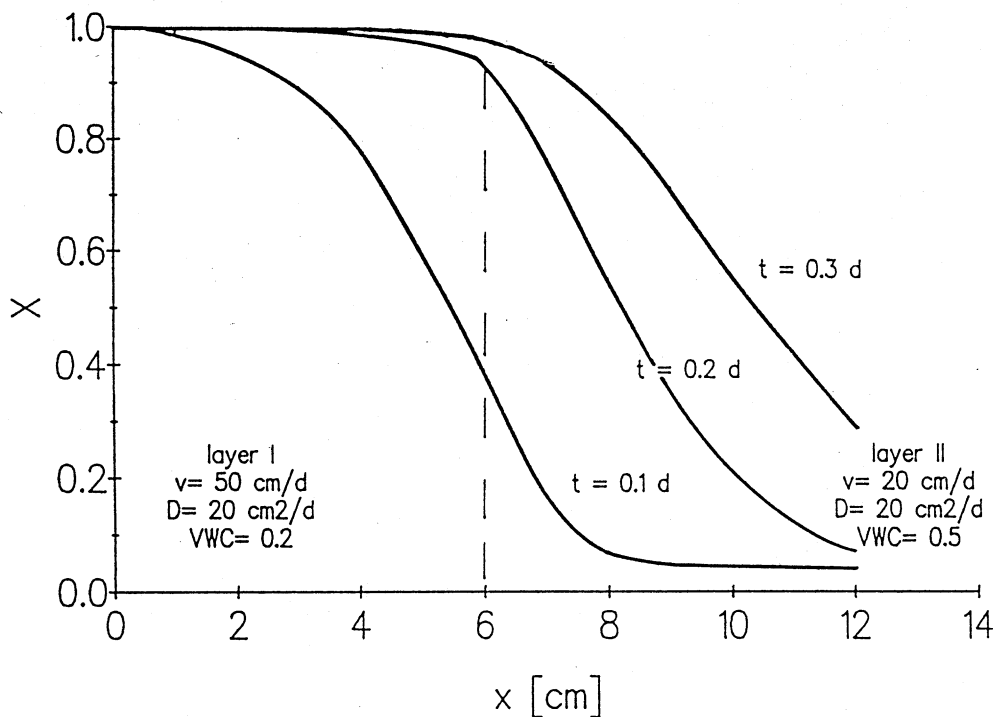


FIG.13A. Analytical solution of the ADE for a two-layer medium ($D_1=D_2$, $v_1>v_2$) using a first-type condition.

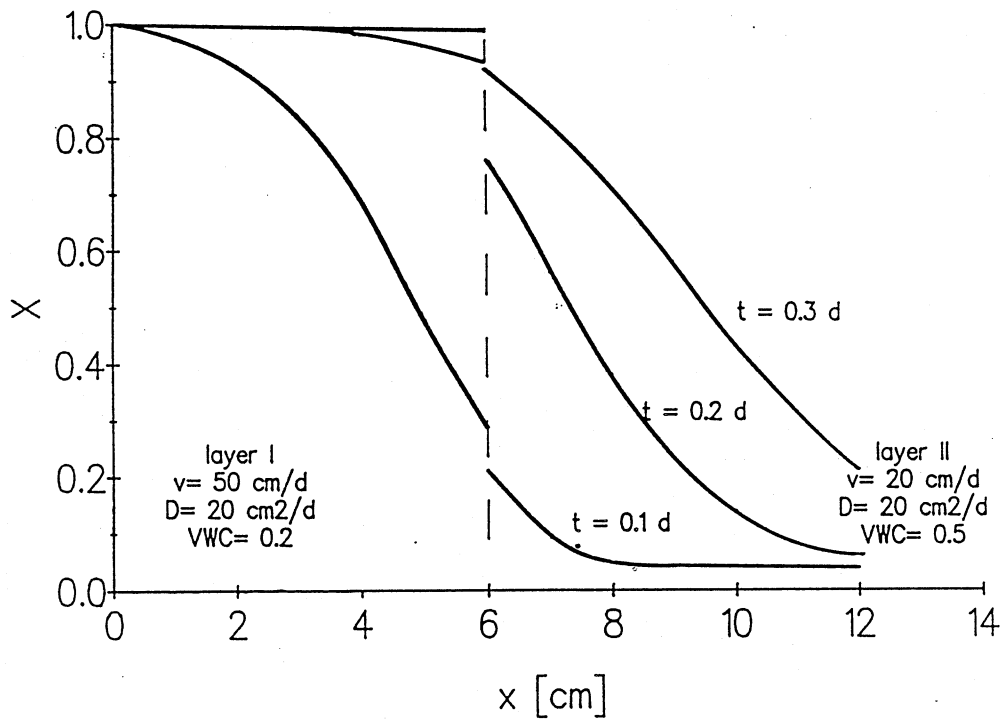


FIG.13B. Analytical solution of the ADE for a two-layer medium ($D_1=D_2$, $v_1>v_2$) using a third-type condition.

The Effect of Nonlinear Exchange on Solute Transport

Reactions between the porous medium and the solute can have a strong impact on the transport of a solute. The only reaction considered here was ion exchange in a binary system. However, other processes or systems could be combined as well with expressions like Eq. (13).

For the purpose of comparison, we considered first the case of linearly exchanging solutes. The relevant parameter values and the type of inlet conditions are given in Appendix F. An arbitrary soil ($S_T=10$ cmol_c/kg, $\rho=1.5$ g/cm³, $\theta=0.4$ cm³/cm³) is saturated with a 0.005 M CaBr₂ solution which is displaced with a 0.01 M KCl solution. The K movement, assuming linear equilibrium exchange between Ca and K, is described using $R=38.5$. The Cl displacement can be described using $R=1$, if neither anion reacts with the soil. The profiles for Cl and K were obtained with an adapted version of Eq. (8) by substituting v^* for v and D^* for D and are shown in figure 14A and 14B, respectively. Although this situation is somewhat idealized, it is clear that the ability of the soil to adsorb the incoming cation greatly increases its travel time through the soil.

In many instances the exchange is not governed by a linear but by a nonlinear exchange isotherm. Therefore, transport of nonlinearly exchanging solutes will be examined for a binary system. Two cases can be distinguished, viz. preferential adsorption of the incoming cation (favorable exchange) or of the resident cation (unfavorable exchange). The shapes of the respective dimensionless exchange curves are convex

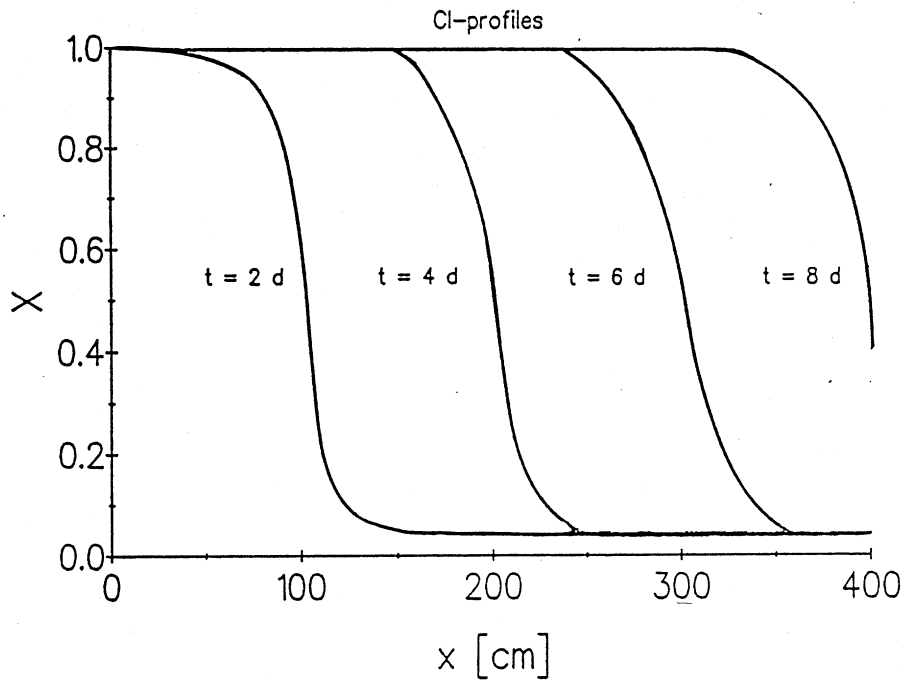


FIG.14A. The effect of front retardation on transport. Analytical solution of the ADE using $R=1$.

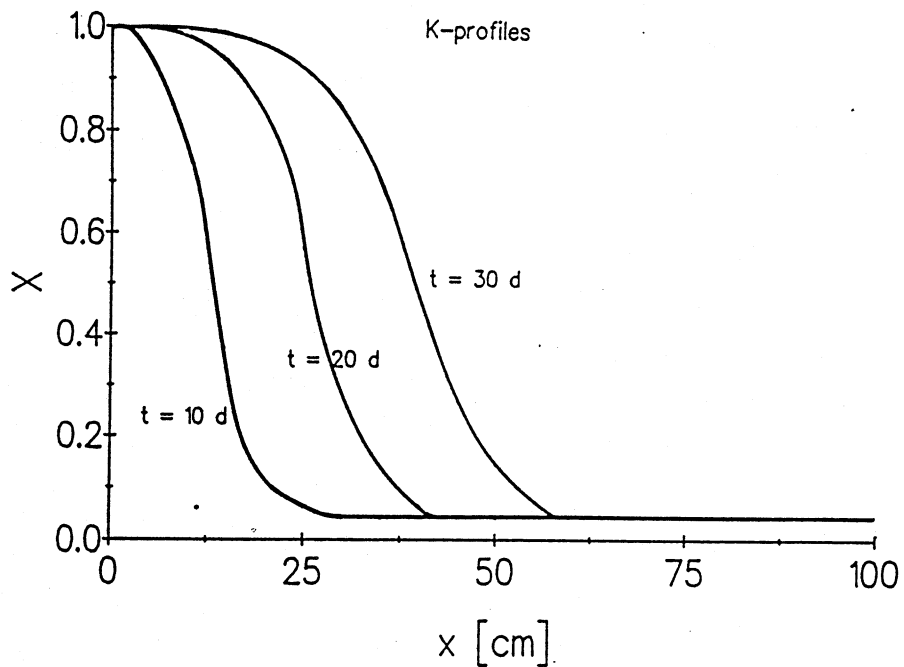


FIG.14B. The effect of front retardation on transport. Analytical solution of the ADE using $R=38.5$.

and concave. A series of simple examples is provided to illustrate how ion exchange influences the transport of solutes. Although complete exchange rarely occurs, usually more than two species participate in the exchange process, and S_T and C_T are not necessarily constant; the illustrations are representative of the exchange behavior expected.

A number of authors have discussed nonlinear exchange during transport. Bolt (5) provided analytical solutions for nonlinear exchange. Lai and Jurinak (17) obtained numerical solutions using an explicit finite difference method. Concentration profiles for unfavorable, linear and favorable exchange are shown in figure 15. The arbitrary exchange isotherms and initial concentration profiles are included as well. All parameter values, as well as the $Y(X)$ -relationships, are given in Appendix F. Because of the choice of an initial value for $X > 0$, a substantial amount of (adsorbed) solute was already present at $t=0$. For the soil with unfavorable exchange, the adsorbed concentration was less than the solution concentration (figure 15A), for linear exchange the two were equal (figure 15B), and for favorable exchange the adsorbed concentration was greater than the solute concentration. It should be noted that Bruggenwert and Kamphorst (6) provided an extensive survey of exchange data which might serve as a guideline for many soil systems where solute transport needs to be modeled. Examining the profile at $t=2$ d, it can be concluded, as was shown by Bolt (5) and Valocchi et al. (30), that favorable exchange (figure 15C) tends to steepen the solute front (counteracts spreading) and nonfavorable exchange flattens the solute front (enhances

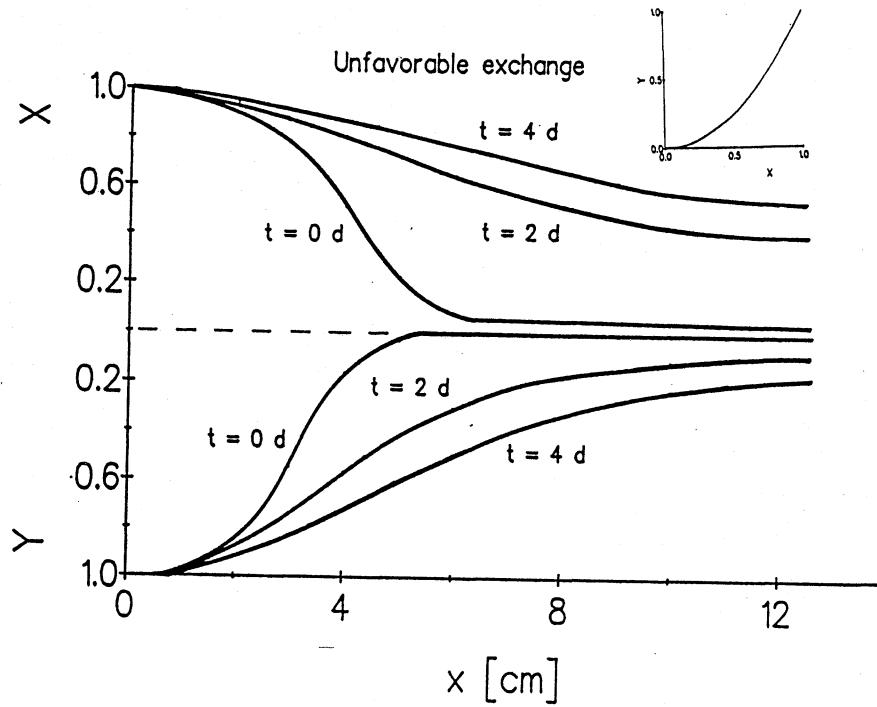


FIG.15A. The effect of nonlinear exchange on transport. Numerical solution of the ADE for unfavorable exchange.

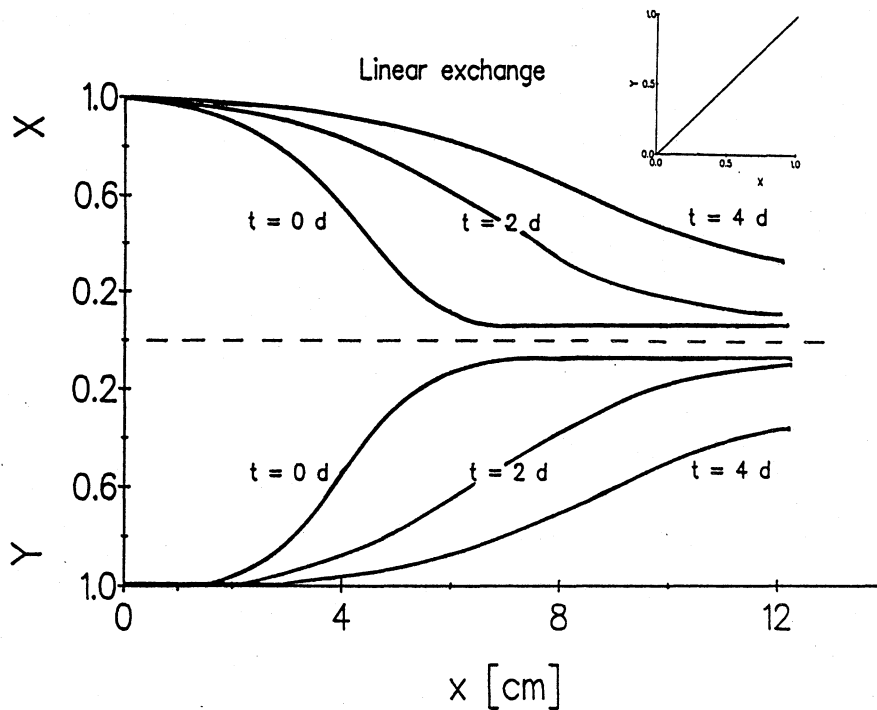


FIG.15B. The effect of nonlinear exchange on transport. Numerical solution of the ADE for linear exchange.

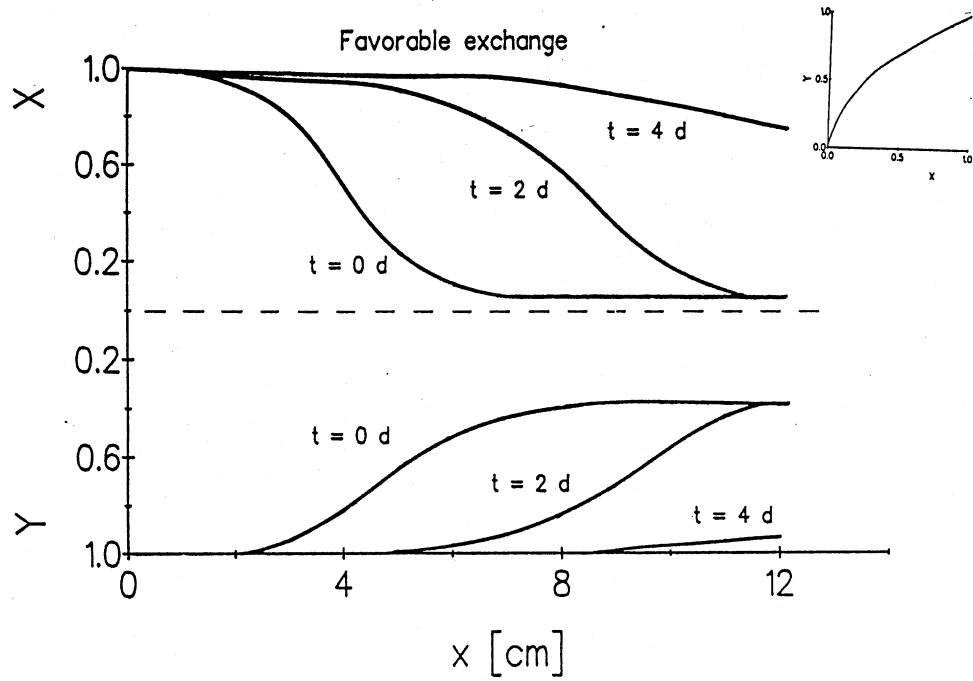


FIG.15C. The effect of nonlinear exchange on transport. Numerical solution of the ADE for favorable exchange.

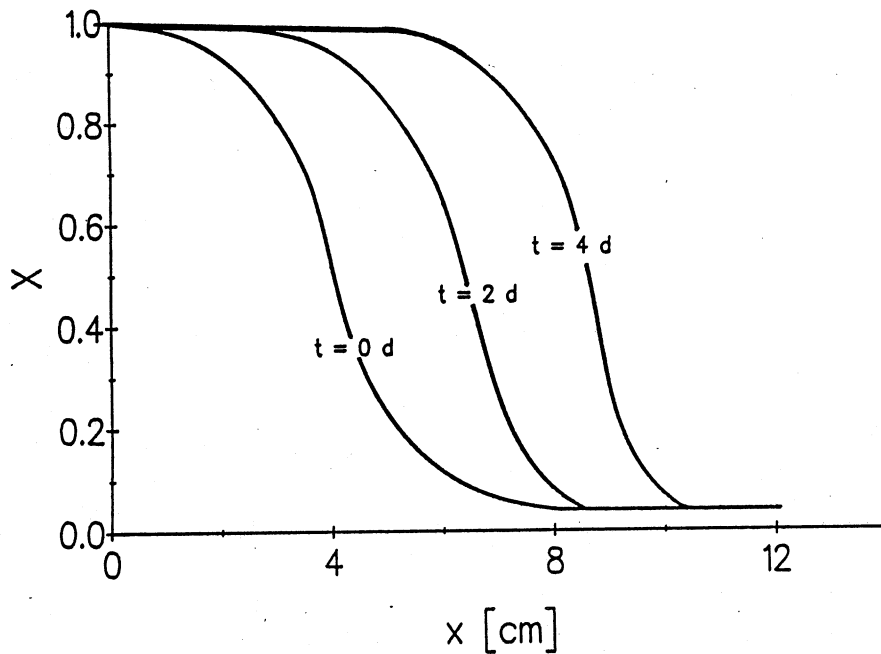


FIG.16. The effect of front sharpening on transport. Numerical solution of the ADE for favorable exchange.

spreading). The self sharpening effect of favorable exchange becomes even more apparent for lower values of v and D (figure 16).

Differences in solute spreading caused by the exchange process are conveniently demonstrated by using a moving coordinate system. Figure 17 contains profiles shown in figure 15 plotted as a function of $x - v^* t$, where v^* is the constant (retarded) advection term for a linearly exchanging solute. The initial concentration profile is given as a dashed line. The differences in steepness of the front can clearly be observed. One of the implications is that the complete displacement of the competing cation is accomplished most easily if the incoming cation is favorably adsorbed. For a speedy, incomplete displacement of the resident cation, an unfavorably adsorbed cation is to be preferred.

The effect of nonlinear exchange on transport is further illustrated using a solute pulse. Consider solute movement through a medium with a constant initial solute concentration ($X_1 = 0.05$). For an unfavorably exchanging solute (figure 18A), considerable spreading occurs at the front end of the pulse, whereas steepening takes place at the tail end of the pulse. The reverse can be observed for a favorably exchanging solute (figure 18C), whereas for a linearly exchanging solute the pulse remains symmetric (figure 18B).

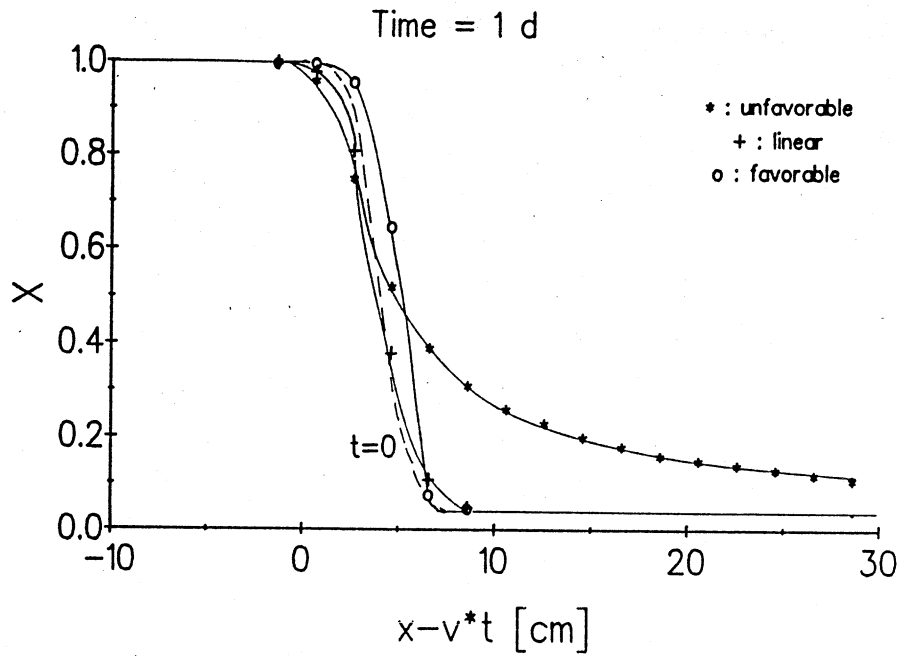


FIG.17A. The effect of nonlinear exchange on dispersion: concentration profiles for various exchange isotherms using a moving coordinate system after 1 d.

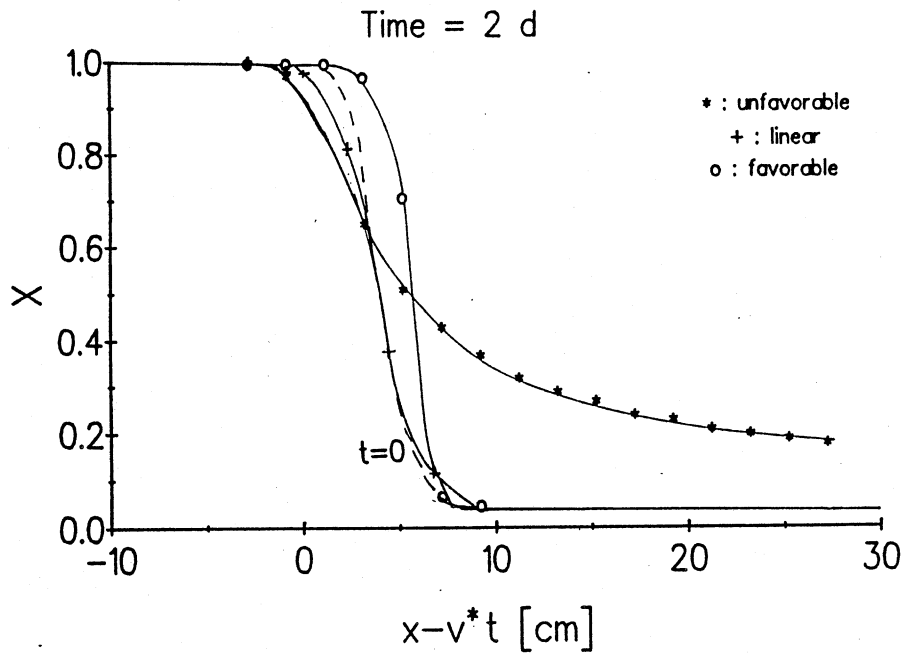


FIG.17B. The effect of nonlinear exchange on dispersion: concentration profiles for various exchange isotherms using a moving coordinate system after 2 d.

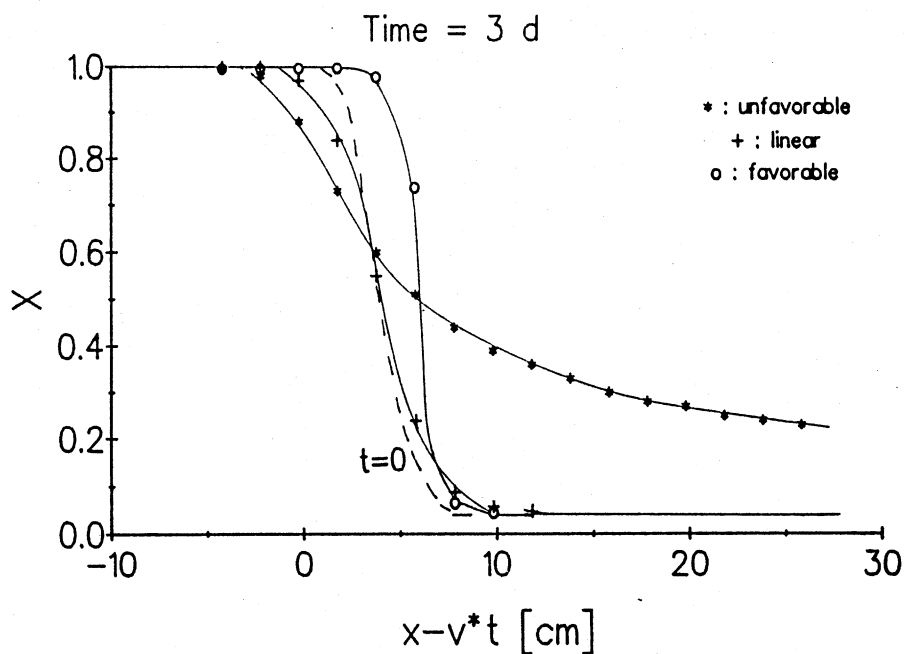


FIG.17C. The effect of nonlinear exchange on dispersion: concentration profiles for various exchange isotherms using a moving coordinate system after 3 d.

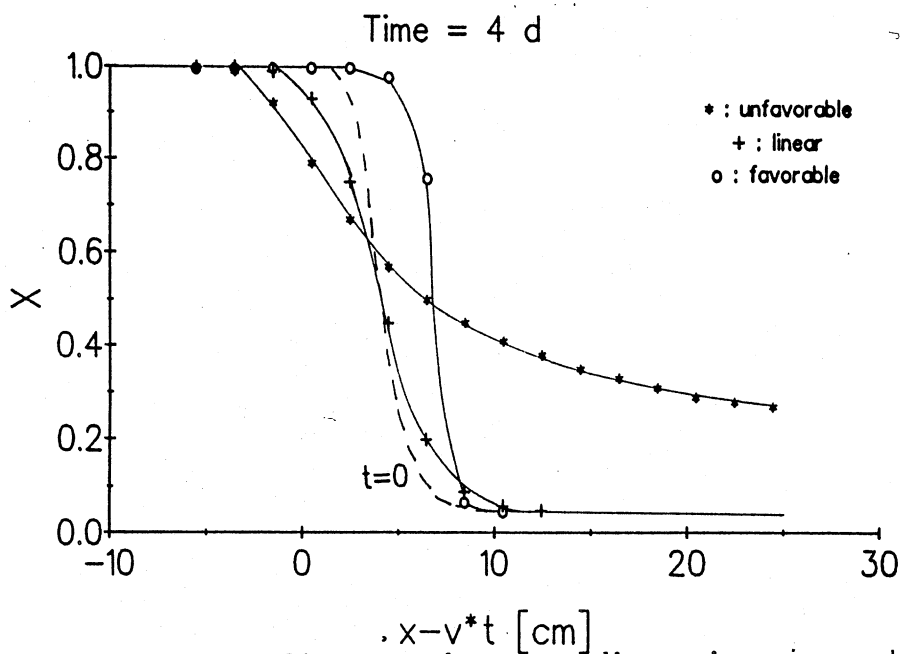


FIG.17D. The effect of nonlinear exchange on dispersion: concentration profiles for various exchange isotherms using a moving coordinate system after 4 d.

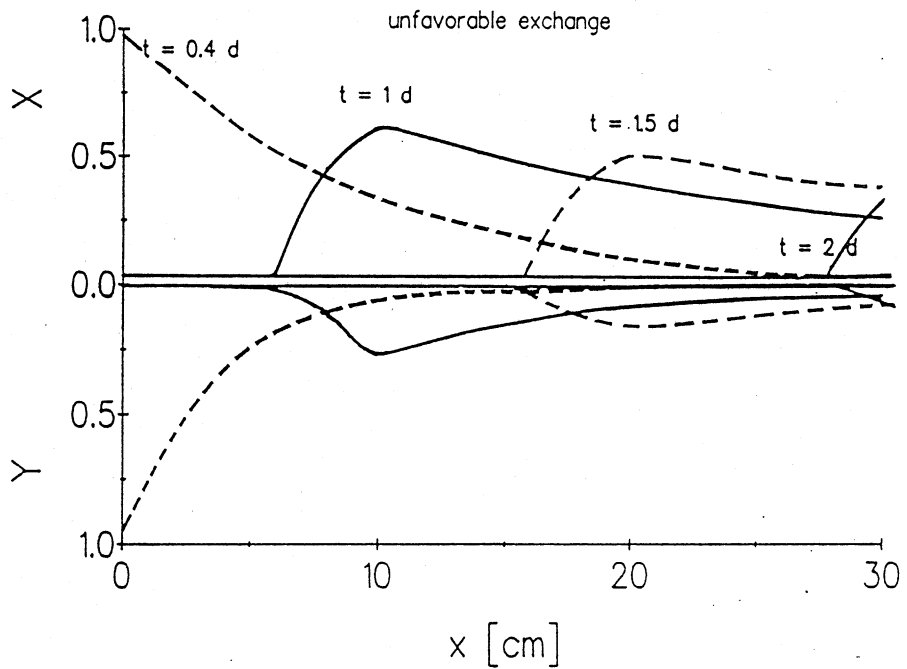


FIG.18A. Numerical solution of the ADE for a pulse input during unfavorable exchange.

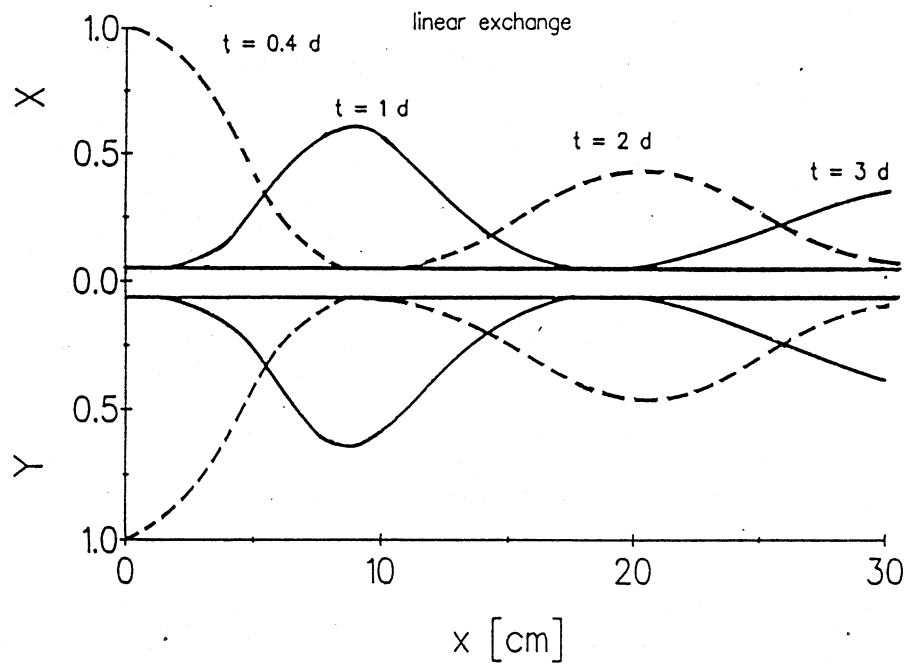


FIG.18B. Numerical solution of the ADE for a pulse input during linear exchange.

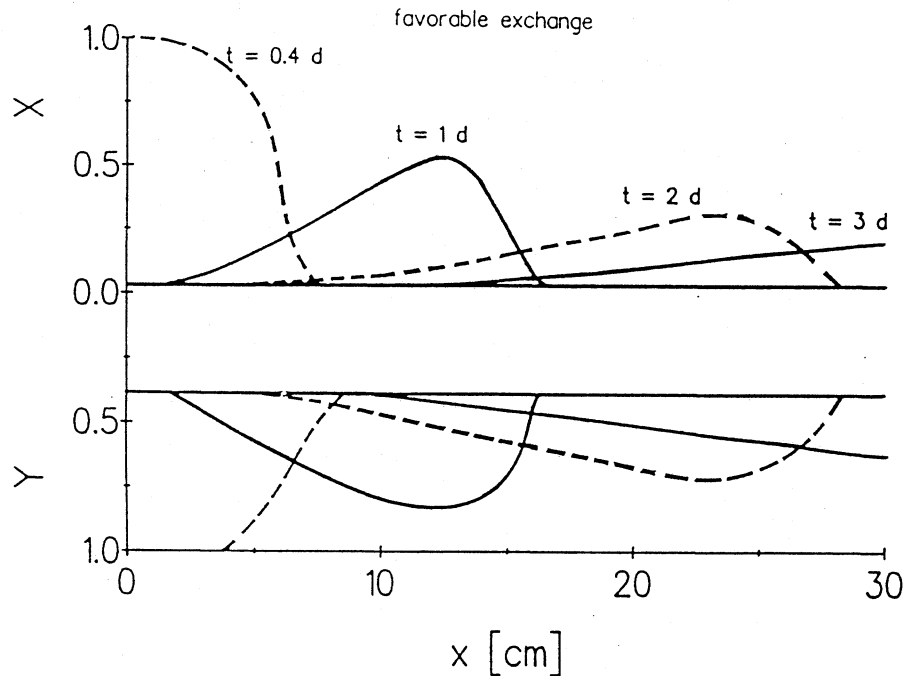


FIG.18C. Numerical solution of the ADE for a pulse input during favorable exchange.

The Influence of Soil Layers with Different Transport
Properties on Solute Transport

Transport of solutes can be influenced by having soil layers with different transport properties. Examination of Eq.(13) shows that the following mechanisms can alter the transport behavior during steady one-dimensional flow.

1) Advection

The continuity condition requires that for an incompressible fluid $\nabla \cdot (\theta v) = 0$ throughout the medium. At the interface of layers k and $k+1$ this leads to $(\theta v)_k = (\theta v)_{k+1}$. In a medium not homogeneous with respect to θ , the solute will, therefore, travel at different velocities through the various layers.

2) Dispersion

Different soils will likely exhibit different mixing behavior. It was already shown how transport is influenced by soil layers having different dispersion values. Although the pore-water velocity varies with each layer, differences in geometry of the pores and the size distribution and orientation of the soil particles is likely to have an even larger impact on spreading (13). This also has implications for transport perpendicular to the direction of flow.

3) Ion exchange

The exchange properties can be of major importance for the transport of reactive solutes. Consequently, differences in exchange properties will result in differences in travel time for the solute.

To illustrate the effect of chemical and physical properties changing from layer to layer, numerical solutions were obtained for transport in layered media with a second- or third-type condition at the interface and a third-type condition at the inlet of the column. We studied transport of a solute pulse in soils with layers that have different values of D and S_T and different exchange isotherms. The influence of different values of D for a step change was already illustrated in figure 10 and 11.

The first example involves the hypothetical case of a pulse of nonreactive solute traveling through a two-layer medium. The value for D is lower in the first than in the second layer. Figure 19A shows the

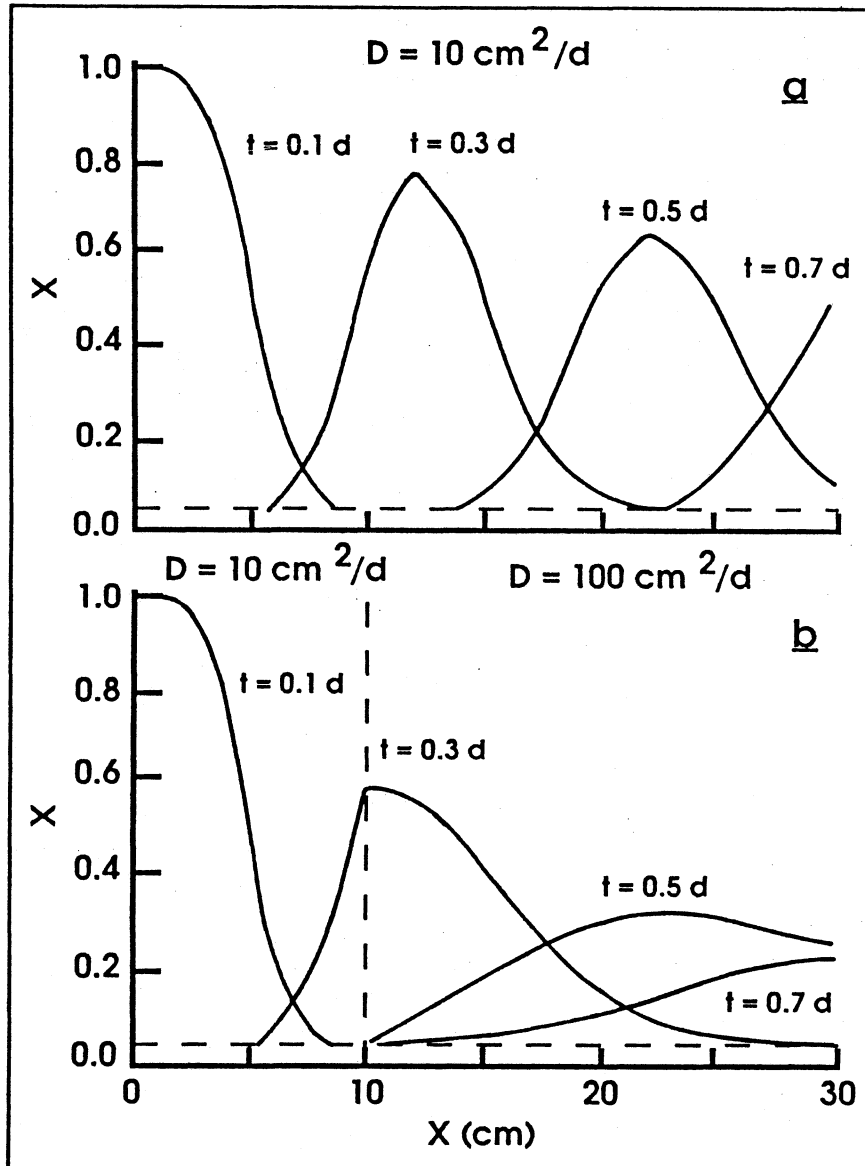


FIG. 19. The effect of layers with different dispersion coefficients on solute transport. Numerical solution of the ADE for a two-layer medium using a third-type condition with: (a) $D_1 = D_2 = 10 \text{ cm}^2/\text{d}$, and (b) $D_1 = 10 \text{ cm}^2/\text{d}$ and $D_2 = 100 \text{ cm}^2/\text{d}$.

resulting concentration profiles for a homogeneous medium, i.e., the bottom layer was assigned the same properties as the top one. The initial concentration, X_1 , is indicated with a dashed line. For a two-layer medium, the first layer ($0 < x < 10$) has the same properties as the homogeneous medium, while the value for D of the second layer ($10 < x < 30$) was, somewhat arbitrarily, increased ten-fold as compared to the homogeneous case. The difference in solute spreading between the two layers (figure 19B) and the discontinuity at the interface as the front passes are apparent. At $t=0.5$ d, the peak concentrations occurred at the same positions in figure 19A and 19B. However, the value of the peak concentration in figure 19A was almost twice the value in figure 19B. A layer with increased dispersion effectively reduces the maximum solute concentration without affecting the average solute movement.

A second example illustrates transport through two consecutive layers with different S_T values. Figure 20A demonstrates how the pulse travels through a homogeneous medium without adsorption capacity (i.e., $S_T=0$). Figure 20B and 20C show results for the medium with the second layer ($10 < x < 30$) having the adsorption capacity $S_T=2$ cmol_c/kg, for a third- and second-type condition at the interface, respectively. The movement of the solute is retarded considerably in the second layer. Also, notice the discontinuity at the interface for a third-type condition, because the concentration was calculated with two independent approximations of the ADE with different values for v^* and D^* . A more correct solution is obtained with the use of a second-type condition. Except at the interface, the solutions obtained with a second- and a third-type condition were similar.

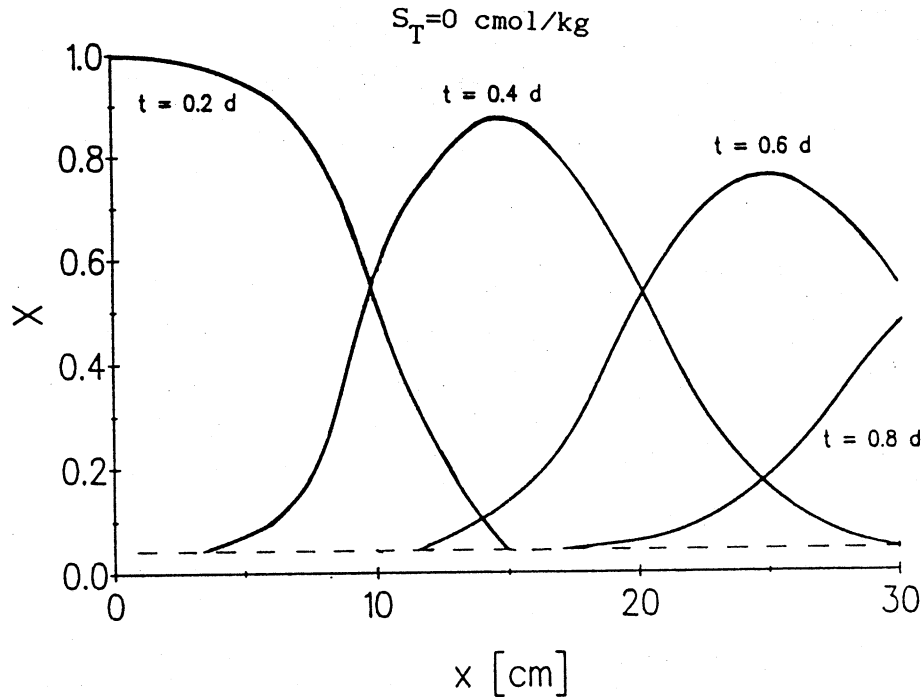


FIG.20A. The effect of layers with different exchange capacities on solute transport. Numerical solution of the ADE for a two-layer medium using a third-type condition with $(S_T)_1 = (S_T)_2 = 0 \text{ cmol/kg}$.

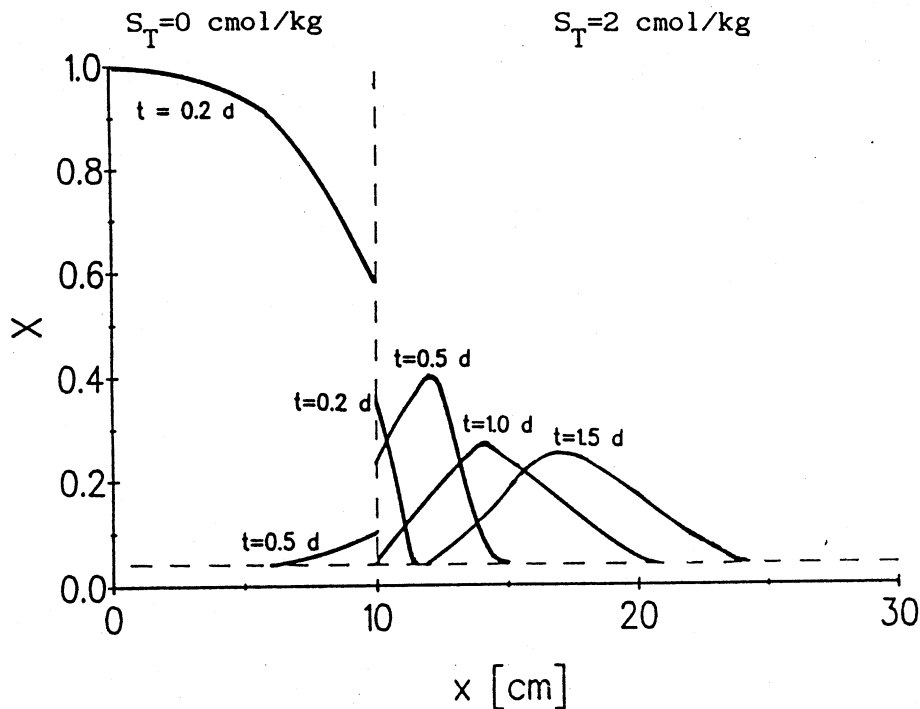


FIG.20B. The effect of layers with different exchange capacities on solute transport. Numerical solution of the ADE for a two-layer medium using a third-type condition with $(S_T)_1 = 0$ and $(S_T)_2 = 2 \text{ cmol/kg}$.

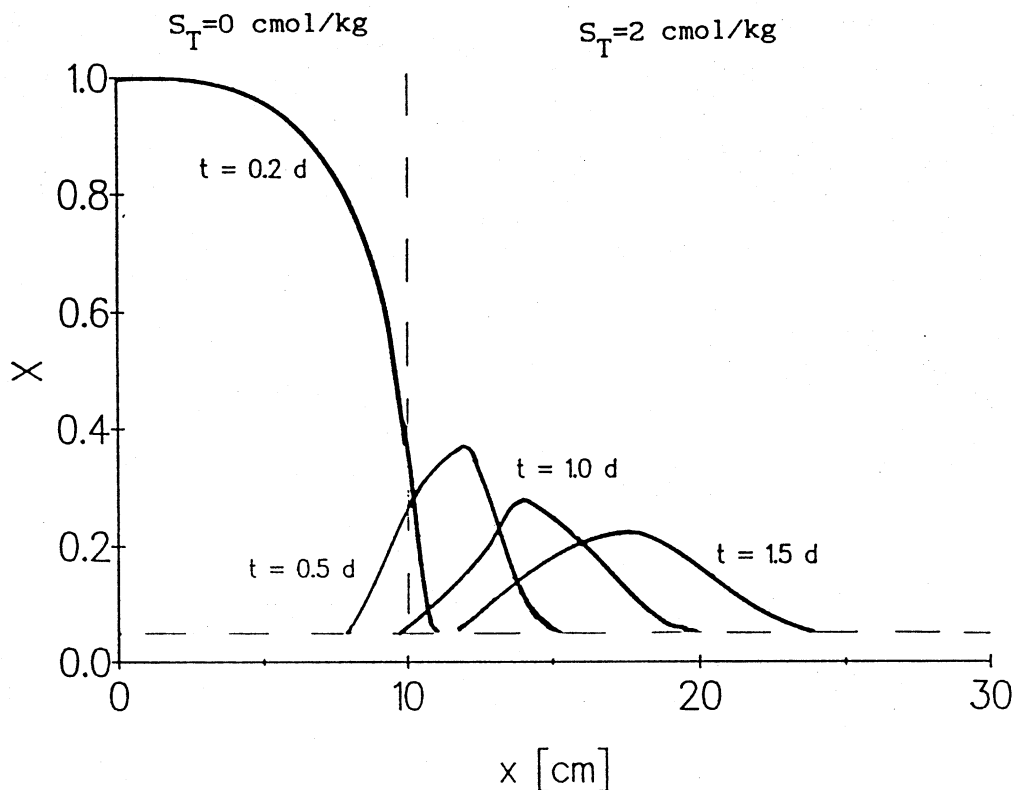


FIG.20C. The effect of layers with different exchange capacities on solute transport. Numerical solution of the ADE for a two-layer medium using a third-type condition at the inlet and a second-type condition at the interface with $(S_T)_1 = 0$ and $(S_T)_2 = 2$ cmol/kg.

In conclusion, a layer with increased adsorption capacity effectively reduces not only the solute movement but also the maximum solute concentration in the liquid phase. This is attractive to minimize the effects of solutes which pose a threat to the quality of ground water.

A third example treats transport of a reactive solute in a medium having layers with different exchange isotherms. Linear exchange occurred in the first layer, whereas the exchange was either unfavorable (figure 21A) or favorable (figure 21B) for the incoming cation in the second layer. The solute distributions were identical in the first layer. However, in the second layer the incoming front of the

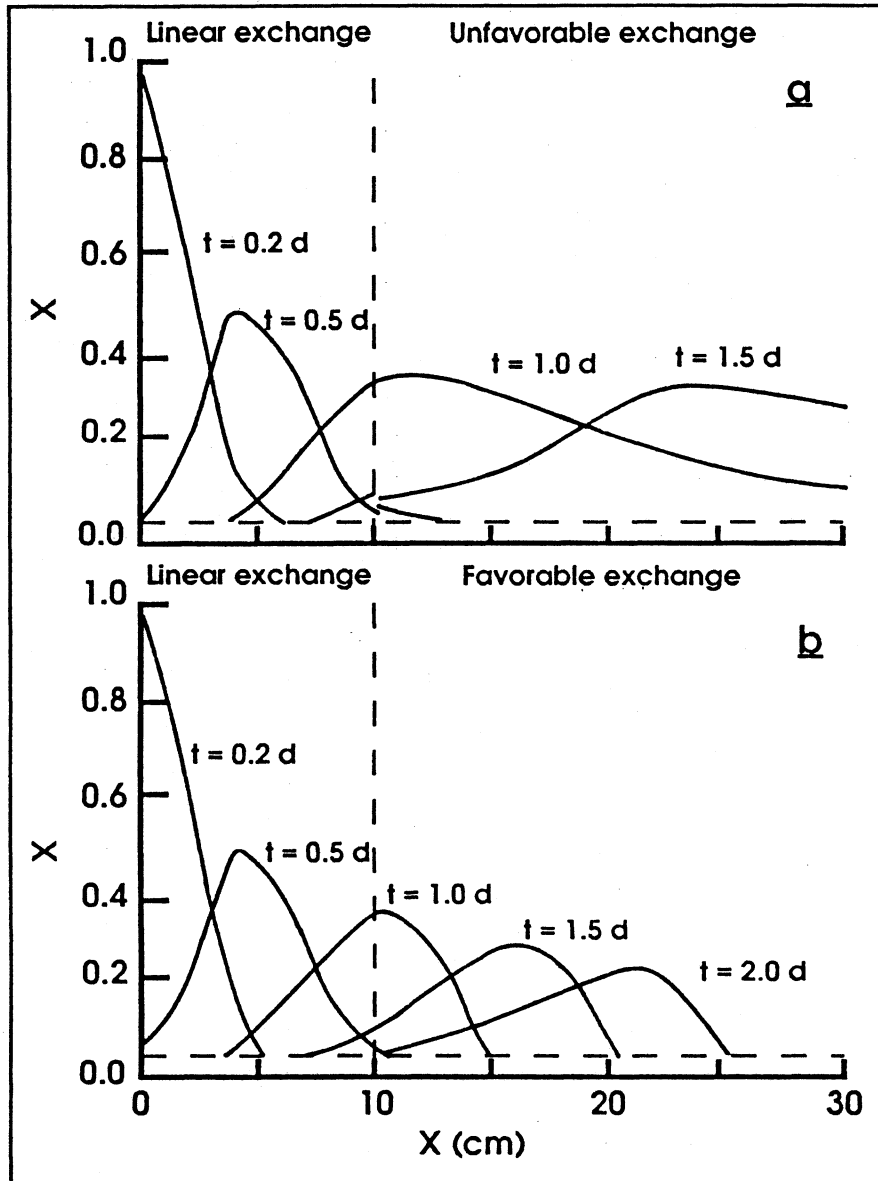


FIG.21. The effect of layers with different exchange isotherms on solute transport. Numerical solution of the ADE for a two-layer medium with: (a) $(dY/dX)_1 = 1$ and $(dY/dX)_2 = 3X^2$ and (b) $(dY/dX)_1 = 1$ and $(dY/dX)_2 = \frac{1}{3}X^{-2/3}$.

pulse showed spreading (figure 21A) and steepening (figure 21B), respectively, for the unfavorable and favorable exchange.

The next two examples were meant to illustrate the effect of a "barrier" to solute (contaminant) transport. First, consider a sandy soil which has a low S_T and where saturated or nearly saturated flow conditions prevail. Evidently, any solute will be transported at a relatively fast pace in such a medium (figure 22A). Movement of the solute can be slowed by incorporating a layer which reduces the solute flux via a decrease in the flow term and via an increase in adsorption. A clay soil generally possesses these characteristics; the hydraulic conductivity is relatively low during saturated conditions and the value of S_T can be significant. Somewhat arbitrary parameter values, listed in Appendix F, were chosen based on these considerations. The effects on the solute concentration profiles of embedding a 2-cm-thick clay layer, in the otherwise homogeneous profile, are shown for a third-type condition (figure 22B) and a second-type condition (figure 22C) at the interfaces. The presence of the clay layer was assumed to result in a ten-fold reduction of v (Appendix F). The value of the dispersion coefficient was calculated according to Eq. (2), using $D_o/\lambda=2$ cm^2/d , while α was assumed equal to 0.5 cm for the sand and 2 cm for the clay.

It can be observed in figure 22B that the concentration in the clay layer was considerably lower than in the sand at either interface. This was caused by the use of two different expressions for the ADE at the interface (i.e., with different values for D^* and v^*).

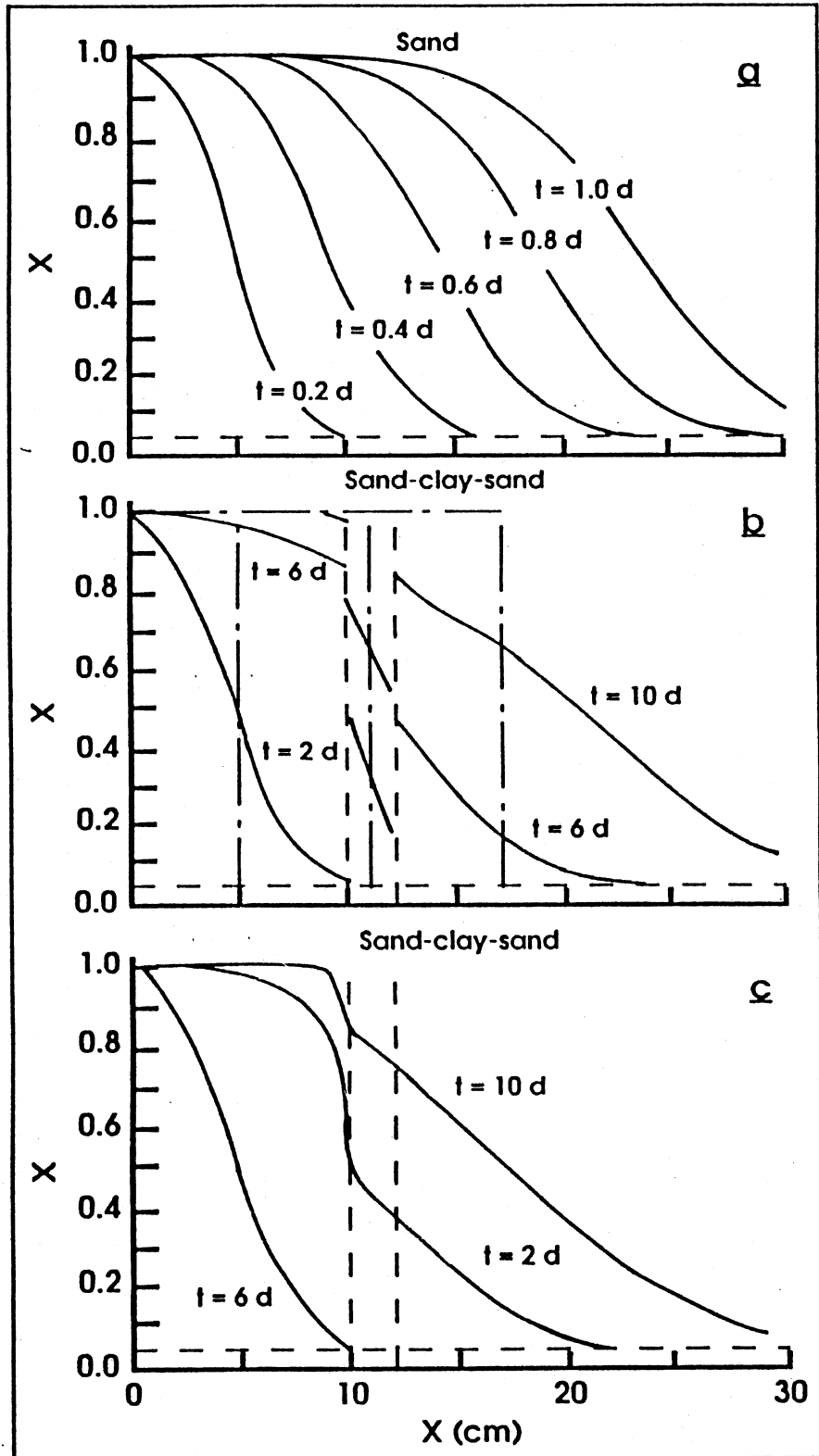


FIG.22. Concentration profiles in a hypothetical sand with a third-type inlet condition: nonlayered profile (a), and profile with a hypothetical clay layer using a third-type interface condition (b), and second-type interface condition (c).

Physically, the concentration in the liquid phase should be continuous at the interface. The use of a second-type condition is, therefore, preferred, although the profiles in figure 22B and 22C were very similar in the clay layer. To investigate the effectiveness of the added adsorption capacity (the clay layer), the locations of the front were also determined for zero dispersion by using the appropriate retarded velocities in each layer. The locations of this "zero-dispersion" front are symbolized with the numerals 1 to 5 (at $C/C_0=0.5$) for the various times listed in figure 22B. The solute moved slower through the sand when no dispersion occurred. Because of dispersion, the adsorption capacity of the clay layer was not fully utilized. It is clear that the magnitude of the dispersion coefficient needs to be known to accurately predict solute movement under these conditions.

Under some circumstances, it can be anticipated that "wet" conditions rarely exist. Solute transport can then be slowed by including a coarse textured layer in the porous medium. Winograd (35) discussed the dry site disposal of waste. Concentration profiles in a homogeneous clay (figure 23A) were compared with those in a clay-sand-clay system for a third- and second-type condition (figure 23B and 23C, respectively) under unsaturated soil water conditions. The inclusion of the sand layer was assumed to result in a ten-fold reduction of the flow (Appendix F), because of the low hydraulic conductivity of the sand. Due to the loss of adsorption capacity, the movement of the solute was reduced to a lesser extent than the movement

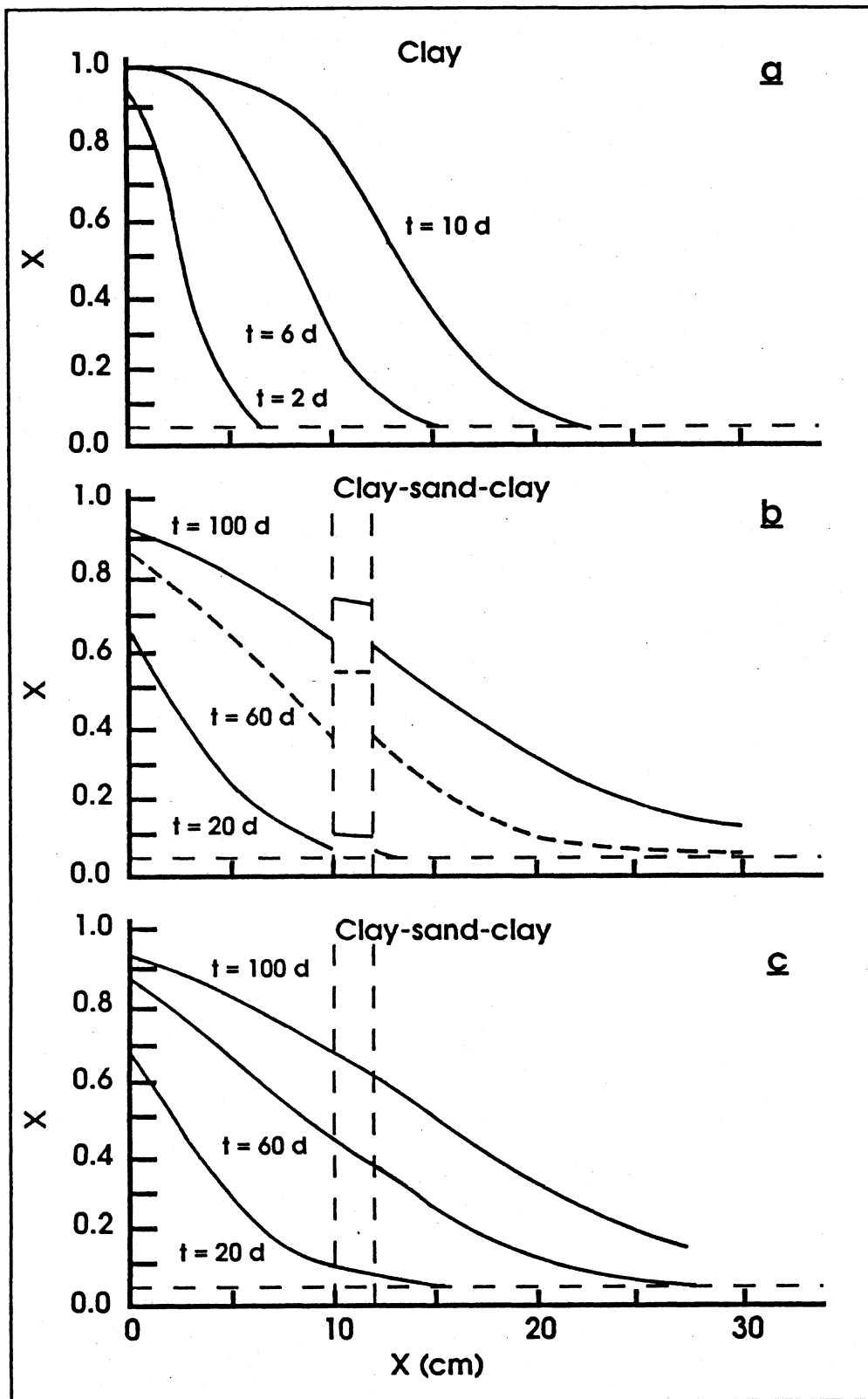


FIG.23. Concentration profiles in a hypothetical clay with a third-type inlet condition: nonlayered profile (a), and profile with a hypothetical sand layer using a third-type interface condition (b), and second-type interface condition (c).

of the water. Because of the lower value of the Peclet number for the 3-layer system, considerable time was needed for the inlet concentration to become equal to the eluent concentration. Notice that the discontinuity at the interface behaved in the opposite manner as for the clay layer in the previous example.

SUMMARY AND CONCLUSIONS

Analytical solutions of the 1-D ADE, subject to a first- or a third-type inlet condition, were obtained to describe transport in a two-layer medium. The 1-D ADE was solved numerically to describe transport of linearly and nonlinearly exchanging solutes in layered and nonlayered soils with the finite difference method. The accuracy of the numerical solutions was checked for a number of situations where analytical solutions were available or could be derived. Both numerical and analytical solutions were used to study transport in layered soils. The solution of the ADE subject to a concentration- or first-type condition at the interface leads to substantial mass balance error. These errors are avoided by using a flux- or third-type condition or a combined concentration/flux- or second-type condition. For a third-type condition, the resident concentration is not continuous at the interface. This is in contrast to the resident concentration obtained with a second-type solution. However, the flux-averaged concentration is continuous at the interface in both cases.

Ion exchange and stratification appeared to have major impacts on the movement of solutes in soils. The choice of cations in the eluent solution is important when the resident cation needs to be

displaced. For complete displacement of the resident solute, an eluent cation which is favorably exchanged with the resident cation is to be preferred. In other instances, one might be interested in a relatively fast displacement of only part of the resident solute and an unfavorably exchanging solute should be applied. Spreading phenomena are then advantageous. The examples which were presented offer some qualitative insight in what might be expected. It was shown that nonlinear exchange can become an important factor for reactive solute transport, which implies that the description of the exchange reaction, over the total concentration range, deserves careful attention. It was also found that the dispersive flux can become quite important at lower pore water velocities. These findings stress the importance of obtaining a good knowledge of the values of physical and chemical parameters.

Although the flow and transport conditions were relatively simple, the developed computer programs can easily be modified to account for different exchange curves, varying C_T and S_T , multi species exchange, sink/source terms, etc. Nonsteady flow conditions can also be included by solving the flow equation along with the ADE.

LITERATURE CITED

- (1) ABRAMOWITZ, M. and I.A. STEGUN. 1964. Handbook of Mathematical Functions. National Bureau of Standards, Applied Mathematics Series 55, U.S. Government Printing Office, Washington, D.C.
- (2) ABRIOLA, L.M. 1987. Modeling Contaminant Transport in the Subsurface: an Interdisciplinary Challenge. *Rev. of Geophys.* 25:125-134.
- (3) AL-NIAMI, A.N.S and K.R. RUSHTON. 1979. Dispersion in Stratified Porous Media: Analytical Solutions. *Water Resour. Res.* 15:1044-1048.
- (4) BARRY, D.A., J.-Y. PARLANGE, and J.L. STARR. 1987. Numerical Analysis of the Precursor Effect. *Soil Sci.* 143:309-317.
- (5) BOLT, G.H. 1982. Movement of Solutes in Soils: Principles of Adsorption/exchange Chromatography. In G.H. Bolt (Ed). *Soil Chemistry: B. Physico-chemical Models.* Elsevier Scientific Publishing Co. Amsterdam.
- (6) BRUGGENWERT, M.G.M. and A. KAMPHORST. 1982. Survey of Experimental Information on Cation Exchange in Soil Systems. In G.H. Bolt (Ed). *Soil Chemistry: B. Physico-chemical Models.* Elsevier Scientific Publishing Co. Amsterdam.
- (7) BURDEN, R.L., J. DOUGLAS FAIRES, and A.C. REYNOLDS. 1981. Numerical Analysis. Prindle Weber & Schmidt. Boston.
- (8) CARSLAW, H.S. and J.C. JAEGER. 1959. Conduction of Heat in Solids. Clarendon Press, Oxford.
- (9) CRUMP, K.S. 1976. Numerical Inversion of Laplace Transforms Using a Fourier Series Approximation. *J. ACM* 23:89-96.
- (10) DAGAN, G. and E. BRESLER. 1985. Comment on "Flux-averaged and Volume-Averaged Concentrations in Continuum Approaches to Solute Transport", by J.C. Parker and M.Th. van Genuchten. *Water Resour. Res.* 21:1299-1300.
- (11) DANCKWERTS, P.V. 1953. Continuous Flow Systems. *Chem. Eng. Sci.* 2:1-13.
- (12) DANE, J.H. and F.H. MATHIS. 1981. An Adaptive Finite Difference Scheme for the One-dimensional Water Flow Equation. *Soil Sci. Soc. Am. J.* 45:1048-1054.

- (13) FRIED, J.J. and M.A. COMBARNOUS. 1971. Dispersion in Porous Media. *Adv. Hydroci.* 9:169-282.
- (14) HUYAKORN, P.S. and G.F. PINDER. 1983. *Computational Methods in Subsurface Flow.* Academic Press. New York.
- (15) JURY, W. A. 1982. Simulation of Solute Transport Using a Transfer Function Model. *Water Resour. Res.* 18:363-368.
- (16) KREFT, A. and A. ZUBER. 1978. On the Physical Meaning of the Dispersion Equation and its Solutions for Different Initial and Boundary Conditions. *Chem. Eng. Sci.* 33:1471-1480.
- (17) LAI, S.-H. and J.J. JURINAK. 1972. Cation Adsorption in One-Dimensional Flow through Soils: a Numerical Solution. *Water Resour. Res.* 8:99-107.
- (18) LAPIDUS, L and N.R. AMUNDSON. 1952. Mathematics of Adsorption in Beds. 6. The Effect of Longitudinal Diffusion in Ion Exchange and Chromatographic Columns. *J. Phys. Chem.* 56:984-988.
- (19) Leij, F.J., and J.H. Dane. 1989. Determination of Transport Parameters from Step and Pulse Displacement of Cations and Anions. *Ala. Agr. Exp. Sta. Dept of Agronomy and Soils Series* 135.
- (20) OBERHETTINGER, F. and L. BADI. 1973. *Tables of Laplace Transforms.* Springer Verlag.
- (21) ÖZİŞİK, M.H. 1980. *Heat Conduction.* Wiley-Interscience. New York.
- (22) PARKER, J.C. and M.Th. VAN GENUCHTEN. 1984. Flux-averaged and Volume-averaged Concentrations in Continuum Approaches to Solute Transport. *Water Resour Res.* 20:866-872.
- (23) PERSAUD, N. and P.J. WIERENGA. 1982. A Differential Model for One-dimensional Cation Transport in Discrete Homoionic Ion-exchange Media. *Soil Sci. Soc. Am. J.* 46:482-490.
- (24) PRESS, W.H., B.P. FLANNERY, S.A. TEUKOLSKY, and W.T. VETTERLING. 1986. *Numerical Recipes.* Cambridge Univ. Press. New York.
- (25) REMSON, I., G.M. HORNBERGER, and F.J. MOLZ. 1971. *Numerical Methods in Subsurface Hydrology.* Wiley-Interscience. New York.
- (26) RUBIN, J. and R.V. JAMES. 1973. Dispersion-affected Transport of Reacting Solutes in Saturated Porous Media: Galerkin Method Applied to Equilibrium-controlled Exchange in Unidirectional Steady Water Flow. *Water Resour. Res.* 9:1332-1356.

- (27) SELIM, H.M., R. SCHULIN, and H. FLUHLER. 1987. Transport and Ion Exchange of Calcium and Magnesium in an Aggregated Soil. Soil Sci. Soc. Am. J. 51:876-884.
- (28) SHAMIR, U.Y. and D.R.F. HARLEMAN. 1967. Dispersion in Layered Porous Media. J. Hydraul. Div. Proc. ASCE 93(HY5):237-260.
- (29) STONE, H.L. and P.T. BRIAN. 1963. Numerical Solution of Convective Transport Problems. AIChE J. 9:681-688.
- (30) VALOCCHI, A.J., R.L. STREET, and P.V. ROBERTS. 1981. Transport of Ion-exchanging Solutes in Groundwater: Chromatographic Theory and Field Simulation. Water Resour. Res. 17:1517-1527.
- (31) VANDERGRAFT, J.S. 1983. Introduction to Numerical Computations. Academic Press. New York.
- (32) VAN GENUCHTEN, M.Th. 1978. Mass Transfer in Saturated-unsaturated Media. I. One-dimensional Solutions. Res Report No.78-WR-11. Princeton Univ., Princeton.
- (33) VAN GENUCHTEN, M.Th. and W.J. ALVES. 1982. Analytical Solutions of the One-dimensional Convective-dispersive Solute Transport Equation. U.S.D.A. Technical Bulletin No. 1661.
- (34) VAN GENUCHTEN, M.Th. and J.C. PARKER. 1984. Boundary Conditions for Displacement Experiments through Short Laboratory Soil Columns. Soil Sci. Soc. Am. J.48:703-708.
- (35) WINOGRAD, I.J. 1974. Radioactive Waste Storage in the Arid Zone. Trans. Am. Geophys. Union 55:884-894.

APPENDIX A: Analytical Solution of the ADE for the Second Layer of
a Porous Medium Using a First-type Condition

The solution of the ADE for the first layer was given by Eq.(7). We will derive more general solutions by considering pulse displacement, and different initial concentrations for both layers. For the second layer, the problem can be formulated as follows:

$$R_2 \frac{\partial C}{\partial t} = D_2 \frac{\partial^2 C}{\partial x^2} - v_2 \frac{\partial C}{\partial x} \quad L_1 < x < L_2 \quad t > 0 \quad (A1)$$

$$C(x, 0) = g_2 \quad L_1 < x < L_2 \quad (A2a)$$

$$C(x, t) \Big|_{x \downarrow L_1} = C(x, t) \Big|_{x \uparrow L_1} \quad t > 0 \quad (A2b)$$

$$\frac{\partial C}{\partial x} \Big|_{x \rightarrow \infty} = 0 \quad t > 0 \quad (A2c)$$

where the subscripts 1 and 2 denote the first and second layer, respectively, and g_2 is the prescribed initial concentration for the second layer. An illustration of the problem for K layers was given in figure 2.

Solution of (A1), subject to (A2), is achieved with the help of Laplace transforms. The Laplace transform of $C(x, t)$ with respect to t , is defined as:

$$\mathcal{L} [C(x, t)] = \int_0^{\infty} C(x, t) \exp(-st) dt = \bar{C}(x, s) \quad (A3)$$

which eliminates the dependency of C on time. By applying the Laplace transform to (A1) and (A2), we obtain:

$$\frac{d^2 \bar{C}}{dx^2} - \frac{v_2}{D_2} \frac{d\bar{C}}{dx} - \frac{sR_2}{D_2} \bar{C} + \frac{g_2 R_2}{D_2} = 0 \quad (A4)$$

$$\bar{C}(L_1, s) = \left[\frac{C_0}{s} \left(1 - \exp(-t_0 s) \right) - \frac{g_1}{s} \right] \exp(\lambda_1 L_1) + \frac{g_1}{s} \quad (A5a)$$

$$\left. \frac{d\bar{C}}{dx} \right|_{x \rightarrow \infty} = 0 \quad (\text{A5b})$$

where $\lambda_1 = \frac{v_1}{2D_1} - \sqrt{\left(\frac{v_1}{2D_1}\right)^2 + \frac{sR_1}{D_1}}$ and C_0 is the prescribed eluent concentration (cf. Eq.(5a)). A general solution of (A4) is:

$$\bar{C}(x,s) = \alpha \exp(\lambda_2^+ x) + \beta \exp(\lambda_2^- x) + \frac{g_2}{s} \quad (\text{A6})$$

where $\lambda_2^\pm = \frac{v_2}{2D_2} \pm \sqrt{\left(\frac{v_2}{2D_2}\right)^2 + \frac{sR_2}{D_2}}$ and α and β are coefficients to be determined by the boundary conditions. By using the outlet condition (A5b), it follows that $\alpha=0$. For convenience, the superscript of λ_2^- will be dropped. Application of the inlet condition (A5a) results in:

$$\beta = \left[\frac{C_0}{s} \left(1 - \exp(-t_0 s) \right) - \frac{g_1}{s} \right] \exp(\lambda_1 L_1 - \lambda_2 L_1) + \left[\frac{g_1 - g_2}{s} \right] \exp(-\lambda_2 L_1) \quad (\text{A7})$$

Substitution of (A7) in (A6) leads to the following solution for $\bar{C}(x,s)$:

$$\begin{aligned} \bar{C}(x,s) = & \left[\frac{C_0 - g_1}{s} \right] \exp(\lambda_1 L_1 + \lambda_2 \xi) - \frac{C_0}{s} \exp(\lambda_1 L_1 + \lambda_2 \xi - t_0 s) + \\ & \left[\frac{g_1 - g_2}{s} \right] \exp(\lambda_2 \xi) + \frac{g_2}{s} = \bar{C}_1 + \bar{C}_2 + \bar{C}_3 + \bar{C}_4 \end{aligned} \quad (\text{A8})$$

where $\xi = x - L_1$. By inverting the various terms of Eq.(A8), we can obtain the desired solution for $C(x,t)$. It is convenient to adopt the following notation:

$$a_1 = v_1 / \sqrt{4R_1 D_1} \quad (\text{A9a})$$

$$k_1 = L_1 \sqrt{R_1 / D_1} \quad (\text{A9b})$$

$$a_2 = v_2 / \sqrt{4R_2 D_2} \quad (\text{A9c})$$

$$k_2 = \xi \sqrt{R_2 / D_2} \quad (\text{A9d})$$

This allows us to write the inverse of \bar{C}_1 as:

$$C_1(x, t) = \mathcal{L}^{-1} \left[\frac{C_0 - g_1}{s} \exp(a_1 k_1 - k_1 \sqrt{a_1^2 + s} + a_2 k_2 - k_2 \sqrt{a_2^2 + s}) \right] =$$

$$(C_0 - g_1) \exp(a_1 k_1 + a_2 k_2) g^* h \quad (A10)$$

where C depends on x because of k_2 . The convolution $g^* h$, defined as

$$g(t) * h(t) = \int_0^t g(t-\tau) h(\tau) d\tau = \int_0^t g(\tau) h(t-\tau) d\tau, \quad (A11)$$

is used to carry out the inverse Laplace transform according to:

$$\mathcal{L}^{-1}[\bar{g}(s)\bar{h}(s)] = g(t) * h(t) \quad (A12)$$

The inverse of $\bar{g}(s)$ and $\bar{h}(s)$ can be obtained with the shift property of the Laplace transform and a table of Laplace transforms (20, 33):

$$g(t) = \exp(-a_1^2 t) \mathcal{L}^{-1} \left[\frac{1}{s - a_1} \exp(-k_1 \sqrt{s}) \right] = \quad (A13)$$

$$\frac{1}{2} \left\{ \exp(-a_1 k_1) \operatorname{erfc} \left[\frac{k_1 - 2a_1 t}{\sqrt{4t}} \right] + \exp(a_1 k_1) \operatorname{erfc} \left[\frac{k_1 + 2a_1 t}{\sqrt{4t}} \right] \right\}$$

$$h(x, t) = \exp(-a_2^2 t) \mathcal{L}^{-1} \left[\exp(-k_2 \sqrt{s}) \right] = \frac{k_2}{\sqrt{4\pi t^3}} \exp \left[-\frac{k_2^2 + 4a_2^2 t^2}{4t} \right] \quad (A14)$$

By applying Eq. (A11), the following expression for C_1 is found:

$$C_1(x, t) = \frac{k_2}{\sqrt{16\pi}} (C_0 - g_1) \int_0^t \left\{ \operatorname{erfc} \left[\frac{k_1 - 2a_1 \tau}{\sqrt{4\tau}} \right] + \exp(2a_1 k_1) \operatorname{erfc} \left[\frac{k_1 + 2a_1 \tau}{\sqrt{4\tau}} \right] \right\} \times$$

$$\times \left\{ (t-\tau)^{-3/2} \exp \left[-\frac{(k_2 - 2a_2(t-\tau))^2}{4(t-\tau)} \right] \right\} d\tau \quad (A15)$$

The inverse of \bar{C}_2 follows from C_1 , using the properties of the Laplace transform for a step function:

$$C_2(x, t) = \begin{cases} 0 & 0 < t \leq t_0 \\ -\frac{C_0}{C_0 - g_1} C_1(x, t - t_0) & t > t_0 \end{cases} \quad (\text{A16})$$

The inverse of \bar{C}_3 is determined according to:

$$C_3(x, t) = \mathcal{L}^{-1} \left[\left[\frac{g_1 - g_2}{s} \right] \exp(a_2 k_2 - k_2 \sqrt{a_2^2 + s}) \right] = \frac{1}{2}(g_1 - g_2) \left\{ \operatorname{erfc} \left[\frac{k_2 - 2a_2 t}{\sqrt{4t}} \right] + \exp(2a_2 k_2) \operatorname{erfc} \left[\frac{k_2 + 2a_2 t}{\sqrt{4t}} \right] \right\} \quad (\text{A17})$$

whereas $C_4 = g_2$. The solution of the problem is:

$$C(x, t) = C_1(x, t) + C_2(x, t) + C_3(x, t) + C_4 \quad (\text{A18})$$

For a step-type displacement, i.e., $t_0 \rightarrow \infty$, and $g_1 = g_2 = C_i$ we obtain

$$C(x, t) = \frac{(C_0 - C_i) k_2}{\sqrt{16\pi}} \int_0^t \left\{ \operatorname{erfc} \left[\frac{k_1 - 2a_1 \tau}{\sqrt{4\tau}} \right] + \exp(2a_1 k_1) \operatorname{erfc} \left[\frac{k_1 + 2a_1 \tau}{\sqrt{4\tau}} \right] \right\} \times \\ \times \left\{ (t - \tau)^{-3/2} \exp \left[-\frac{(k_2 - 2a_2(t - \tau))^2}{4(t - \tau)} \right] \right\} d\tau + C_i \quad (\text{A19})$$

The integrals in Eqs. (A15) and (A19) can be evaluated via standard numerical methods.

The approach outlined in this Appendix is similar to that originally described by Shamir and Harleman (28), which we were not aware of at the time we derived (A19). It should be noted that their Eq. (18) contains a misprint: the term $\pi D_{L_2}(t - \pi)$ should be read as $\pi D_{L_2}(t - \pi)^3$. Shamir and Harleman (28) extended their analysis to a medium of K layers to obtain the concentration at the end of the K-th layer. However, it can be verified that $\bar{C}(x, s)$ for an arbitrary

position in this layer is given by:

$$\bar{C}(x, s) = \frac{C_o - C_i}{s} \exp\left[\sum_{k=1}^{K-1} (\lambda_k \ell_k)\right] \exp(\lambda_K \xi_K) + \frac{C_i}{s} \quad (\text{A20})$$

where ℓ_k is the thickness of the k-th layer and $\xi_K = x - L_{K-1}$. Equation (A20) can be inverted using the convolution theorem while making use of the results for layer K-1. It is apparent from (A20) that the order in which the layers appear does not affect the concentration in the final layer K, as was already concluded by Shamir and Harleman (28).

APPENDIX B: Analytical solution of the ADE for the Second Layer of a
Porous Medium Using a Third-type Condition

In this Appendix we seek a solution of the ADE for the second layer, using the principle of continuity of flux rather than concentration, as in Appendix A. The use of a flux- or third-type condition is preferred over a first-type condition for volume-averaged concentrations because it leads to conservation of mass (34). The solution in the first layer was given by Eq.(8). The problem can be stated as follows:

$$R_2 \frac{\partial C}{\partial t} = D_2 \frac{\partial^2 C}{\partial x^2} - v_2 \frac{\partial C}{\partial x} \quad L_1 < x < L_2 \quad t > 0 \quad (B1)$$

$$C(x, 0) = g_2 \quad L_1 < x < L_2 \quad (B2a)$$

$$(-\theta_1 D_1 \frac{\partial C}{\partial x} + \theta_1 v_1 C) \Big|_{x \uparrow L_1} = (-\theta_2 D_2 \frac{\partial C}{\partial x} + \theta_2 v_2 C) \Big|_{x \downarrow L_1} \quad t > 0 \quad (B2b)$$

$$\frac{\partial C}{\partial x} \Big|_{x \rightarrow \infty} = 0 \quad t > 0 \quad (B2c)$$

Again, the method of Laplace transforms is employed to obtain a solution of (B1) subject to (B2). Transformation of (B1) and (B2) leads to:

$$\frac{d^2 \bar{C}}{dx^2} - \frac{v_2}{D_2} \frac{d\bar{C}}{dx} - \frac{sR_2}{D_2} \bar{C} + \frac{g_2 R_2}{D_2} = 0 \quad (B3)$$

$$(-\theta_1 D_1 \frac{d\bar{C}}{dx} + \theta_1 v_1 \bar{C}) \Big|_{x \uparrow L} = (-\theta_2 D_2 \frac{d\bar{C}}{dx} + \theta_2 v_2 \bar{C}) \Big|_{x \downarrow L} \quad (B4a)$$

$$\frac{d\bar{C}}{dx} \Big|_{x \rightarrow \infty} = 0 \quad (B4b)$$

The Laplace transform of the concentration in the first layer is:

$$\bar{C}(x, s) = \frac{v_1}{v_1 - D_1 \lambda_1} \left[\left[\frac{C_0 - g_1}{s} \right] - \frac{C_0}{s} \exp(-t_0 s) \right] \exp(\lambda_1 x) + \frac{g_1}{s} \quad (B5)$$

where λ_1 was defined in Appendix A.

The general solution of (B3) subject to (B4) is:

$$\bar{C}(x,s) = \alpha \exp(\lambda_2^+ x) + \beta \exp(\lambda_2^- x) + \frac{g_2}{s} \quad (\text{B6})$$

where α , β , λ_2^+ and λ_2^- were defined before. Boundary condition (B4b) requires that α equals zero. An expression for β is found by using the inlet condition and assuming steady flow (i.e., $\nabla \cdot (v\theta) = 0$):

$$\beta = \frac{v_2}{v_2 - D_2 \lambda_2^-} \left\{ \left[\frac{g_1 - g_2}{s} \right] + \frac{C_0}{s} [1 - \exp(-t_0 s)] \exp(\lambda_1 L_1) \right\} \exp(-\lambda_2^- L_1) \quad (\text{B7})$$

Substitution of Eq.(B7) into Eq.(B6) yields the solution of the ordinary differential equation (B3). Using the notation according to Eq.(A9) we obtain:

$$\begin{aligned} \bar{C}(x,s) = & \frac{2a_2}{a_2 + \sqrt{a_2^2 + s}} \left\{ \left[\left[\frac{C_0 - g_1}{s} \right] - \frac{C_0}{s} \exp(-t_0 s) \right] \exp(a_1 k_1 - k_1 \sqrt{a_1^2 + s}) + \left[\frac{g_1 - g_2}{s} \right] \right\} \times \\ & \times \exp(a_2 k_2 - k_2 \sqrt{a_2^2 + s}) + \frac{g_2}{s} = \bar{C}_1(x,t) + \bar{C}_2(x,t) + \bar{C}_3(x,t) + \bar{C}_4 \quad (\text{B8}) \end{aligned}$$

To obtain $C(x,t)$ we proceed by taking the inverse in a similar manner as in Appendix A.

$$C_1(x,t) = 2a_2 (C_0 - g_1) \exp(a_1 k_1 + a_2 k_2) \mathcal{L}^{-1} \left[\frac{\exp \left[-k_1 \sqrt{a_1^2 + s} - k_2 \sqrt{a_2^2 + s} \right]}{s \left[a_2 + \sqrt{a_2^2 + s} \right]} \right] \quad (\text{B9})$$

The inverse part of C_1 is determined by using the expression for the Laplace transform of the convolution of two functions $g(t)$ and $h(t)$, for completeness, we also include the expressions for $\bar{g}(s)$ and $\bar{h}(s)$:

$$\bar{g}(s) = \frac{1}{s} \exp \left[\sqrt{-k_1 (a_1^2 + s)} \right] \quad (\text{B10})$$

$$g(t) = \frac{1}{2} \left\{ \exp(-a_1 k_1) \operatorname{erfc} \left[\frac{k_1 - 2a_1 t}{\sqrt{4t}} \right] + \exp(a_1 k_1) \operatorname{erfc} \left[\frac{k_1 + 2a_1 t}{\sqrt{4t}} \right] \right\} \quad (\text{B11})$$

$$\bar{h}(x, s) = \frac{1}{a_2 + \sqrt{a_2^2 + s}} \exp\left[-k_2 \sqrt{a_2^2 + s}\right] \quad (\text{B12})$$

$$h(x, t) = \frac{1}{\sqrt{\pi t}} \exp\left[-\frac{(4a_2^2 t^2 + k_2^2)}{4t}\right] - a_2 \exp(a_2 k_2) \operatorname{erfc}\left[\frac{k_2 + 2a_2 t}{\sqrt{4t}}\right] \quad (\text{B13})$$

After applying Eq. (A11) we obtain:

$$C_1(x, t) = a_2 (C_0 - g_1) \int_0^t \left\{ \operatorname{erfc}\left[\frac{k_1 - 2a_1 \tau}{\sqrt{4\tau}}\right] + \exp(2a_1 k_1) \operatorname{erfc}\left[\frac{k_1 + 2a_1 \tau}{\sqrt{4\tau}}\right] \right\} \times \quad (\text{B14})$$

$$\times \left\{ (\pi(t-\tau))^{-1/2} \exp\left[-\frac{(k_2 - 2a_2(t-\tau))^2}{4(t-\tau)}\right] - a_2 \exp(2a_2 k_2) \operatorname{erfc}\left[\frac{k_2 + 2a_2(t-\tau)}{\sqrt{4(t-\tau)}}\right] \right\} d\tau$$

Using the properties of the Laplace transform:

$$C_2(x, t) = \begin{cases} 0 & 0 < t \leq t_0 \\ -\frac{C_0}{C_0 - g_1} C_2(x, t - t_0) & t > t_0 \end{cases} \quad (\text{B15})$$

$$C_3(x, t) = 2a_2 (g_1 - g_2) \exp(a_2 k_2) \mathcal{L}^{-1} \left[\frac{\exp\left[-k_2 \sqrt{a_2^2 + s}\right]}{s \left[a_2 + \sqrt{a_2^2 + s} \right]} \right] =$$

$$\frac{1}{2} (g_1 - g_2) \left\{ \sqrt{\frac{16a_2^2 t}{\pi}} \exp\left[-\frac{(k_2 - 2a_2 t)^2}{4t}\right] + \operatorname{erfc}\left[\frac{k_2 - 2a_2 t}{\sqrt{4t}}\right] + \right.$$

$$\left. - (1 + 2a_2 k_2 + 4a_2^2 t) \exp(2a_2 k_2) \operatorname{erfc}\left[\frac{k_2 + 2a_2 t}{\sqrt{4t}}\right] \right\} \quad (\text{B16})$$

$$C_4(x, t) = g_2 \quad (\text{B17})$$

The solution of the problem is:

$$C(x, t) = C_1(x, t) + C_2(x, t) + C_3(x, t) + C_4 \quad (\text{B18})$$

For a step-type displacement, i.e., $t_0 \rightarrow \infty$, and $g_1 = g_2 = C_1$ we obtain

$$\begin{aligned}
C(x,t) = & a_2(C_o - C_i) \int_0^t \left\{ \operatorname{erfc} \left[\frac{k_1 - 2a_1 \tau}{\sqrt{4\tau}} \right] + \exp(2a_1 k_1) \operatorname{erfc} \left[\frac{k_1 + 2a_1 \tau}{\sqrt{4\tau}} \right] \right\} \times \\
& \times \left\{ (\pi(t-\tau))^{-1/2} \exp \left[-\frac{(k_2 - 2a_2(t-\tau))^2}{4(t-\tau)} \right] - a_2 \exp(2a_2 k_2) \operatorname{erfc} \left[\frac{k_2 + 2a_2(t-\tau)}{\sqrt{4(t-\tau)}} \right] \right\} d\tau + \\
& + C_i
\end{aligned} \tag{B19}$$

For the K-th layer, the solution in the Laplace domain is given by:

$$\bar{C}(x,s) = \frac{v_K}{s} \frac{C_o - C_i}{(v_K - D_K \lambda_K)} \exp \left[\sum_{k=1}^{K-1} \lambda_k \ell_k \right] \exp(\lambda_K \xi_K) + \frac{C_i}{s} \tag{B17}$$

Again, it appears that the order of layers between $k=2$ and $k-1$ is irrelevant for the concentration in the K-th layer ($L_{K-1} < x < L_K$).

APPENDIX C. Analytical Solution of the ADE for a Two-layer Porous
Medium Using a Third-Type Condition at the Inlet and a Combined
First- and Third-type Condition at the Interface

Physically, it is realistic that both concentration and flux are continuous at the interface. This problem is similar to that of heat flow in a composite medium where the heat flux across the interface is continuous and intimate contact between different layers at the interface, i.e., no thermal resistance, ensures continuity in temperature (8). The application of continuity in both solute flux and concentration at the inlet is not feasible, therefore a third-type condition will be used at the inlet.

In this appendix, we seek a solution for the ADE in a medium consisting of a finite layer ($-L < x < 0$) and a semi-infinite layer ($x > 0$) (cf. 8, p.319). In contrast with the two previously investigated problems, the concentration in the first layer depends on the properties of the second layer. The problem can be stated as follows:

$$R_1 \frac{\partial C_1}{\partial t} = D_1 \frac{\partial^2 C_1}{\partial x^2} - v_1 \frac{\partial C_1}{\partial x} \quad -L < x < 0 \quad t > 0 \quad (C1a)$$

$$R_2 \frac{\partial C_2}{\partial t} = D_2 \frac{\partial^2 C_2}{\partial x^2} - v_2 \frac{\partial C_2}{\partial x} \quad x > 0 \quad t > 0 \quad (C1b)$$

$$C_1(x, 0) = g_1 \quad -L < x < 0 \quad (C2a)$$

$$C_2(x, 0) = g_2 \quad x > 0 \quad (C2b)$$

$$\left(v_1 C_1 - D_1 \frac{\partial C_1}{\partial x} \right) \Big|_{x \downarrow -L} = v_1 f = \begin{cases} v_1 C_o & 0 < t \leq t_o \\ 0 & t > t_o \end{cases} \quad (C2c)$$

$$C_1 \Big|_{x \uparrow 0} = C_2 \Big|_{x \downarrow 0} \quad t > 0 \quad (C2d)$$

$$\theta_1 v_1 C_1 - \theta_1 D_1 \frac{\partial C_1}{\partial x} \Big|_{x \uparrow 0} = \theta_2 v_2 C_2 - \theta_2 D_2 \frac{\partial C_2}{\partial x} \Big|_{x \downarrow 0} \quad t > 0 \quad (C2e)$$

$$\frac{\partial C_2}{\partial x} \Big|_{x \rightarrow \infty} = 0 \quad t > 0 \quad (C2f)$$

The Laplace transforms of (C1) and (C2) are:

$$\frac{d^2 \bar{C}_1}{dx^2} - \frac{v_1}{D_1} \frac{d\bar{C}_1}{dx} - \frac{sR_1}{D_1} \bar{C}_1 + \frac{g_1 R_1}{D_1} = 0 \quad (C3a)$$

$$\frac{d^2 \bar{C}_2}{dx^2} - \frac{v_2}{D_2} \frac{d\bar{C}_2}{dx} - \frac{sR_2}{D_2} \bar{C}_2 + \frac{g_2 R_2}{D_2} = 0 \quad (C3b)$$

$$(v_1 \bar{C}_1 - D_1 \frac{d\bar{C}_1}{dx}) \Big|_{x \downarrow -L} = v_1 f = \frac{C_0}{s} [1 - \exp(-t_0 s)] \quad t > 0 \quad (C4a)$$

$$\bar{C}_1 \Big|_{x \uparrow 0} = \bar{C}_2 \Big|_{x \downarrow 0} \quad t > 0 \quad (C4b)$$

$$\theta_1 D_1 \frac{d\bar{C}_1}{dx} \Big|_{x \uparrow 0} = \theta_2 D_2 \frac{d\bar{C}_2}{dx} \Big|_{x \downarrow 0} \quad t > 0 \quad (C4c)$$

$$\frac{d\bar{C}_2}{dx} \Big|_{x \rightarrow \infty} = 0 \quad t > 0 \quad (C4d)$$

Note that Eq.(C4c) follows from Eq.(C2e) assuming steady flow and continuity in concentration. The general solution of Eq.(C3) can be written as:

$$\bar{C}_1(x, s) = \left[\alpha \exp(\lambda_1 x) + \beta \exp(-\lambda_1 x) \right] \exp\left(\frac{v_1 x}{2D_1}\right) + \frac{g_1}{s} \quad (C5a)$$

$$\bar{C}_2(x, s) = \left[\gamma \exp(\lambda_2 x) + \mu \exp(-\lambda_2 x) \right] \exp\left(\frac{v_2 x}{2D_2}\right) + \frac{g_2}{s} \quad (C5b)$$

where α , β , γ and μ are coefficients determined by the boundary

conditions and $\lambda_1 = \sqrt{\left(\frac{v_1}{2D_1}\right)^2 + \frac{sR_1}{D_1}}$.

Application of Eq.(C4d) gives $\gamma=0$, whereas the use of (C4b) shows

that $\mu = \alpha + \beta$. During steady flow, the following relationship between α and β can be established with Eq. (C4c):

$$\alpha \left[v_2 D_1 \lambda_1 + v_1 D_2 \lambda_2 \right] = \beta \left[v_2 D_1 \lambda_1 - v_1 D_2 \lambda_2 \right] \quad (C6a)$$

or using $q_1 = (D_1 \lambda_1) / v_1$:

$$\alpha = \left[\frac{q_1 - q_2}{q_1 + q_2} \right] \beta \quad (C6b)$$

whereas application of Eq. (C4a) yields:

$$\alpha \left[\frac{1}{2} - q_1 \right] \exp(-\lambda_1 L) + \beta \left[\frac{1}{2} + q_1 \right] \exp(\lambda_1 L) = \frac{v_1}{s} \left[C_o - g_1 - \exp(-t_o s) \right] \exp\left(\frac{v_1 L}{2D_1} \right) \quad (C7)$$

Explicit expressions for α and β can be found by using both Eq. (C6) and (C7). It is convenient to transform the position coordinate such that the interface is located at $x=0$. The resulting equations for \bar{C}_1 and \bar{C}_2 are:

$$\bar{C}_1(x, s) = \frac{g_1}{s} + \frac{C_o - g_1 - \exp(-t_o s)}{\left(\frac{1}{2} - q_1 \right) (q_1 - q_2) \exp(-\lambda_1 L) + \left(\frac{1}{2} + q_1 \right) (q_1 + q_2) \exp(\lambda_1 L)} \times \frac{v_1}{s} \left\{ (q_1 - q_2) \exp\left[\frac{v_1 x}{2D_1} + \lambda_1 (x-L) \right] + (q_1 + q_2) \exp\left[\frac{v_1 x}{2D_1} - \lambda_1 (x-L) \right] \right\} \quad (C8)$$

$$\bar{C}_2(x, s) = \frac{g_2}{s} + \frac{2q_1 [C_o - g_1 - \exp(-t_o s)] \exp\left(\frac{v_1 L}{2D_1} \right)}{\left(\frac{1}{2} - q_1 \right) (q_1 - q_2) \exp(-\lambda_1 L) + \left(\frac{1}{2} + q_1 \right) (q_1 + q_2) \exp(\lambda_1 L)} \times \left\{ \frac{v_1}{s} \exp\left[\frac{v_2 (x-L)}{2D_2} - \lambda_2 (x-L) \right] \right\} \quad (C9)$$

Inversion as described in Appendix A and B or application of the inversion theorem or the expansion procedure (8) did not seem feasible. Concentration profiles were therefore obtained via numerical inversion of the Laplace transform according to the algorithm by Crump (9). As an approximate analytical solution, Eq. (B14) can be used.

APPENDIX D. Numerical Integration with the Gauss Chebyshev Formula

Numerical integration can be performed in many ways (7). We attempted Gaussian quadrature and the Gauss-Chebyshev method. The latter one gave more accurate results at the end points and was easier to code. In particular, the flexibility in the number of points is attractive.

In order to evaluate the integrals appearing in Eq.(11) to (13), the integration variable τ , varying between 0 and t, needs to be transformed to a variable η varying between -1 and +1. This was accomplished by the linear transformation $\eta = [\frac{1}{t}(2\tau-t)]$. For a function $f(\tau)$ the integration changes as follows:

$$\int_0^t f(\tau) d\tau = \int_{-1}^{+1} \frac{t}{2} f\left(\frac{t\eta + t}{2}\right) d\eta \quad (D1)$$

The Gauss-Chebyshev formula yields (31):

$$\int_{-1}^{+1} \frac{f(\eta)}{\sqrt{1-\eta^2}} d\eta = a_1 f(\eta_1) + a_2 f(\eta_2) + \dots + a_n f(\eta_n) + E_T \quad (D2)$$

where E_T is the truncation error, and a and η are the coefficients and points, respectively, which are defined for n points as:

$$\begin{aligned} \eta_k &= \cos\left(\frac{(2k-1)\pi}{2n}\right) \\ a_1 &= a_2 = \dots = a_k = \dots = a_n = \frac{\pi}{n} \quad k=1,2,\dots,n \end{aligned} \quad (D3)$$

In our case, the transformation of variables is straightforward. Because the denominator does not contain a term $\sqrt{(1-\eta^2)}$, both denominator and numerator of the transformed function are multiplied with this factor (cf. Appendix G).

APPENDIX E. Expressions for a_i , b_i , c_i , and f_i to Solve
the ADE for a Non-layered and a Layered Soil

Non-layered soil

inlet condition ($x=0$) $j \geq 0$

$c_1 = 0, b_1 = 1, f_1 = X_0$ first-type

 $c_1 = -2\Delta t G$

$b_1 = R_1^j + 2\Delta t(G + 2H(1 + \frac{H}{G}))$ third-type

$f_1 = (2R_1^j - b_1) X_1^j + 2\Delta t G X_2^j + 8\Delta t H(1 + \frac{H}{G}) X_0$

 $a_i = -G - H$

$b_i = 2G + \frac{R_i^j}{\Delta t}$

$i=2, 3, \dots, n-1$

$c_i = -G + H$

$j \geq 0$

$f_i = -a_i X_{i-1}^j + (b_i - 4G) X_i^j - c_i X_{i+1}^j$

outlet condition ($x=L$) $j \geq 0$

$a_n = -1,$

$b_n = 1 + \frac{R_n^j}{2\Delta t G}$

$f_n = X_{n-1}^j + (b_n - 2) X_n^j$

initial condition ($t=0$)

$X_i^0 = \begin{cases} X_0 & i=1 \\ X_i & i>1 \end{cases}$ first-type

$X_i^0 = \begin{cases} \frac{24H}{24H+25G} X_0 & i=1 \\ X_i & i>1 \end{cases}$ third-type

Note that $G=D/(2\Delta x^2)$ and $H=v/(4\Delta x)$

APPENDIX E. Continued

Layered soil

inlet condition ($x=0$) $j \geq 0, k=1$

$$a_1 = c_1 = 0, \quad b_1 = 1, \quad f_1 = X_0 \quad \text{first-type}$$

$$a_1 = 0, \quad c_1 = -2\Delta t G_1$$

$$b_1 = R_{11}^j + 2\Delta t(G_1 + 2H_1(1 + \frac{H_1}{G_1})) \quad \text{third-type}$$

$$f_1 = (2R_{11}^j - b_1) X_1^j + 2\Delta t G_1 X_2^j + 8\Delta t H_1(1 + \frac{H_1}{G_1}) X_0$$

coefficients for nodes not located at the boundaries or interface

$$a_i = -G_k - H_k$$

$$b_i = 2G_k + \frac{R_{ik}^j}{\Delta t} \quad j=0, 1, 2, \dots$$

$$c_i = -G_k + H_k \quad k=1, 2, \dots, K$$

$$f_i = -a_i X_{i-1}^j + (b_i - 4G_k) X_i^j - c_i X_{i+1}^j$$

interface condition ($x=L_k$) $j \geq 0, k=1, 2, \dots, K-1$

$$a_i = -w_k G_k - w_{k+1} G_{k+1} - w_k H_k - w_{k+1} H_{k+1}$$

$$b_i = \frac{w_k R_{ik}^j + w_{k+1} R_{i,k+1}^j}{\Delta t} + 2w_k G_k + 2w_{k+1} G_{k+1} \quad \text{first-type}$$

$$c_i = -w_k G_k - w_{k+1} G_{k+1} + w_k H_k + w_{k+1} H_{k+1}$$

$$f_i = -a_i X_{i-1}^j + (b_i + 4w_k G_k + 4w_{k+1} G_{k+1}) X_i^j - c_i X_{i+1}^j$$

$$\zeta_k = 2\Delta x \left(\frac{v}{D}\right)_k \quad \phi_k = \frac{2}{\Delta x} \left(\frac{D}{v}\right)_{k+1}$$

$$a_{i\uparrow} = -2G_k$$

$$b_{i\uparrow} = \frac{R_{ik}^j}{\Delta t} + 2G_k + \zeta_k (H_k - G_k) \quad \text{third-type}$$

$$c_{i\uparrow} = \zeta_k (G_k - H_k)$$

$$f_{i\uparrow} = 2G_k X_{i-1}^j + \left[\frac{R_{ik}^j}{\Delta t} - 2G_k + \zeta_k (G_k - H_k) \right] X_{i\uparrow}^j + \left[(\phi_{k+1} + 1) \zeta_k (H_k - G_k) \right] X_{i\downarrow}^j \\ + \left[\phi_{k+1} \zeta_k (G_k - H_k) \right] X_{i+1}^j$$

APPENDIX E. Continued.

$$a_i = -\theta_k D_k,$$

$$b_i = \theta_k D_k + \theta_{k+1} D_{k+1}$$

second-type

$$c_i = -\theta_{k+1} D_{k+1}$$

$$f_i = -a_i X_{i-1}^j - b_i X_i^j - c_i X_{i+1}^j$$

$$a_{i\downarrow} = -\zeta_{k+1} (G_{k+1} + H_{k+1})$$

$$b_{i\downarrow} = \frac{R_{i,k+1}^j}{\Delta t} + 2G_{k+1} + \zeta_{k+1} (G_{k+1} + H_{k+1})$$

$$c_{i\downarrow} = -2G_{k+1}$$

third-type

$$f_{i\downarrow} = \left[\phi_k \zeta_{k+1} (G_{k+1} + H_{k+1}) \right] X_{i-1}^j + \left[(1-\phi_k) \zeta_{k+1} (G_{k+1} + H_{k+1}) \right] X_{i\uparrow}^j +$$

$$\left[\frac{R_{i,k+1}^j}{\Delta t} - 2G_{k+1} - \zeta_{k+1} (G_{k+1} + H_{k+1}) \right] X_{i\downarrow}^j + 2G_{k+1} X_{i+1}^j$$

outlet condition ($x=L_k$) $j \geq 0$

$$a_n = -1, \quad c_n = 0$$

$$b_n = 1 + \frac{R_{n,k}^j}{2\Delta t G_k}$$

$$f_n = X_{n-1}^j + (b_n - 2) X_n^j$$

initial condition ($t=0$) $j=0$ $k=1, 2, \dots, K$

$$X_i^0 = \begin{cases} X_0 & i=1 \\ X_i & i>1 \end{cases} \quad \text{first-type}$$

$$X_i^0 = \begin{cases} \frac{24H_k}{24H_k + 25G_k} X_0 & i=1 \\ X_i & i>1 \end{cases} \quad \text{third-type}$$

Note that $G_k = D_k / (2\Delta x^2)$ and $H_k = v_k / (4\Delta x)$

APPENDIX F. List of Parameter Values Used for Simulations

Fig.	k	v	D	θ	ρ	S_T	$\frac{dY}{dX}$	X_i	t_o
condition		cm/d	cm ² /d		g/cm ³	cmol /kg			d
3 ^a	1	50	50			0.0		0.05	∞
3 ^b	1	50	50			0.0		0.05	∞
4	1	50	0			0.0		0.05	∞
5 ^a	1	50	50			0.0		0.05	∞
5 ^b	3	50	50			0.0		0.05	∞
6 ^a	1	1	50	50		0.0		0.05	∞
		2	50	50		0.0		0.05	∞
6 ^b	3	1	50	50	0.4	0.0		0.05	∞
		2	50	50	0.4	0.0		0.05	∞
7 ^a	1	1	50	50		0.0		0.05	∞
		2	50	50		0.0		0.05	∞
7 ^b	3	1	50	50	0.4	0.0		0.05	∞
		2	50	50	0.4	0.0		0.05	∞
7 ^c	3	1	50	50	0.4	0.0		0.05	∞
		2	50	50	0.4	0.0		0.05	∞
8 ^a	1	1	25	12.5	0.4	0.0		0.05	∞
		2	100	100	0.1	0.0		0.05	∞
8 ^b	3	1	25	12.5	0.4	0.0		0.05	∞
		2	100	100	0.1	0.0		0.05	∞
8 ^c	2	1	25	12.5	0.4	0.0		0.05	∞
		2	100	100	0.1	0.0		0.05	∞
9 ^a	1	1	100	100	0.1	0.0		0.05	∞
		2	25	12.5	0.4	0.0		0.05	∞
9 ^b	3	1	100	100	0.1	0.0		0.05	∞
		2	25	12.5	0.4	0.0		0.05	∞
9 ^c	2	1	100	100	0.1	0.0		0.05	∞
		2	25	12.5	0.4	0.0		0.05	∞
10 ^a	1	1	10	10		0.0		0.05	∞
		2	10	5		0.0		0.05	∞
10 ^b	3	1	10	10	0.4	0.0		0.05	∞
		2	10	5	0.4	0.0		0.05	∞
11 ^a	1	1	10	40		0.0		0.05	∞
		2	10	5		0.0		0.05	∞
11 ^b	3	1	10	40	0.4	0.0		0.05	∞
		2	10	5	0.4	0.0		0.05	∞
12 ^a	1	1	20	20	0.5	0.0		0.05	∞
		2	50	20	0.2	0.0		0.05	∞
12 ^b	3	1	20	20	0.5	0.0		0.05	∞
		2	50	20	0.2	0.0		0.05	∞

APPENDIX F. Continued.

Fig.	k	v	D	θ	ρ	S_T	$\frac{dY}{dX}$	X_i	t_o	
condition		cm/d	cm ² /d		g/cm ³	cmol /kg			d	
13 ^a	1	1	50	20	0.2	0.0		0.05	∞	
		2	20	20	0.5	0.0		0.05	∞	
13 ^b	3	1	50	20	0.2	0.0		0.05	∞	
		2	20	20	0.5	0.0		0.05	∞	
14 ^a	3	50	50			0.0		0.05	∞	
14 ^b	3	50	50	0.4	1.5	10.0	1	0.05	∞	
15 ^a	3	50	50	0.4	1.4	10.0	$3X^2$	shown	∞	
15 ^b	3	50	50	0.4	1.4	10.0	1		∞	
15 ^c	3	50	50	0.4	1.4	10.0	$\frac{1}{3}X^{-2/3}$	s	∞	
16	3	25	10	0.4	1.4	10.0	$\frac{1}{3}X^{-2/3}$	h	∞	
17 ^a	3	50	20	0.4	1.4	10.0	$3X^2$	o	∞	
17 ^b	3	50	20	0.4	1.4	10.0	1	w		
17 ^c	3	50	20	0.4	1.4	10.0	$\frac{1}{3}X^{-2/3}$	n	∞	
18 ^a	3	50	20	0.4	1.4	1.0	$3X^2$	0.05	0.4	
18 ^b	3	50	20	0.4	1.4	1.0	1	0.05	0.4	
18 ^c	3	50	20	0.4	1.4	1.0	$\frac{1}{3}X^{-2/3}$	0.05	0.4	
19 ^a	3	1	50	10	0.4	0.0		0.05	0.1	
		2	50	10	0.4	0.0		0.05	0.1	
19 ^b	3	1	50	10	0.4	0.0		0.05	0.1	
		2	50	100	0.4	0.0		0.05	0.1	
20 ^a	3	1	50	20	0.4	0.0		0.05	0.2	
		2	50	20	0.4	0.0		0.05	0.2	
20 ^b	3	1	50	20	0.4	1.4	0.0	1	0.05	0.2
		2	50	20	0.4	1.4	2.0	1	0.05	0.2
21 ^a	3	1	50	20	0.4	1.4	1.0	1	0.05	0.2
		2	50	20	0.4	1.4	1.0	$3X^2$	0.05	0.2
21 ^b	3	1	50	20	0.4	1.4	1.0	1	0.05	0.2
		2	50	20	0.4	1.4	1.0	$\frac{1}{3}X^{-2/3}$	0.05	0.2

APPENDIX F. Continued.

Fig.	k	v	D	θ	ρ	S_T	$\frac{dY}{dX}$	X_i	t_o	
condition		cm/d	cm ² /d		g/cm ³	cmol /kg			d	
22 ^a	3	1	100	52	0.4	1.3	1.0	1	0.05	∞
		2	100	52	0.4	1.3	1.0	1	0.05	∞
		3	100	52	0.4	1.3	1.0	1	0.05	∞
22 ^b	3	1	10	7	0.4	1.3	1.0	1	0.05	∞
		2	8	18	0.5	1.3	5.0	1	0.05	∞
		3	10	7	0.4	1.3	1.0	1	0.05	∞
23 ^a	3	1	10	7	0.2	1.3	1.0	1	0.05	∞
		2	10	7	0.2	1.3	1.0	1	0.05	∞
		3	10	7	0.2	1.3	1.0	1	0.05	∞
23 ^b	3	1	1	4	0.2	1.3	1.0	1	0.05	∞
		2	0.5	2.5	0.4	1.3	0.0	1	0.05	∞
		3	1	4	0.2	1.3	1.0	1	0.05	∞

APPENDIX G. Listing of Computer Programs

This Appendix contains the various WATFIV programs for the IBM-mainframe used in this study. The values of the input parameters are entered as program parameters in the declaration section, which is followed by a brief explanation of these variables. Initial concentration profiles can be entered as input variables (cf. HOMSOIL). Any set of consistent units can be used. The output format is specified in the program. The structure is similar for all programs and should be self explanatory.

- FISEC : Analytical solution of the ADE for the second layer of a two-layer medium using a first-type condition
- THSEC : Analytical solution of the ADE for the second layer of a two-layer medium using a third-type condition
- HOMSOIL : Numerical solution of the ADE for a homogeneous medium using a first- or a third-type condition
- VARTIM : Numerical solution of the ADE for a homogeneous medium using a first- or a third-type condition with a variable time step
- LAY1 : Numerical solution of the ADE for a layered medium using a first-type condition
- LAY3 : Numerical solution of the ADE for a layered medium using a third-type condition

Listing of FISEC

```
//FIG10A JOB (AYL59FL,124),'FEIKE LEIJ',MSGCLASS=P,
// NOTIFY=AYL59FL,MSGLEVEL=(1,1),REGION=1024K,TIME=(1,59)
/*ROUTE PRINT RMT4
/*JOBPARM LINES=10
//STEP1 EXEC WATFIV
//WATFIV.SYSIN DD *
/JOB FEIKE,TIME=(5),PAGES=60
```

C

```
INTEGER NUM/7/,I,J,UP/100/
REAL R/1.0/,POS(7),VELO1/10./,VELO2/10./,DIF01/100./,DIF02/10./
REAL A1,A2,C(30),F,H,M,N,K1,K2(25),DELPOS/1./,DUM
REAL ROOT(100),COEF,SUM,CON(12),DIMCON(12),X(12)
REAL NO/0.0/,CIN/.0005/,CZERO/.01/,FACT,TEL1(100),TEL2(100)
REAL NOEM2(100),NOEM3(100),LEN1/6./,REPOS(25)
REAL EXF,FACT4(100),B(100),D(100),E(100),G(100),NOEM1(100)
REAL BOUND/170./,LOEF,DELTIM/0.1/,TIMMAX/4.0/
```

C

C VARIABLES TO BE SPECIFIED

C	NUM	: NUMBER OF POSITIONS IN SECOND LAYER	
C	VELO1	: PORE WATER VELOCITY IN FIRST LAYER	L/T
C	VELO2	: PORE WATER VELOCITY IN SECOND LAYER	L/T
C	DIF01	: DISPERSION COEFFICIENT IN FIRST LAYER	L2/T
C	DIF02	: DISPERSION COEFFICIENT IN SECOND LAYER	L2/T
C	CON	: CONCENTRATION	M/L3
C	DIMCON	: (C-CI)/(CO-CI)	-
C	X	: C/CO	-
C	DELPOS	: SPACE INCREMENT FOR ANALYTICAL SOLUTION	L
C	CIN	: INITIAL CONCENTRATION	M/L3
C	CZERO	: ELUENT CONCENTRATION	M/L3
C	LEN1	: POSTION OF INTERFACE	L
C	DELTIM	: TIME INCREMENT FOR ANALYTICAL SOLUTION	T
C	TIMMAX	: MAXIMUM TIME FOR ANALYTICAL SOLUTION	T

C

```
PRINT, '*****'
PRINT, '*
PRINT, '*
PRINT, '* ANALYTICAL SOLUTION OF THE ADVECTION-DISPERSION
PRINT, '* EQUATION FOR 1-D TRANSPORT IN THE 2-ND LAYER OF
PRINT, '* A SEMI-INFINITE POROUS MEDIUM
PRINT, '* 1-ST TYPE BOUNDARY CONDITION
PRINT, '*
PRINT, '*****'
```

C

C INITIALIZE SOME BASIC VARIABLES

C

```
A1=VELO1/(2.0*SQRT(DIF01))
A2=VELO2/(2.0*SQRT(DIF02))
K1=LEN1/(SQRT(DIF01))
POS(1)=LEN1
REPOS(1)=0.0
K2(1)=0.0
```

```

DO 10 I=2,NUM
  POS(I)=POS(I-1)+DELPOS
  REPOS(I)=POS(I)-LEN1
  K2(I)=REPOS(I)/(SQRT(DIF02))
10 CONTINUE
C
PRINT, ' '
PRINT, '
PRINT 113, 'TIME', ' ', (POS(I), I=1, NUM)
113 FORMAT(' ', A7, A15, 7F7.3)
PRINT, ' '
C
C INITIALIZE ROOTS AND COEFFICIENTS FOR GAUSS-CHEBYSHEV
C
DO 23 J=1,UP
  DUM=((2*J-1)*1.57096327)/FLOAT(UP)
  ROOT(J)=COS(DUM)
23 CONTINUE
C
COEF=3.141592654/FLOAT(UP)
C
TIME=DELTIM
WHILE(TIME.LE.TIMMAX) DO
C
C INITIALIZE VARIABLES FOR COMPLEMENTARY ERROR AND EXPONENTIAL FUNCTIONS
C
DO 20 J=1,UP
  TEL1(J)=A1*TIME*(ROOT(J)+1.0)
  TEL2(J)=A2*TIME*(1.0-ROOT(J))
  NOEM1(J)=2.0*TIME*(ROOT(J)+1)
  NOEM2(J)=0.25*NOEM1(J)*SQRT(0.25*NOEM1(J))
  NOEM3(J)=SQRT(2.*TIME*(1.-ROOT(J)))
  FACT4(J)=SQRT(1.0-ROOT(J)*ROOT(J))
20 CONTINUE
C
C INITIALIZE POSITION DEPENDENT VARIABLES
C
DO 99 I=1,NUM
  C(I)=2*A2*K2(I)
  DO 30 J=1,UP
    B(J)=-((K1-TEL1(J))**2)/NOEM1(J)
    D(J)=(K2(I)-TEL2(J))/NOEM3(J)
    E(J)=1.0/NOEM2(J)
    G(J)=(K2(I)+TEL2(J))/NOEM3(J)
30 CONTINUE
C
FACT=(CZERO-CIN)*K1*0.070523697*TIME
C
C EVALUATE THE INTEGRAL
C
SUM=0.0

```

POSITIONS'

```

DO 40 J=1,UP
  IF (B(J).LE.-BOUND) THEN
    LOEF=0.0
  ELSE
    LOEF=EXP(B(J))
  ENDIF
SUM=SUM+COEF*FACT4(J)*E(J)*LOEF*(EXF(NO,D(J))+EXF(C(I),G(J)))
40 CONTINUE
C
  CON(I)=SUM*FACT+CIN
  DIMCON(I)=(CON(I)-CIN)/(CZERO-CIN)
  X(I)=CON(I)/CZERO
99 CONTINUE
C
  PRINT 114,TIME,'C-CI/CO-CI',(DIMCON(I),I=1,NUM)
114 FORMAT(' ',F7.3,A15,7F7.3)
C
  PRINT 113,' ','C/CO',(X(I),I=1,NUM)
C
  PRINT,' '
C
  TIME=TIME+DELTIM
  ENDWHILE
C
  STOP
  END
C
  REAL FUNCTION EXF(Q,Z)
C
  REAL Q,Z,T,STUP1,STUP2,XX,YY,QQ
C
  EXF=0.0
  STUP1=ABS(Q)
C
  IF (STUP1.GT.170 .AND. Z.LE.0.0) GO TO 40
  IF(Z.NE.0.) GO TO 31
  EXF=EXP(Q)
  GO TO 40
31 QQ=Q-Z*Z
  STUP2=ABS(QQ)
  IF((STUP2.GT.170) .AND. (Z.GT.0.0)) GO TO 40
  IF(QQ.LT.-170) GO TO 34
  XX=ABS(Z)
  IF (XX .GT. 3.0) GO TO 32
  T=1.0/(1.0+0.3275911*XX)
  YY=T*(.2548296-T*(.2844967-T*(1.421414-
$   T*(1.453152-1.061405*T))))
  GO TO 33
32 YY=0.56418958/(XX+.5/(XX+.1/(XX+1.5/(XX+2./
$   (XX+2.5/(XX+1.))))))
33 EXF=YY*EXP(QQ)

```

```
C
 34   IF(Z.LT.0.0)THEN
      EXF=2.*EXP(Q)-EXF
      ENDIF
C
 40   CONTINUE
C
      RETURN
      END
/GO
```

Listing of THSEC

```
//FIG10B JOB (AYL59FL,124),'FEIKE LEIJ',MSGCLASS=P,
// NOTIFY=AYL59FL,MSGLEVEL=(1,1),REGION=1024K,TIME=(0,59)
/*ROUTE PRINT RMT4
/*JOBPARM LINES=10
//STEP1 EXEC WATFIV
//WATFIV.SYSIN DD *
/JOB FEIKE,TIME=(05),PAGES=60
```

```
C
INTEGER NUM/7/,I,J,UP/100/
REAL R/1.0/,POS(7),VELO1/10./,VELO2/10./,DIFO1/100./,DIFO2/10./
REAL TEL2(100),A1,A2,C,G(100),F(25),H,M,N,K1,K2(25),DELPOS/1.0/
REAL ROOT(100),COEF,TERM1,TERM2,CON(25),DIMCON(25),X(25)
REAL DUMMY,CIN/.0005/,CZERO/.01/,FACT1,FACT2,TEL1(100)
REAL NO/0.0/,NOEM1(100),NOEM2(100),LEN1/6./,REPOS(25),TIME
REAL DUM,LOEF,CHECK,EXF,FACT3(100),DUMMY2,B(100),D(100),E(100)
REAL NOEM3(100),NOEM4(100),BOUND/150./,DELTIM/.1/,TIMMAX/4.0/
REAL GG(100),VMC1/0.5/,VMC2/0.5/
```

```
C
C VARIABLES TO BE SPECIFIED
C NUM : NUMBER OF POINTS IN SECOND LAYER
C VELO1 : PORE WATER VELOCITY IN FIRST LAYER L/T
C VELO2 : PORE WATER VELOCITY IN SECOND LAYER L/T
C DIFO1 : DISPERSION COEFFICIENT IN FIRST LAYER L2/T
C DIFO2 : DISPERSION COEFFICIENT IN SECOND LAYER L2/T
C CIN : INITIAL CONCENTRATION M/L3
C CZERO : ELUENT CONCENTRATION M/L3
C LEN1 : POSITION OF INTERFACE L
C DELTIM : TIME STEP FOR ANALYTICAL SOLUTION T
C DELPOS : SPACE STEP FOR ANALYTICAL SOLUTION L
C TIMMAX : MAXIMUM TIME FOR ANALYTICAL SOLUTION T
C VMC1 : VOLUMETRIC WATER CONTENT IN FIRST LAYER L3/L3
C VMC2 : VOLUMETRIC WATER CONTENT IN SECOND LAYER L3/L3
C
```

```
PRINT, '*****'
PRINT, '*
T H S E C *
PRINT, '*
PRINT, '* ANALYTICAL SOLUTION OF THE ADVECTION-DISPERSION *
PRINT, '* EQUATION FOR 1-D TRANSPORT IN THE 2-ND LAYER OF *
PRINT, '* A SEMI-INFINITE POROUS MEDIUM *
PRINT, '* 3-RD TYPE BOUNDARY CONDITION *
PRINT, '*
PRINT, '*****'
```

```
C
TIME=DELTIM
C
C INITIALIZE SOME BASIC VARIABLES
C
A1=VELO1/(2.0*SQRT(DIFO1))
A2=VELO2/(2.0*SQRT(DIFO2))
K1=LEN1/(SQRT(DIFO1))
POS(1)=LEN1
```

```

REPOS(1)=0.0
K2(1)=0.0
DO 10 I=2,NUM
    POS(I)=POS(I-1)+DELPOS
    REPOS(I)=POS(I)-LEN1
    K2(I)=REPOS(I)/(SQRT(DIFO2))
10 CONTINUE
C
PRINT,'DEPTH OF FIRST LAYER      ',LEN1
PRINT,'DEPTH OF SECOND LAYER    ',REPOS(NUM)
C
PRINT,' '
PRINT,' '
PRINT 113,'TIME', ' ',(POS(I),I=1,NUM)
113 FORMAT(' ',A7,A15,7F7.3)
PRINT,' '
C
C INITIALIZE ROOTS AND COEFFICIENTS GAUSS-CHEBYSHEV
C
DO 23 J=1,UP
    DUM=((2*J-1)*1.57096327)/FLOAT(UP)
    ROOT(J)=COS(DUM)
23 CONTINUE
C
COEF=3.141592654/FLOAT(UP)
C
WHILE(TIME.LE.TIMMAX) DO
C
C INITIALIZE VARIABLES FOR COMPLEMENTARY ERROR AND EXPONENTIAL FUNCTIONS
C
DO 20 J=1,UP
    TEL1(J)=A1*TIME*(ROOT(J)+1)
    TEL2(J)=A2*TIME*(1.0-ROOT(J))
    NOEM1(J)=SQRT(2.0*TIME*(ROOT(J)+1))
    NOEM2(J)=2.*TIME*(1.-ROOT(J))
    NOEM3(J)=SQRT(NOEM2(J))
    DUMMY=0.785398163*NOEM2(J)
    NOEM4(J)=SQRT(DUMMY)
    FACT3(J)=SQRT(1.0-ROOT(J)*ROOT(J))
20 CONTINUE
C
C INITIALIZE POSITION DEPENDENT VARIABLES
C
DO 99 I=1,NUM
    C=2.*A1*K1
    F(I)=2.*A2*K2(I)
    DO 30 J=1,UP
        B(J)=(K1-TEL1(J))/NOEM1(J)
        D(J)=(K1+TEL1(J))/NOEM1(J)
        GG(J)=(K2(I)+TEL2(J))/NOEM3(J)
        E(J)=1./NOEM4(J)
30 CONTINUE
99 CONTINUE

```

```

          G(J)=-((K2(I)-TEL2(J))**2)/NOEM2(J)
30      CONTINUE
C
      FACT2=(CIN*(VELO1*(VMC1/VMC2)-VELO2))/(SQRT(DIFO2))
      FACT1=0.25*VMC1*VELO1*(CZERO-CIN)*TIME*COEF/(VMC2*SQRT(DIFO2))
C
      H=-((K2(I)-2.0*A2*TIME)**2)/(4.0*TIME)
      M=0.5*(K2(I)-2.0*A2*TIME)/(SQRT(TIME))
      N=0.5*(K2(I)+2.0*A2*TIME)/(SQRT(TIME))
C
C EVALUATE THE INTEGRAL WITH GAUSS-CHEBYSHEV
C
      TERM1=0.0
      DO 40 J=1,UP
          IF(G(J).LT.-BOUND)THEN
              LOEF=0.0
          ELSE
              LOEF=EXP(G(J))
          ENDIF
C
          TERM1=TERM1+FACT3(J)*(EXF(NO,B(J))+EXF(C,D(J)))*
$          (E(J)*LOEF-A2*EXF(F(I),GG(J)))
40      CONTINUE
C
      TERM1=FACT1*TERM1
C
C EVALUATE SECOND PART OF THE ANALYTICAL SOLUTION
C
      DUMMY=TIME/3.141592654
      DUMMY=SQRT(DUMMY)
      IF(H.LE.-BOUND) THEN
          LOEF=0.
      ELSE
          LOEF=EXP(H)
      ENDIF
C
      TERM2=FACT2*(DUMMY*LOEF+((0.25*EXF(NO,M))/A2)
$      -((0.25*(1.+F(I)+4.*A2*A2*TIME)*EXF(F(I),N))/A2))
C
      CON(I)=TERM1+TERM2+CIN
      DIMCON(I)=(CON(I)-CIN)/(CZERO-CIN)
      X(I)=CON(I)/CZERO
99      CONTINUE
C
      PRINT 114,TIME,'C-CI/CO-CI',(DIMCON(I),I=1,NUM)
114     FORMAT(' ',F7.3,A15,7F7.3)
C
      PRINT 113,' ','C/CO',(X(I),I=1,NUM)
C
      TIME=TIME+DELTIM
      ENDWHILE

```



```

C      STOP
      END
C
C      REAL FUNCTION EXF(Q,Z)
C
C      REAL LOEF,Q,Z,T,STUP1,STUP2,XX,YY,QQ,BOUND2/120./
C
      EXF=0.0
      STUP1=ABS(Q)
      IF((STUP1.GT.BOUND2) .AND. (Z.LE.0.0)) GO TO 40
      IF(Z.NE.0.0) GO TO 31
      EXF=EXP(Q)
      GO TO 40
31     QQ=Q-Z*Z
      STUP2=ABS(QQ)
      IF((STUP2.GT.BOUND2) .AND. (Z.GT.0.)) GO TO 40
      IF(QQ.LT.-BOUND2) GO TO 34
      XX=ABS(Z)
      IF(XX.GT.3.) GO TO 32
          T=1.0/(1.0+0.3275911*XX)
          YY=T*(.2548296-T*(.2844967-T*(1.421414-
$           T*(1.453152-1.061405*T))))
      GO TO 33
32     YY=0.56418958/(XX+.5/(XX+.1/(XX+1.5/(XX+2./
$           (XX+2.5/(XX+1.))))))
33     EXF=YY*EXP(QQ)
C
C      34     IF(Z.LT.0.0) THEN
          EXF=2.*EXP(Q)-EXF
          ENDIF
C
C      40     CONTINUE
C
      RETURN
      END
/GO

```

Listing of HOMSOIL

```
//FIG22 JOB (AYL59FL,124),'FEIKE LEIJ',MSGCLASS=P,
// NOTIFY=AYL59FL,MSGLEVEL=(1,1),REGION=1024K,TIME=(1,59)
/*ROUTE PRINT RMT4
/*JOBPARM LINES=10
//STEP1 EXEC WATFIV
//WATFIV.SYSIN DD *
/JOB FEIKE,TIME=(05),PAGES=60
```

C

C VARIABLE DECLARATION

```
INTEGER I,J,K,SIZE/25/,DUMBOU,INLET/3/
REAL DELTIM/0.005/,DELPOS/0.5/,COLD(63),CNEW(63),CTOT/0.01/
REAL TIMMAX/5.0/,TIME,POS(63),CIN/1./
REAL DBD/1.4/,CEC/0.0/,VMC/0.4/,VELO/50./,DIFO/50./
REAL A(63),B(63),C(63),F(63),CINIT/0.05/
REAL DBDVMC,G,H,RETCO(63),ADS(63)
REAL ACCNEW,ACCOLD,ACCIN,ORMB,RMB,SUMFLU,SUMACC,FLUX
```

C

C VARIABLES

```
C INLET : INLET CONDITION(FIRST=1,THIRD=3)
C SIZE : NUMBER OF SPATIAL NODES
C K : PRINT COUNTER
C DELTIM : TIME STEP T
C DELPOS : SPACE STEP L
C COLD : CONCENTRATION AT OLD TIME LEVEL -
C CNEW : CONCENTRATION AT NEW TIME LEVEL -
C CTOT : TOTAL SOLUTE CONCENTRATION M/L3
C TIMMAX : MAXIMUM TIME FOR NUMERICAL SIMULATION T
C CIN : ELUENT CONCENTRATION -
C DBD : DRY BULK DENSITY M/L3
C CEC : CATION EXCHANGE CAPACITY (MMOL/G) M/M
C VMC : VOLUMETRIC WATER CONTENT L3/L3
C VELO : PORE WATER VELOCITY L/T
C DIFO : DISPERSION COEFFICIENT L2/T
C CINIT : INITIAL CONCENTRATION -
```

```
PRINT, ' '
PRINT, ' *****'
PRINT, ' * H O M S O I L *'
PRINT, ' * *'
PRINT, ' * SOLUTION OF ADVECTION DISPERSION EQUATION *'
PRINT, ' * IN DIMENSIONLESS FORM, INCLUDING NON-LINEAR *'
PRINT, ' * EXCHANGE, USING THE CRANK-NICHOLSON METHOD *'
IF (INLET.EQ.1) THEN
PRINT, ' * FIRST TYPE IBC HOMOGENEOUS SYSTEM *'
ELSE
PRINT, ' * THIRD TYPE IBC HOMOGENEOUS SYSTEM *'
ENDIF
PRINT, ' * *'
PRINT, ' *****'
PRINT, ' '
C
```

```
PRINT, 'Timestep =', DELTIM
```

```

PRINT, 'SPACE-INCREMENT=', DELPOS
PRINT, ' '
C
TIME=0.0
K=1
DUMBOU=SIZE-1
C
G=DIFO/(2.*DELPOS*DELPOS)
H=VELO/(4.*DELPOS)
C
DBDVMC=DBD*CEC/(VMC*CTOT)
C
C DEFINE INITIAL CONDITIONS AND BOUNDARY CONDITIONS FOR THE PROBLEM
C POSED, AND POSITIONS
C
READ, (COLD(I), I=1, 10)
READ, (COLD(I), I=11, 20)
C
READ, (COLD(I), I=21, SIZE)
C
DO 11 I=21, SIZE
    COLD(I)=CINIT
11 CONTINUE
C
ACCOLD=0.0
DO 26 I=2, SIZE
    CALL ADSORB(I, ADS, COLD)
    ACCOLD=ACCOLD+0.5*DELPOS*(CTOT*VMC*(COLD(I-1)+COLD(I))+
$         DBD*CEC*(ADS(I-1)+ADS(I)))
26 CONTINUE
C
SUMFLU=0.0
ACCIN=ACCOLD
C
PRINT, 'ACCIN=', ACCIN
ORMB=0.0
RMB=0.0
CIN=1.
C
IF(INLET.EQ.1) THEN
    COLD(1)=CIN
ELSE
    COLD(1)=12.*VELO*DELPOS*CIN/(12.*VELO*DELPOS+25*DIFO)
ENDIF
C
DO 10 I=1, SIZE
    POS(I)=(I-1)*DELPOS
10 CONTINUE
C
PRINT, '
PRINT 113, ' TIME ', ' ORMB ', ' RMB ', (POS(I), I=1, SIZE, 4)
113 FORMAT(' ', 3A6, 16F6.1)
114 FORMAT(' ', 19F6.2)

```

```

115 FORMAT(' ',3A6,16F6.2)
PRINT, ' '
PRINT 114, TIME, ORMB, RMB, (COLD(I), I=1, SIZE, 4)
PRINT 115, ' ', ' ', ' ', ' ', (ADS(I), I=1, SIZE, 4)
C
C INITIALIZE DUMMY VARIABLES AND TRIDIAGONAL MATRIX
C
      A(SIZE)=-1.0
      C(SIZE)=0.0
C
      WHILE (TIME.LE.TIMMAX) DO
C
      CALL EXCHAN(SIZE, COLD, DBDVMC, RETCO)
C
      IF (INLET.EQ.1) THEN
        A(1)=0.0
        B(1)=1.0
        C(1)=0.0
        F(1)=CIN
      ELSE
        A(1)=0.0
        B(1)=RETCO(1)+2.*DELTIM*(G+2.*H*(1+(H/G)))
        C(1)=-G*2.*DELTIM
        F(1)=(-B(1)+2.*RETCO(1))*COLD(1)+
$         2.*DELTIM*(G*COLD(2)+4.*H*(1+(H/G))*CIN)
      ENDIF
C
      DO 25 I=2, DUMBOU
        A(I)=-G-H
        C(I)=-G+H
        B(I)=2.0*G+(RETCO(I)/DELTIM)
        F(I)=-A(I)*COLD(I-1)+(B(I)-4.0*G)*COLD(I)-
$         C(I)*COLD(I+1)
      25 CONTINUE
C
      B(SIZE)=1.+0.5*RETCO(SIZE)/(G*DELTIM)
      F(SIZE)=COLD(DUMBOU)+(B(SIZE)-2.)*COLD(SIZE)
C
C SOLVE THE DIFFERENTIAL EQUATION WITH THE CRANK-NICOLSON METHOD
C BY USING THE THOMAS ALGORITHM
C
      CALL TRIDIA(A, B, C, CNEW, F, SIZE, INLET)
C
C REQUIRED PRINTOUT
C
      TIME=TIME+DELTIM
C
      ACCNEW=0.0
      DO 29 I=2, SIZE
        CALL ADSORB(I, ADS, CNEW)
        ACCNEW=ACCNEW+0.5*DELPOS*(CTOT*VMC*(CNEW(I-1)+CNEW(I)))+

```

```

$          DBD*CEC*(ADS(I-1)+ADS(I))
29      CONTINUE
C
      FLUX=0.5*VELO*DELTIM*CTOT*VMC*(2*CIN-CNEW(SIZE)-COLD(SIZE))
      SUMACC=ACCNEW-ACCIN
      SUMFLU=SUMFLU+FLUX
      RMB=100.*ABS((ACCNEW-ACCOLD-FLUX)/FLUX)
      ORMB=100.*ABS((SUMACC-SUMFLU)/SUMACC)
      ACCOLD=ACCNEW
C
      IF (K.EQ.PRINT) THEN
        PRINT 114,TIME,ORMB,RMB,(CNEW(I),I=1,SIZE,4)
        PRINT 115,' ',' ',' ',(ADS(I),I=1,SIZE,4)
        K=0
      ENDIF
      K=K+1
C
      DO 60 I=1,SIZE
        COLD(I)=CNEW(I)
60      CONTINUE
C
      ENDWHILE
C
      STOP
      END
C
C*****
C
      SUBROUTINE TRIDIA(A,B,C,CNEW,F,SIZE,INLET)
C
C THIS SUBROUTINE CONTAINS THE THOMAS-ALGORITHM, THE SOLUTION IS
C CONTAINED IN THE CNEW-ARRAY
C
      REAL A(63),B(63),C(63),CNEW(63),F(63)
      INTEGER SIZE,INLET
C
      REAL GAMMA(63),BETA(63)
      INTEGER I,J,DUMBOU
C
      DUMBOU=SIZE-1
C
      BETA(1)=B(1)
      GAMMA(1)=F(1)/B(1)
      DO 200 I=2,SIZE
        BETA(I)=B(I)-(A(I)*C(I-1)/BETA(I-1))
        GAMMA(I)=(F(I)-A(I)*GAMMA(I-1))/BETA(I)
200      CONTINUE
C
C BEGIN BACKWARD SUBSTITUTION FROM LAST ROW, INCLUDE BOUNDARY CONDITIONS
C
      I=SIZE-1

```

```

CNEW(SIZE)=GAMMA(SIZE)
WHILE (I.GE.1) DO
    CNEW(I)=GAMMA(I)-(C(I)*CNEW(I+1)/BETA(I))
    I=I-1
ENDWHILE
C
RETURN
END
C
C *****
C
SUBROUTINE EXCHAN(SIZE,COLD,DBDVMC,RETCO)
C
REAL COLD(63),DBDVMC,RETCO(63)
INTEGER I,SIZE
REAL SLOPE(63)
C
DO 300 I=1,SIZE
    SLOPE(I)=1.
    RETCO(I)=1.+DBDVMC*SLOPE(I)
300 CONTINUE
C
RETURN
END
C
C *****
C
SUBROUTINE ADSORB(I,ADS,CNEW)
C
REAL ADS(63),CNEW(63)
INTEGER I
C
ADS(I)=CNEW(I)
ADS(I-1)=CNEW(I-1)
C
RETURN
END
C
/GO
1.000 0.990 0.980 0.960 0.940 0.900 0.810 0.700 0.525 0.350
0.240 0.150 0.110 0.090 0.070 0.060 0.050 0.050 0.050 0.050
0.050 0.050 0.050 0.050 0.050 0.050 0.050 0.050 0.050 0.050

```

Listing of LAY1

```
//FIG19B JOB (AYL59FL,124),'FEIKE LEIJ',MSGCLASS=P,
// NOTIFY=AYL59FL,MSGLEVEL=(1,1),REGION=1024K,TIME=(1,59)
/*ROUTE PRINT RMT4
/*JOBPARM LINES=10
//STEP1 EXEC WATFIV
//WATFIV.SYSIN DD *
/JOB FEIKE,TIME=(05),PAGES=60
```

C

C VARIABLE DECLARATION

```
INTEGER I,J,K,NUMLAY/2/,LAY(2)/11,70/,SIZE/61/,DUMBOU,PRINT/10/,PC
REAL DELTIM/0.005/,DELPOS/0.5/,COLD(63),CNEW(63),CTOT/0.01/
REAL TIMMAX/5.0/,TIME,POS(63),CIN,ADS(63)
REAL DBD(2)/2*1.4/,CEC(2)/0.01,0.01/,PULSE/0.5/
REAL VMC(2)/2*0.4/,VELO(2)/50.,50./,DIFO(2)/20.,20./
REAL A(63),B(63),C(63),F(63),CINIT/0.05/
REAL DBDVMC(2),G(2),H(2),RETCO(63),W(2),FLU(2)
REAL ACCNEW,ACCOLD,ACCIN,ORMB,RMB,SUMFLU,SUMACC,FLUX
```

C

C VARIABLES

```
C NUMLAY : NUMBER OF LAYERS
C LAY : INTERFACE NODES
C SIZE : NUMBER OF SPATIAL NODES
C PRINT : PRINT COUNTER
C DELTIM : TIME STEP T
C DELPOS : SPACE STEP L
C TIMMAX : MAXIMUM TIME FOR NUMERICAL SIMULATION T
C DBD : DRY BULK DENSITY M/L3
C CEC : CATION EXCHANGE CAPACITY (MMOL/KG) M/M
C PULSE : TIME OF PULSE DURATION T
C VMC : VOLUMETRIC WATER CONTENT L3/L3
C VELO : PORE WATER VELOCITY L/T
C DIFO : DISPERSION COEFFICIENT L2/T
C CINIT : INITIAL CONCENTRATION
C CTOT : TOTAL CONCENTRATION M/L3
```

C

```
PRINT 80,' '
PRINT 85,' *****'
PRINT 85,' * L A Y O N E *'
PRINT 85,' * *'
PRINT 85,' * SOLUTION OF ADVECTION DISPERSION EQUATION *'
PRINT 85,' * IN DIMENSIONLESS FORM, INCLUDING NON-LINEAR *'
PRINT 85,' * EXCHANGE, USING THE CRANK-NICHOLSON METHOD *'
PRINT 85,' * FIRST TYPE IBC *'
PRINT 85,' * LINEAR & FAVORABLE EXCHANGE *'
PRINT 85,' *****'
PRINT,' '

```

C

```
PRINT 85,' -----'
DO 15 K=1,NUMLAY
PRINT 95,' LAYER # ',K
PRINT,' '

```

```

PRINT 90, 'DISPERSION COEFFICIENT ', DIFO(K), 'CM2/D'
PRINT 90, 'PORE WATER VELOCITY ', VELO(K), 'CM/D'
PRINT 90, 'CATION EXCHANGE CAPACITY', CEC(K), 'ME/G'
PRINT 90, 'DRY BULK DENSITY ', DBD(K), 'G/CM3'
PRINT, ' '
PE(K)=VELO(K)*DELPOS/DIFO(K)
CR(K)=VELO(K)*DELTIM/DELPOS
PRINT 90, 'PECLET NUMBER', PE(K), ' '
PRINT 90, 'COURANT NUMBER', CR(K), ' '
PRINT 85, ' -----'
15 CONTINUE
C
PRINT, ' '
PRINT 90, 'TIMESTEP', DELTIM, 'D'
PRINT 90, 'SPACE-INCREMENT', DELPOS, 'CM'
PRINT, ' '
80 FORMAT('1', A60)
85 FORMAT(A60)
90 FORMAT(A32, 3X, F7.3, A10)
95 FORMAT(A40, 3X, I2)
C
DUMBOU=SIZE-1
CIN=1.
C
DO 21 K=1, NUMLAY
G(K)=DIFO(K)/(2.*DELPOS*DELPOS)
H(K)=VELO(K)/(4.*DELPOS)
DBDVMC(K)=DBD(K)*CEC(K)/(VMC(K)*CTOT)
W(K)=0.5
21 CONTINUE
C
C DEFINE INITIAL CONDITIONS AND BOUNDARY CONDITIONS FOR THE PROBLEM
C POSED, AND POSITIONS
C
DO 11 I=1, SIZE
COLD(I)=CINIT
11 CONTINUE
C
DO 10 I=1, SIZE
POS(I)=(I-1)*DELPOS
10 CONTINUE
C
C DETERMINE INITIAL AMOUNT OF SOLUTE
C
K=1
ACCOLD=0.0
C
DO 27 I=2, SIZE
CALL ADSORB(I, K, ADS, COLD)
ACCOLD=ACCOLD+0.5*DELPOS*(CTOT*VMC(K)*(COLD(I-1)+COLD(I))+
$ DBD(K)*CEC(K)*(ADS(I-1)+ADS(I)))

```



```

        IF (I.EQ.LAY(K)) K=K+1
27  CONTINUE
C
        SUMFLU=0.0
        ACCIN=ACCOLD
C
        COLD(1)=CIN
C
        PRINT, '
        PRINT 113, ' TIME ', ' ORMB ', ' RMB ', (POS(I), I=1, SIZE, 4)
113  FORMAT(' ', 3A6, 16F6.1)
114  FORMAT(' ', 19F6.2)
115  FORMAT(' ', 3A6, 16F6.2)
        PRINT, ' '
C
        TIME=0.
        ORMB=0.
        RMB=0.
C
        PRINT 114, TIME, ORMB, RMB, (COLD(I), I=1, SIZE, 4)
        PRINT 115, ' ', ' ', ' ', (ADS(I), I=1, SIZE, 4)
        PC=1
C
C  INITIALIZE DUMMY VARIABLES AND TRIDIAGONAL MATRIX
C
        A(SIZE)=-1.0
        C(SIZE)=0.0
C
        WHILE (TIME.LE.TIMMAX) DO
C
        CALL EXCHAN(SIZE, W, LAY, COLD, DBDVMC, RETCO)
C
        IF(TIME.LT.PULSE) THEN
            CIN=1.
        ELSE
            CIN=CINIT
        ENDIF
C
        K=1
C
        A(1)=0.0
        B(1)=1.0
        C(1)=0.0
        F(1)=CIN
C
        DO 25 I=2, DUMBOU
            IF(I.EQ.LAY(K)) THEN
                FLU(K)=(VMC(K)*VELO(K)*COLD(I)-VMC(K)*DIFO(K)*
$                 (COLD(I)-COLD(I-1))/DELPOS)
                FLU(K+1)=VMC(K+1)*VELO(K+1)*COLD(I)-VMC(K+1)*DIFO(K+1)*
$                 (COLD(I+1)-COLD(I))/DELPOS

```

```

W(K)=1./(1.+(FLU(K)/FLU(K+1)))
A(I)=-W(K)*(G(K)+H(K))-(1-W(K))*(G(K+1)+H(K+1))
B(I)=(RETCO(I)/DELTIM)+2.*(W(K)*G(K)+(1-W(K))*G(K+1))
C(I)=W(K)*(H(K)-G(K))+(1-W(K))*(H(K+1)-G(K+1))
F(I)=-A(I)*COLD(I-1)+(B(I)-4.*(W(K)*G(K)+(1-W(K))*G(K+1)))*
$      COLD(I)-C(I)*COLD(I+1)
      K=K+1
ELSE
A(I)=-G(K)-H(K)
C(I)=-G(K)+H(K)
B(I)=2.0*G(K)+(RETCO(I)/DELTIM)
F(I)=-A(I)*COLD(I-1)+(B(I)-4.0*G(K))*COLD(I)-
$      C(I)*COLD(I+1)
ENDIF
25 CONTINUE
C
B(SIZE)=1.+0.5*RETCO(SIZE)/(G(K)*DELTIM)
F(SIZE)=COLD(DUMBOU)+(B(SIZE)-2.)*COLD(SIZE)
C
C SOLVE THE DIFFERENTIAL EQUATION WITH THE CRANK-NICOLSON METHOD
C BY USING THE THOMAS ALGORITHM
C
CALL TRIDIA(A,B,C,CNEW,F,SIZE,INLET)
C
CALL EXCHAN(SIZE,W,LAY,CNEW,DBDVMC,RETCO)
C
C REQUIRED PRINTOUTANDMASS BALANCE CALCULATIONS
C
TIME=TIME+DELTIM
C
ACCNEW=0.0
K=1
DO 29 I=2,SIZE
CALL ADSORB(I,K,ADS,CNEW)
ACCNEW=ACCNEW+0.5*DELPOS*(CTOT*VMC(K)*(CNEW(I-1)+CNEW(I))+
$      DBD(K)*CEC(K)*(ADS(I-1)+ADS(I)))
IF (I.EQ.LAY(K)) K=K+1
29 CONTINUE
C
FLUX=DELTIM*CTOT*(VELO(1)*VMC(1)*CIN-0.5*VELO(NUMLAY)*
$      VMC(NUMLAY)*(CNEW(SIZE)+COLD(SIZE)))
SUMACC=ACCNEW-ACCIN
SUMFLU=SUMFLU+FLUX
RMB=100.*ABS((ACCNEW-ACCOLD-FLUX)/FLUX)
ORMB=100.*ABS((SUMACC-SUMFLU)/SUMACC)
ACCOLD=ACCNEW
C
IF (PC.EQ.PRINT) THEN
PRINT 114,TIME,ORMB,RMB,(CNEW(I),I=1,SIZE,4)
PRINT 115,' ',' ',' ',' ',(ADS(I),I=1,SIZE,4)
PC=0

```

```

        ENDIF
        PC=PC+1
C
        DO 60 I=1,SIZE
            COLD(I)=CNEW(I)
60      CONTINUE
C
        ENDWHILE
C
        STOP
        END
C
C*****
C
        SUBROUTINE TRIDIA(A,B,C,CNEW,F,SIZE,INLET)
C
C THIS SUBROUTINE CONTAINS THE THOMAS-ALGORITHM, THE SOLUTION IS
C CONTAINED IN THE CNEW-ARRAY
C
        REAL A(63),B(63),C(63),CNEW(63),F(63)
        INTEGER SIZE,INLET
C
        REAL GAMMA(63),BETA(63)
        INTEGER I,J,DUMBOU
C
        DUMBOU=SIZE-1
C
        BETA(1)=B(1)
        GAMMA(1)=F(1)/B(1)
        DO 200 I=2,SIZE
            BETA(I)=B(I)-(A(I)*C(I-1)/BETA(I-1))
            GAMMA(I)=(F(I)-A(I)*GAMMA(I-1))/BETA(I)
200     CONTINUE
C
C BEGIN BACKWARD SUBSTITUTION FROM LAST ROW, INCLUDE BOUNDARY CONDITIONS
C
        I=SIZE-1
        CNEW(SIZE)=GAMMA(SIZE)
        WHILE (I.GE.1) DO
            CNEW(I)=GAMMA(I)-(C(I)*CNEW(I+1)/BETA(I))
            I=I-1
        ENDWHILE
C
        RETURN
        END
C
C*****
C
        SUBROUTINE EXCHAN(SIZE,W,LAY,COLD,DBDVMC,RETCO)
C
        REAL COLD(63),DBDVMC(2),RETCO(63),W(2)

```

```

INTEGRER I,K,LAY(2),SIZE
REAL SLOPE(63)
C
K=1
DO 300 I=1,SIZE
  IF(I.LT.LAY(1)) THEN
    SLOPE(I)=1.
    RETCO(I)=1.+DBDVMC(K)*SLOPE(I)
  ELSE IF (I.EQ.LAY(1)) THEN
    RETCO(I)=W(K)*(1.+DBDVMC(K))+(1-W(K))*(1.+DBDVMC(K+1))*
$      (0.333333333333/(COLD(I)**0.666666666666)))
    K=2
  ELSE
    SLOPE(I)=0.333333333333/(COLD(I)**0.666666666666)
    RETCO(I)=1.+DBDVMC(K)*SLOPE(I)
  ENDIF
300 CONTINUE
C
RETURN
END
C
C *****
C
SUBROUTINE ADSORB(I,K,ADS,CNEW)
C
REAL ADS(63),CNEW(63)
INTEGRER I,K
C
IF(K.GT.1) THEN
  ADS(I-1)=CNEW(I-1)**0.333333333333
  ADS(I)=CNEW(I)**0.333333333333
ELSE
  ADS(I-1)=CNEW(I-1)
  ADS(I)=CNEW(I)
ENDIF
C
RETURN
END
/GO

```

Listing of LAY3

```
//FIG21B JOB (AYL59FL,124),'FEIKE LEIJ',MSGCLASS=P,
// NOTIFY=AYL59FL,MSGLEVEL=(1,1),REGION=1024K,TIME=(1,59)
/*ROUTE PRINT RMT4
/*JOBPARM LINES=10
//STEP1 EXEC WATFIV
//WATFIV.SYSIN DD *
/JOB FEIKE,TIME=(05),PAGES=60
```

C

C VARIABLE DECLARATION

```
INTEGER I,J,K,NUMLAY/3/,LAY(3)/21,26,80/,SIZE/63/,DUMBOU,PRINT/20/
INTEGER UPLAY(3),PC
REAL DELTIM/0.05/,DELPOS/0.5/,COLD(63),CNEW(63),CTOT/0.01/
REAL TIMMAX/100./,TIME,POS(63),CIN/1./,ADSOLD(63),ADSNEW(63)
REAL DBD(3)/3*1.3/,CEC(3)/0.01,0.0,0.01/
REAL PE(3),CR(3),VMC(3)/0.2,.4,.2/,DIFO(3)/4.,2.5,4./
REAL A(63),B(63),C(63),F(63),CINIT/0.05/,VELO(3)/1.,.5,1./
REAL DBDVMC(3),G(3),H(3),DV(3),VD(3),RETCO(63)
REAL ACCNEW,ACCOLD,ACCIN,ORMB,RMB,SUMFLU,SUMACC,FLUX
```

C

C VARIABLES

```
C   NUMLAY      : NUMBER OF LAYERS
C   LAY         : INTERFACE NODES
C   SIZE        : NUMBER OF SPACE NODES
C   PRINT       : PRINT FREQUENCY
C   DELTIM      : TIME STEP                      T
C   DELPOS      : SPACE STEP                      L
C   CTOT        : TOTAL CONCENTRATION            M/L3
C   TIMMAX      : MAXIMUM TIME OF SIMULATION     T
C   CIN         : ELUENT CONCENTRATION           -
C   CINIT       : INITIAL CONCENTRATION          -
C   DBD         : DRY BULK DENSITY                M/L3
C   CEC         : CATION EXCHANGE CAPACITY (MMOL/KG) M/M
C   VMC         : VOLUMETRIC WATER CONTENT       L3/L3
C   VELO        : PORE WATER VELOCITY           L/T
```

C

```
PRINT 80,' '
PRINT 85,' *****'
PRINT 85,' *                L A Y T H R E E                *'
PRINT 85,' *
PRINT 85,' *      SOLUTION OF ADVECTION DISPERSION EQUATION      *'
PRINT 85,' *      IN DIMENSIONLESS FORM, INCLUDING NON-LINEAR          *'
PRINT 85,' *      EXCHANGE, USING THE CRANK-NICHOLSON METHOD              *'
PRINT 85,' *                THIRD TYPE IBC                              *'
PRINT 85,' *                S A N D                                        *'
PRINT 85,' *****'
PRINT,' '
C
```

C

```
PRINT 85,' -----'
DO 15 K=1,NUMLAY
PRINT 95,' LAYER      #      ',K
PRINT,' '
C
```

```

PRINT 90, 'DISPERSION COEFFICIENT ', DIFO(K), 'CM2/D'
PRINT 90, 'PORE WATER VELOCITY ', VELO(K), 'CM/D'
PRINT 90, 'CATION EXCHANGE CAPACITY', CEC(K), 'ME/G'
PRINT 90, 'DRY BULK DENSITY ', DBD(K), 'G/CM3'
PRINT 90, 'VOLUMETRIC WATER CONTENT', VMC(K), 'CM3/CM3'
PRINT, ' '
PE(K)=VELO(K)*DELPOS/DIFO(K)
CR(K)=VELO(K)*DELTIM/DELPOS
PRINT 90, 'PECLET NUMBER', PE(K), ' '
PRINT 90, 'COURANT NUMBER', CR(K), ' '
PRINT 85, ' -----'
15 CONTINUE
C
PRINT, ' '
PRINT 90, 'TIMESTEP', DELTIM, 'D'
PRINT 90, 'SPACE-INCREMENT', DELPOS, 'CM'
PRINT, ' '
80 FORMAT('1', A60)
85 FORMAT(A60)
90 FORMAT(A32, 3X, F7.3, A10)
95 FORMAT(A40, 3X, I2)
C
DUMBOU=SIZE-1
C
DO 21 K=1, NUMLAY
  G(K)=DIFO(K)/(2.*DELPOS*DELPOS)
  H(K)=VELO(K)/(4.*DELPOS)
  DBDVMC(K)=DBD(K)*CEC(K)/(VMC(K)*CTOT)
  UPLAY(K)=LAY(K)+1
  VD(K)=2.*DELPOS*VELO(K)/DIFO(K)
  DV(K)=2.*DIFO(K)/(VELO(K)*DELPOS)
21 CONTINUE
C
C DEFINE INITIAL CONDITIONS AND BOUNDARY CONDITIONS FOR THE PROBLEM
C POSED, AND POSITIONS
C
DO 11 I=1, SIZE
  COLD(I)=CINIT
11 CONTINUE
C
K=1
DO 10 I=1, SIZE
  POS(I)=(I-K)*DELPOS
  IF (I.EQ.LAY(K)) K=K+1
10 CONTINUE
C
C DETERMINE INITIAL AMOUNT OF SOLUTE
C
K=1
ACCOLD=0.0
C

```

```

I=2
WHILE (I.LE.SIZE) DO
  CALL ADSORB(I,K,ADSOLD,COLD)
  ACCOLD=ACCOLD+0.5*DELPOS*(CTOT*VMC(K)*(COLD(I-1)+COLD(I))+
$   DBD(K)*CEC(K)*(ADSOLD(I-1)+ADSOLD(I)))
  IF (I.EQ.LAY(K)) THEN
    K=K+1
    I=I+1
  ENDIF
  I=I+1
ENDWHILE

C
  SUMFLU=0.0
  ACCIN=ACCOLD

C
  COLD(1)=12.*VELO(1)*DELPOS*CIN/(12.*VELO(1)*DELPOS+25.*DIFO(1))

C
  PRINT, '                                POSITIONS'
  PRINT 113, ' TIME ', ' ORMB ', ' RMB ', (POS(I),I=1,21,4),
$   (POS(I),I=22,26,2), (POS(I),I=27,SIZE,4)
113 FORMAT(' ',3A5,19F5.1)
114 FORMAT(' ',22F5.2)
  PRINT, ' '

C
  PC=1
  TIME=0.0

C
C INITIALIZE DUMMY VARIABLES AND TRIDIAGONAL MATRIX
C
  A(SIZE)=-1.0
  C(SIZE)=0.0

C
  CALL EXCHAN(SIZE,LAY,COLD,DBDVMC,RETCO)

C
  WHILE (TIME.LE.TIMMAX) DO

C
  K=1

C
  A(1)=0.0
  B(1)=RETCO(1)+2.*DELTIM*(G(1)+2.*H(1)*(1.+(H(1)/G(1))))
  C(1)=-G(1)*2.*DELTIM
  F(1)=(-B(1)+2.*RETCO(1))*COLD(1)+
$   2.*DELTIM*(G(1)*COLD(2)+4.*H(1)*(1.+(H(1)/G(1)))*CIN)

C
  DO 25 I=2,DUMBOU
    IF(I.EQ.LAY(K)) THEN
      A(I)=-2.*G(K)
      B(I)=(RETCO(I)/DELTIM)+2.*G(K)+(H(K)-G(K))*VD(K)
      C(I)=(G(K)-H(K))*VD(K)
      F(I)=2.*G(K)*COLD(I-1)+((RETCO(I)/DELTIM)-2.*G(K)+(G(K)-H(K))
$   *VD(K))*COLD(I)+((H(K)-G(K))*(DV(K+1)+1.)*VD(K))*

```

```

$      COLD(I+1)+((G(K)-H(K))*DV(K+1)*VD(K))*COLD(I+2)
ELSE IF(I.EQ.UPLAY(K)) THEN
  A(I)=- (G(K+1)+H(K+1))*VD(K+1)
  B(I)=(RETCO(I)/DELTIM)+2.*G(K+1)+(G(K+1)+H(K+1))*VD(K+1)
  C(I)=-2.*G(K+1)
  F(I)=((G(K+1)+H(K+1))*DV(K)*VD(K+1))*COLD(I-2)+
$      ((G(K+1)+H(K+1))*(1.-DV(K))*VD(K+1))*COLD(I-1)+
$      ((RETCO(I)/DELTIM)-2.*G(K+1)-(G(K+1)+H(K+1))*VD(K+1))*
$      COLD(I)+2.*G(K+1)*COLD(I+1)
      K=K+1
ELSE
  A(I)=-G(K)-H(K)
  C(I)=-G(K)+H(K)
  B(I)=2.0*G(K)+(RETCO(I)/DELTIM)
  F(I)=-A(I)*COLD(I-1)+(B(I)-4.0*G(K))*COLD(I)-
$      C(I)*COLD(I+1)
      ENDIF
25 CONTINUE
C
  B(SIZE)=1.+0.5*RETCO(SIZE)/(G(NUMLAY)*DELTIM)
  F(SIZE)=COLD(DUMBOU)+(B(SIZE)-2.)*COLD(SIZE)
C
C SOLVE THE DIFFERENTIAL EQUATION WITH THE CRANK-NICOLSON METHOD
C BY USING THE THOMAS ALGORITHM
C
      CALL TRIDIA(A,B,C,CNEW,F,SIZE,INLET)
C
      CALL EXCHAN(SIZE,LAY,CNEW,DBDVMC,RETCO)
C
C REQUIRED PRINTOUTANDMASS BALANCE CALCULATIONS
C
      TIME=TIME+DELTIM
C
      ACCNEW=0.0
      I=2
      K=1
      WHILE (I.LE.SIZE) DO
        CALL ADSORB(I,K,ADSNEW,CNEW)
        ACCNEW=ACCNEW+0.5*DELPOS*(CTOT*VMC(K)*(CNEW(I-1)+CNEW(I))+
$          DBD(K)*CEC(K)*(ADSOLD(I-1)+ADSOLD(I)))
        IF (I.EQ.LAY(K)) THEN
          I=I+1
          K=K+1
        ENDIF
        I=I+1
      ENDWHILE
C
      FLUX=DELTIM*CTOT*(VELO(1)*VMC(1)*CIN-0.5*VELO(NUMLAY)*
$      VMC(NUMLAY)*(CNEW(SIZE)+COLD(SIZE)))
      SUMACC=ACCNEW-ACCIN
      SUMFLU=SUMFLU+FLUX

```



```

RMB=100.*ABS(ACCNEW-ACCOLD-FLUX)/FLUX
ORMB=100.*ABS(SUMACC-SUMFLU)/SUMACC
ACCOLD=ACCNEW
C
  IF (PC.EQ.PRINT) THEN
    PRINT 114,TIME,ORMB,RMB,(CNEW(I),I=1,21,4),
$      (CNEW(I),I=22,26,2),(CNEW(I),I=27,SIZE,4)
    PC=0
  ENDIF
  PC=PC+1
C
    DO 60 I=1,SIZE
      COLD(I)=CNEW(I)
      ADSOLD(I)=ADSNEW(I)
60    CONTINUE
C
  ENDWHILE
C
  STOP
  END
C
C*****
C
  SUBROUTINE TRIDIA(A,B,C,CNEW,F,SIZE,INLET)
C
C THIS SUBROUTINE CONTAINS THE THOMAS-ALGORITHM, THE SOLUTION IS
C CONTAINED IN THE CNEW-ARRAY
C
  REAL A(63),B(63),C(63),CNEW(63),F(63)
  INTEGER SIZE,INLET
C
  REAL GAMMA(63),BETA(63)
  INTEGER I,J,DUMBOU
C
  DUMBOU=SIZE-1
C
  BETA(1)=B(1)
  GAMMA(1)=F(1)/B(1)
  DO 200 I=2,SIZE
    BETA(I)=B(I)-(A(I)*C(I-1)/BETA(I-1))
    GAMMA(I)=(F(I)-A(I)*GAMMA(I-1))/BETA(I)
200  CONTINUE
C
C BEGIN BACKWARD SUBSTITUTION FROM LAST ROW, INCLUDE BOUNDARY CONDITIONS
C
  I=SIZE-1
  CNEW(SIZE)=GAMMA(SIZE)
  WHILE (I.GE.1) DO
    CNEW(I)=GAMMA(I)-(C(I)*CNEW(I+1)/BETA(I))
    I=I-1
  ENDWHILE

```

```

C
    RETURN
    END
C
C *****
C
    SUBROUTINE EXCHAN(SIZE, LAY, COLD, DBDVMC, RETCO)
C
    REAL COLD(63), DBDVMC(3), RETCO(63)
    INTEGER I, K, LAY(3), SIZE
    REAL SLOPE(63)
C
    K=1
    DO 300 I=1, SIZE
        IF (I.LE.LAY(1)) THEN
            SLOPE(I)=1.
            RETCO(I)=1.+DBDVMC(1)*SLOPE(I)
        ELSE IF (I.GT.LAY(2)) THEN
            SLOPE(I)=1.
            RETCO(I)=1.+DBDVMC(3)*SLOPE(I)
        ELSE
            SLOPE(I)=1.
            RETCO(I)=1.+DBDVMC(2)*SLOPE(I)
        ENDIF
    300 CONTINUE
C
    RETURN
    END
C
C *****
C
    SUBROUTINE ADSORB(I, K, ADS, CNEW)
C
    REAL ADS(63), CNEW(63)
    INTEGER I, K
C
        ADS(I)=CNEW(I)
        ADS(I-1)=CNEW(I-1)
C
    RETURN
    END
/GO

```

Listing of VARTIM

```
//FIG22 JOB (AYL59FL,124),'FEIKE LEIJ',MSGCLASS=P,
// NOTIFY=AYL59FL,MSGLEVEL=(1,1),REGION=1024K,TIME=(1,59)
/*ROUTE PRINT RMT4
/*JOBPARM LINES=10
//STEP1 EXEC WATFIV
//WATFIV.SYSIN DD *
/JOB FEIKE,TIME=(05),PAGES=60
```

C

C VARIABLE DECLARATION

```
INTEGER I,J,PC,SIZE/25/,DUMBOU,INLET/3/
REAL DELTIM,DELPOS/0.5/,COLD(33),CNEW(33),CTOT/0.01/
REAL TIMMAX/4.0/,TIME,POS(33),CIN/1./
REAL DBD/1.45/,CEC/0.0/,VMC/0.4/,VELO/50./,DIFO/50./
REAL A(33),B(33),C(33),F(33),CINIT/0.05/
REAL DBDVMC,G,H,RETCO(33),ADS(33),PRSTEP/0.2/,PRTIME,SFT
REAL ACCNEW,ACCOLD,ACCIN,ORMB,RMB,SUMFLU,SUMACC,FLUX
LOGICAL CHANGE
```

C

C VARIABLES

```
C SIZE : NUMBER OF SPATIAL NODES
C INLET : CONDITION AT INLET BOUNDARY (FIRST=1, THIRD=3)
C DELPOS : SPACE STEP L
C DELTIM : (VARIABLE) TIME STEP T
C CTOT : TOTAL CONCENTRATION M/L3
C CINIT : INITIAL CONCENTRATION -
C PRSTEP : TIME STEP FOR PRINTING T
C CIN : ELUENT CONCENTRATION -
C TIMMAX : MAXIMUM TIME FOR NUMERICAL SIMULATION T
C DBD : DRY BULK DENSITY M/L3
C CEC : CATION EXCHANGE CAPACITY (MOL/KG) M/M
C VELO : PORE WATER VELOCITY L/T
C DIFO : DISPERSION COEFFICIENT L2/T
C VMC : VOLUMETRIC WATER CONTENT L3/L3
```

C

```
PRINT,' '
PRINT,' *****'
PRINT,' * V A R T I M E *'
PRINT,' * *'
PRINT,' * SOLUTION OF ADVECTION DISPERSION EQUATION *'
PRINT,' * IN DIMENSIONLESS FORM, INCLUDING NON-LINEAR *'
PRINT,' * EXCHANGE, USING THE CRANK-NICHOLSON METHOD *'
IF (INLET.EQ.1) THEN
PRINT,' * FIRST TYPE IBC HOMOGENEOUS SYSTEM *'
ELSE
PRINT,' * THIRD TYPE IBC HOMOGENEOUS SYSTEM *'
ENDIF
PRINT,' * *'
PRINT,' *****'
PRINT,' '
C
```

```
PRINT,'SPACE-INCREMENT=',DELPOS
```

```

PRINT, ' '
C
DELTIM=0.005
TIME=0.0
PC=1
DUMBOU=SIZE-1
CHANGE=.TRUE.
C
G=DIFO/(2.*DELPOS*DELPOS)
H=VELO/(4.*DELPOS)
C
DBDVMC=DBD*CEC/(VMC*CTOT)
C
C DEFINE INITIAL CONDITIONS AND BOUNDARY CONDITIONS FOR THE PROBLEM
C POSED, AND POSITIONS
C
DO 11 I=1,SIZE
  COLD(I)=CINIT
11 CONTINUE
C
ACCOLD=0.0
DO 26 I=2,SIZE
  CALL ADSORB(I,ADS,COLD)
  ACCOLD=ACCOLD+0.5*DELPOS*(CTOT*VMC*(COLD(I-1)+COLD(I))+
    $ DBD*CEC*(ADS(I-1)+ADS(I)))
26 CONTINUE
C
SUMFLU=0.0
ACCIN=ACCOLD
C
ORMB=0.0
RMB=0.0
CIN=1.
C
IF(INLET.EQ.1) THEN
  COLD(1)=CIN
ELSE
  COLD(1)=12.*VELO*DELPOS*CIN/(12.*VELO*DELPOS+25*DIFO)
ENDIF
C
DO 10 I=1,SIZE
  POS(I)=(I-1)*DELPOS
10 CONTINUE
C
PRINT, ' POSITIONS'
PRINT 113, ' TIME ', ' ORMB ', ' RMB ', (POS(I),I=1,SIZE,2)
113 FORMAT(' ',3A7,13F7.1)
114 FORMAT(' ',16F7.3)
115 FORMAT(' ',3A7,13F7.3)
PRINT, ' '
PRINT 114, TIME, ORMB, RMB, (COLD(I), I=1, SIZE, 2)

```

```

      PRINT 115, ' ', ' ', ' ', ' ', (ADS(I), I=1, SIZE, 2)
C
C INITIALIZE DUMMY VARIABLES AND TRIDIAGONAL MATRIX
C
      A(SIZE)=-1.0
      C(SIZE)=0.0
C
      WHILE (TIME.LE.TIMMAX) DO
C
      CALL EXCHAN(SIZE, COLD, DBDVMC, RETCO)
C
126  CONTINUE
C
      IF (INLET.EQ.1) THEN
          A(1)=0.0
          B(1)=1.0
          C(1)=0.0
          F(1)=CIN
      ELSE
          A(1)=0.0
          B(1)=RETCO(1)+2.*DELTIM*(G+2.*H*(1+(H/G)))
          C(1)=-G*2.*DELTIM
          F(1)=(-B(1)+2.*RETCO(1))*COLD(1)+
$          2.*DELTIM*(G*COLD(2)+4.*H*(1+(H/G))*CIN)
      ENDIF
C
      DO 25 I=2, DUMBOU
          A(I)=-G-H
          C(I)=-G+H
          B(I)=2.0*G+(RETCO(I)/DELTIM)
          F(I)=-A(I)*COLD(I-1)+(B(I)-4.0*G)*COLD(I)-
$          C(I)*COLD(I+1)
25  CONTINUE
C
      B(SIZE)=1.+0.5*RETCO(SIZE)/(G*DELTIM)
      F(SIZE)=COLD(DUMBOU)+(B(SIZE)-2.)*COLD(SIZE)
C
C SOLVE THE DIFFERENTIAL EQUATION WITH THE CRANK-NICOLSON METHOD
C BY USING THE THOMAS ALGORITHM
C
      CALL TRIDIA(A,B,C,CNEW,F,SIZE,INLET)
C
C MASS BALANCE CALCULATIONS
C
      ACCNEW=0.0
      DO 29 I=2, SIZE
          CALL ADSORB(I, ADS, CNEW)
          ACCNEW=ACCNEW+0.5*DELPOS*(CTOT*VMC*(CNEW(I-1)+CNEW(I))+
$          DBD*CEC*(ADS(I-1)+ADS(I)))
29  CONTINUE
C

```

```

FLUX=0.5*VELO*DELTIM*CTOT*VMC*(2*CIN-CNEW(SIZE)-COLD(SIZE))
SUMACC=ACCNEW-ACCIN
SFT=SUMFLU+FLUX
RMB=100.*ABS((ACCNEW-ACCOLD-FLUX)/FLUX)
ORMB=100.*ABS(SUMACC-SUMFLU)/SFT
C
IF(TIME.GT.0.1) THEN
C
    IF(DELTIM.LT.0.00000001) THEN
        PRINT,'MASS BALANCE ERROR AT T=',TIME
        STOP
    ELSE IF(ORMB.LE.0.5 .AND. CHANGE) THEN
        DELTIM=2.*DELTIM
        CHANGE=.FALSE.
        GO TO 126
    ELSE IF (ORMB.GT.3 .AND. CHANGE) THEN
        DELTIM=0.5*DELTIM
        CHANGE=.FALSE.
        GO TO 126
    ENDIF
C
ENDIF
C
CHANGE=.TRUE.
SUMFLU=SUMFLU+FLUX
ACCOLD=ACCNEW
C
C REQUIRED PRINT OUT
C
    TIME=TIME+DELTIM
    PRTIM=PC*PRSTEP
    IF (TIME.GE.PRTIM) THEN
        PRINT 114,TIME,ORMB,RMB,(CNEW(I),I=1,SIZE,2)
        PRINT 115,' ',' ',' ',' ',' ',(ADS(I),I=1,SIZE,2)
        PC=PC+1
    ENDIF
C
    DO 60 I=1,SIZE
        COLD(I)=CNEW(I)
60    CONTINUE
C
ENDWHILE
C
STOP
END
C
C*****
C
SUBROUTINE TRIDIA(A,B,C,CNEW,F,SIZE,INLET)
C
C THIS SUBROUTINE CONTAINS THE THOMAS-ALGORITHM, THE SOLUTION IS

```

```

C CONTAINED IN THE CNEW-ARRAY
C
REAL A(33),B(33),C(33),CNEW(33),F(33)
INTEGER SIZE,INLET
C
REAL GAMMA(33),BETA(33)
INTEGER I,J,DUMBOU
C
DUMBOU=SIZE-1
C
BETA(1)=B(1)
GAMMA(1)=F(1)/B(1)
DO 200 I=2,SIZE
    BETA(I)=B(I)-(A(I)*C(I-1)/BETA(I-1))
    GAMMA(I)=(F(I)-A(I)*GAMMA(I-1))/BETA(I)
200 CONTINUE
C
C BEGIN BACKWARD SUBSTITUTION FROM LAST ROW, INCLUDE BOUNDARY CONDITIONS
C
I=SIZE-1
CNEW(SIZE)=GAMMA(SIZE)
WHILE (I.GE.1) DO
    CNEW(I)=GAMMA(I)-(C(I)*CNEW(I+1)/BETA(I))
    I=I-1
ENDWHILE
C
RETURN
END
C
C *****
C
SUBROUTINE EXCHAN(SIZE,COLD,DBDVMC,RETCO)
C
REAL COLD(33),DBDVMC,RETCO(33)
INTEGER I,SIZE
REAL SLOPE(33)
C
DO 300 I=1,SIZE
    SLOPE(I)=1.
    RETCO(I)=1.+DBDVMC*SLOPE(I)
300 CONTINUE
C
RETURN
END
C
C *****
C
SUBROUTINE ADSORB(I,ADS,CNEW)
C
REAL ADS(33),CNEW(33)
INTEGER I
C
ADS(I)=CNEW(I)
ADS(I-1)=CNEW(I-1)
C
RETURN
END
C

```